LIGAND EXCHANGE EQUILIBRIUM STUDIES OF SOME MO_8 ANIONIC β-DIKETONATE COMPLEXES OF YTTRIUM(III), AND KINETIC AND MECHANISTIC STUDIES OF INTERMOLECULAR LIGAND EXCHANGE IN SOME ORGANOTIN(IV) ACETYLACETONATE COMPLEXES BY ^1H NMR SPECTROSCOPY

Rouben Ishayek

A THESIS

in

The Department

of

Chemistry

Presented in Partial Fulfillment of the Requirements for
the Degree of Master of Science at
Sir George Williams University
Montreal, Canada

June, 1973

ABSTRACT

Ligand exchange equilibria for the [pip][Y(tfac)$_4$]-[pip][Y(bzac)$_4$], [pip][Y(hfac)$_4$]-[pip][Y(bzbz)$_4$], and [pip][Y(hfac)$_4$]- [pip][Y(tfac)$_4$] systems, where pip is piperidinium and bzac, bzbz, tfac, and hfac stand for benzoylacetonate, dibenzoylmethanate, trifluoroacetylacetonate, and hexafluoroacetylacetonate, respectively, have been studied in deuteriochloroform by proton nmr spectroscopy. The [pip][Y(hfac)$_4$]-[pip][Y(tfac)$_4$] system has been characterized quantitatively in the methylene proton nmr region. The complexes [pip][Y(hfac)$_4$] and [pip] [Y(bzbz)$_4$] have not been reported previously. In the temperature range -58 to -16^o, the equilibrium quotients for the formation of mixed complexes for the [pip][Y(hfac)$_4$]- [pip][Y(tfac)$_4$] system are 3 to 5 times larger than statistical assuming a total random distribution of ligands. Deviations from statistical behaviour are ascribed to enthalpy changes, entropy changes being zero or nearly zero within experimental error. Relative rates of ligands exchanging between two complexes are discussed in terms of the coalescence behaviour of the methylene proton resonances from which it appears that the hexafluoroacetylacetonate ligands exchange faster than the trifluoroacetylacetonate ligands. Room temperature and variable temperature chemical shifts are reported. Room temperature shifts of [pip][Y(bzbz)$_4$] and [pip][Y(hfac)$_4$] are discussed in terms of the electric field model. Downfield shifts of the methylene proton resonances of the

five $[pip][Y(hfac)_n(tfac)_{4-n}]$ (where n = 0, 1, 2, 3, or 4) complexes with decreasing temperature are attributed to greater solvent-solute interactions at the lower temperatures.

The kinetics and mechanisms of intermolecular ligand exchange of acetylacetonate (acac) groups between $(C_6H_5)_2Sn(acac)_2$ and $(CH_3)_2Sn(acac)_2$ have been investigated in deuteriochloroform and bromoform solutions by ^1H nmr spectroscopy in the temperature range 17.5-58.5°($CDCl_3$) and 57-102°($CHBr_3$). The activation energies and entropies of activation are: 7.5 ± 1.5 kcal/mole ($CDCl_3$) and 5.4 ± 0.9 kcal/mole ($CHBr_3$), -33 ± 5 eu ($CDCl_3$) and -42 ± 3 eu ($CHBr_3$), respectively. Concentration dependence studies in $CHBr_3$ indicate that the rate of acetylacetonate exchange is first order in $(C_6H_5)_2Sn(acac)_2$ and zero order in $(CH_3)_2Sn(acac)_2$ concentration. A mechanism is proposed in which the rate-controlling step, in contrast to earlier studies, is identified as a metal-oxygen bond rupture in $(C_6H_5)_2Sn(acac)_2$ to yield a five-coordinate tin species with a dangling unidentate acac ligand.

Biographical Sketch

The author, son of Mr. and Mrs. Salim Ishayek, was born January 8, 1947 in Baghdad, Iraq. His secondary education was completed in June 1965, at University Tutorial College in London, England.

In September of 1965, he entered McGill University in Montreal where he graduated in June 1969 with a B.Sc. degree with a Major in Chemistry.

The author entered the Graduate Chemistry Program at Sir George Williams University in September 1969.

He is co-author of (1a) "Ligand-Exchange Equilibrium Studies of Some Octacoordinate Yttrium(III)-β-Diketonate Complexes by Hydrogen-1 Nuclear Magnetic Resonance Spectroscopy" by N. Serpone* and R. Ishayek, Inorg. Chem., 10, 2650-2656 (1971), and (1b) by N. Serpone and R. Ishayek*, 162nd National Meeting of the American Chemical Society, Washington, D.C., September 1971, Abstracts of Papers No. INOR 81; (2) "Kinetics and Mechanisms of Intermolecular Ligand Exchange. I. Diphenyltin- and Dimethyltin Acetylacetonate" by N. Serpone* and R. Ishayek, Inorg. Chem., submitted for publication.

Acknowledgement

I want to express my sincere and deep gratitude to Professor N. Serpone for his patience and supervision on the work reported here. He has put in a great deal of time and effort into this work and has been most kind when things got bogged down.

I also wish to express thanks to Professors P.H. Bird and R. Townshend for serving on my research committee, and to Professor L.D. Colebrook for serving on this committee while Professor Townshend was on sabbatical. The department of Chemistry is acknowledged for the financial assistance during the course of this work.

Helpful discussions with other members of the faculty and graduate students is gratefully acknowledged, especially Miss K. Bennett who also ran some of the thermograms.

TABLE OF CONTENTS

LIST OF TABLES

LIST OF FIGURES

I. INTRODUCTION

The chemistry of β-diketonate metal complexes has in the past decade been the subject of numerous studies as evidenced by the several review articles (1-9) that have recently appeared. These studies have dealt with the syntheses of the β-diketones and their metal complexes, with the stereochemistry and reactivity of the metal complexes, with the kinetic and mechanistic aspects of configurational rearrangement processes, and with ligand redistribution reactions and kinetics of ligand exchange in these metal complexes. It is upon the last two types of studies that attention is focussed in this work.

Some thirty years ago, Calingaert and Beatty (10,11) recognized the redistribution reaction between $Pb(CH_3)_4$ and $Pb(C_2H_5)_4$ to yield the mixed alkyl compounds $Pb(CH_3)(C_2H_5)_3$, $Pb(CH_3)_2(C_2H_5)_2$, and $Pb(CH_3)_3(C_2H_5)$ as a general class of chemical reactions in which distinguishable ligands are redistributed between polyfunctional central metal moieties. A vast majority of redistribution reactions that have been investigated have involved exchange of monofunctional substituents, while little attention was paid to exchange of polyfunctional substituents though some examples of the latter type of reaction were reported prior to the work of Calingaert and Beatty. One of these examples was reported in a study by Moore and Young (12) who found that the copper concentration, in a solution saturated with respect to two β-diketonate compounds, was considerably

greater than the sum of the separate solubilities. Such increase in the concentration of copper, as for example in the system copper acetylacetonate, $Cu(acac)_2$, and copper benzoylacetonate, $Cu(bzac)_2$, was attributed to the formation of a mixed complex *via* a ligand redistribution reaction as depicted in equation 1.

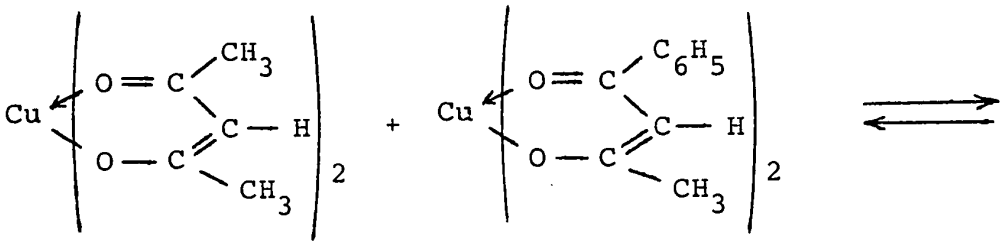

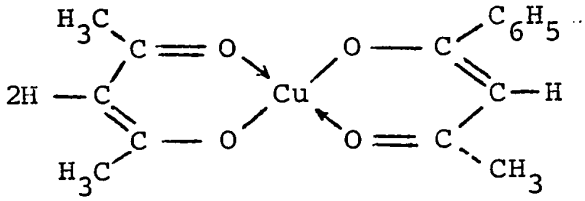

1

The current interest in redistribution reactions has been stimulated by their importance in chemical syntheses (13-15) and utility as models in understanding the discriminating behaviour of ligands and metal ions in biological systems (16). In addition to this, scrambling reactions are useful to study because the resulting mixed ligand complexes not only are of structural interest in that they may exist in several diastereomeric forms, but they are also well-suited for kinetic and mechanistic studies of configurational rearrangements of the chelate rings (1,2). The availability of nuclear magnetic resonance (nmr) spectro-

scopy in the past decade has stimulated studies of the kind.

Apart from this, eight-coordinate tetrakis-β-diketonate complexes have been the subject of many interesting investigations in the past several years. These investigations were directed toward structure elucidation (8,17,18), laser action in these chelates (8,17,19,20), magnetic properties (21-23), ligand dissociation equilibria (8,17), volatility and thermal properties (24-29), kinetics of ligand exchange (30), vibrational properties (31), electric field effects on proton chemical shifts (32), and ligand exchange equilibria (33-35). Of special interest are the latter studies in which lability of the β-diketonate ligands* in octacoordinate neutral complexes of the type $M(dik)_4$ (33,34,36) (M is Zr(IV), Hf(IV), Th(IV), or Ce(IV); dik is acac or tfac), and in octacoordinate ion-pair complexes, $[(C_6H_5)_4As][Y(dik)_4]$ (35) (dik is tfac or hfac) has been demonstrated by proton (33,35) and fluorine (34) nmr spectroscopy. For example, a benzene solution of $Zr(acac)_4$-$Zr(tfac)_4$ (Type III exchange#) contains the mixed complexes, $Zr(acac)_3(tfac)$, $Zr(acac)_2(tfac)_2$, and $Zr(acac)(tfac)_3$ as well as the parent complexes. The mixed complexes appear to be thermodynamically more stable

* The following abbreviations are used throughout the text: acac = anion of acetylacetone, bzac = anion of benzoylacetone, tfac = anion of trifluoroacetylacetone, hfac = anion of hexafluoroacetylacetone, bzbz = anion of dibenzoylmethane, dpm = anion of dipivaloylmethane, β-T = anion of β-isopropyltropolone, bztf = anion of benzoyltrifluoroacetone.

#For a definition of these types of exchange, see text.

than $Zr(acac)_4$ and $Zr(tfac)_4$. Deviations from a purely random distribution of ligands have been ascribed to entropy effects, enthalpy changes being zero or nearly zero (34). The need for measurement of enthalpy and entropy changes in studies of ligand exchange equilibria has been strongly emphasized by Fay(6).

Except for $Zr(acac)_4$-$Zr(tfac)_4$ (34), $Ga(acac)_3$-$Ga(bzbz)_3$ and $Ga(acac)_3$-$Ga(hfac)_3$ (37), and $Al(dik)_3$-$Al(dik')_3$ (38) systems (where dik and dik' are acac, hfac, or dpm), relatively little thermodynamic data are available in the literature for bidentate ligand exchange. Pinnavaia and Nweke (37) have shown that $Ga(acac)_3$-$Ga(hfac)_3$ is the first system in which deviations from statistical scrambling are due mainly to enthalpy changes. Similar enthalpy changes can probably be found in cases where the equilibrium quotients are two or more orders of magnitude larger than the expected statistical values (37,38).

More recently, in a comprehensive study of ligand exchange reactions, Pinnavaia and co-workers (39) investigated several ligand redistribution equilibria# by nmr spectroscopy for six-coordinate aluminum(III) [dik = acac; dik' = bzbz or hfac] and eight-coordinate zirconium(IV)

#The ligand exchange equilibria were defined by the reaction

$$\frac{i}{n}\,M(dik)_n + \frac{n-i}{n}\,M(dik')_n \overset{K_{fi}}{\rightleftharpoons} M(dik)_i(dik')_{n-i}$$

where dik and dik' are distinguishable β-diketonate ligands, n = 3 when M = aluminum and n = 4 when M = zirconium; i = 1, 2, 3,.....n-1.

[dik = acac or dpm; dik' = bzbz, β-T, or hfac] β-diketonates in solvents of low donor ability, in order to assess the various factors which might influence the stabilization of mixed ligand d^0 metal complexes containing MO_6 and MO_8 cores. The results of these studies (39), along with those reported previously for related systems (33-35,37,38,40,41), indicate that when dik and dik' both possess protonated terminal groups (Type I exchange), the values of the equilibrium constants are equal to, or slightly smaller than, the values (3.00 for MO_6 and 4.00 or 6.00 for MO_8) expected for a random statistical distribution of ligands. However, when dik is protonated and dik' is fluorinated (Type II exchange) the values of the equilibrium constants were two to five orders of magnitude larger than the statistical values. The driving force for Type I exchange has been ascribed to entropy effects, enthalpy changes being zero or nearly zero within experimental error. In Type II exchange reactions were found substantial enthalpy changes (-1.2 to -5.5 kcal/mole) and entropy changes (1.5 to 4.8 eu) which are somewhat larger than the values expected for random exchange (ΔH_{stat} = 0.00 kcal/mole and ΔS_{stat} = 2.18 eu for MO_6; ΔH_{stat} = 0.00 kcal/mole and ΔS_{stat} = 2.75, 3.56 eu for MO_8). The enthalpy changes were attributed to differences in mean metal-oxygen bond energies between the mixed ligand and parent complexes. Solvent polarity over the dielectric constant range 2.2-34.8 did not appreciably affect enthalpy changes for the acac-hfac exchange in aluminum(III) complexes (39). It was

also postulated that decreases in the repulsive energies between the donor oxygen atoms of the β-diketonate ligands probably play an important role in the stabilization of the mixed complexes formed in the Type II exchange reactions.

To further ascertain the importance of enthalpy and entropy changes as impetus behind ligand exchange equilibrium reactions, the systems $[pip][M(hfac)_4]$-$[pip][M(tfac)_4]$, $[pip][M(hfac)_4]$- $[pip][M(bzbz)_4]$, $[pip]$ $[M(hfac)_4]$-$[pip][M(bzac)_4]$ and $[pip][M(tfac)_4]$-$[pip][M(bzac)_4]$ (M = Y(III) or La(III)) were investigated by ^1H nmr spectroscopy. The second and third systems of the above series represent a Type II exchange, while the remaining two systems are further examples of a Type III exchange in which either dik is a fully fluorinated ligand and dik' a partially fluorinated or dik is a partially fluorinated ligand and dik' is fully protonated.

Another facet of ligand exchange reactions is the study of the kinetics of exchange of ligands from one complex to another. In the above cases, where ligands can exchange between eight-coordinate complexes, such kinetic studies are rendered complicated because a particular ligand exchanges between the five complexes present in an equilibrium mixture. However, the kinetics are made simpler if the ligands were to exchange only between two sites.

In a recent related study, Serpone and Hersh (42) have reported that the complex $(C_6H_5)_2Sn(acac)_2$ exists in

solution in the cis configuration. This complex (point group C_2) contains symmetry nonequivalent terminal methyl groups on the Sn-acac heterochelate rings, and thus configurational rearrangements of the rings can occur whereby the environment of the terminal CH_3 groups is averaged between the two sites. It was speculated that an intermolecular mechanism for configurational rearrangements in the acetylacetonate chelate rings might not be insignificant vis-á-vis an intramolecular pathway on the basis of the values of the rate constants: k = ca. 600 sec^{-1} (40^{o}) for the environmental averaging of the methyl groups in $(C_6H_5)_2Sn(acac)_2$ while k = 4.0 sec^{-1} (40^{o}) for the intermolecular ligand exchange between $(C_6H_5)_2Sn(acac)_2$ and $(CH_3)_2Sn(acac)_2$ (43). Unfortunately, the latter studies reported by Glass and Tobias (43) for the $(C_6H_5)_2Sn(acac)_2$-$(CH_3)_2Sn(acac)_2$ system were done only at one temperature (40^{o}). In order to shed more light into the possible mechanism(s) of configurational rearrangement phenomena in $(C_6H_5)_2Sn(acac)_2$ and related complexes (44), a more thorough study of the ligand exchange between $(C_6H_5)_2Sn(acac)_2$ and $(CH_3)_2Sn(acac)_2$ in deuteriochloroform and bromoform was undertaken.

II. EXPERIMENTAL SECTION

A. Preparation of Compounds

1. Reagents and Solvents

Columbia Organic Chemical trifluoroacetylacetone (1,1,1-trifluoro-2,4-pentanedione) and hexafluoroacetylacetone (1,1,1,5,5,5-hexafluoro-2,4-pentanedione) were used as purchased without further purification. Acetylacetone (2,4-pentanedione) was Fisher reagent grade and used as received. Yttrium(III) chloride ($YCl_3.6H_2O$; 99.9%), lanthanum(III) chloride ($LaCl_3.6H_2O$; 99.9%), diphenyltin dichloride, $(C_6H_5)_2SnCl_2$, and dimethyltin dichloride, $(CH_3)_2SnCl_2$, were purchased from Alpha Inorganics and used as received. Eastman Organic Chemicals dibenzoylmethane (1,3-diphenyl-1,3-propanedione) was used without further purification. Fisher certified reagent grade dichloromethane was dried over calcium hydride and distilled therefrom before use. Ethanol (95%) was used as received from the supplier (Fisher Scientific Co.). Hexane was of practical grade and distilled over calcium hydride before use.

2. General Techniques

Where synthesis and handling of moisture sensitive compounds was involved, all operations were carried out in a glove bag under anhydrous conditions in a dry nitrogen atmosphere. All glassware was dried in an oven at 140^{o} for

a few hours and cooled in a nitrogen atmosphere before use.

Unless otherwise noted, recrystallizations were carried out by dissolving the compound in a minimum amount of dichloromethane in an Erlenmeyer flask equipped with a side arm. Enough hexane was then added dropwise until the first signs of turbidity. The stoppered flask was placed in the freezer (ca 0°) for some time to allow crystallization of the desired product. The supernatant liquid was then decanted under nitrogen and the crystals were dried in vacuo. In other cases the product was filtered through a modified frit funnel as described previously (45).

3. Melting Points

Melting points were measured in capillaries, sealed with putty, with a Gallenkamp Melting Point Apparatus and are not corrected.

4. Analyses

Unless otherwise noted, elemental analyses were performed by Galbraith Laboratories Inc., Knoxville, Tennessee.

5. Piperidinium Tetrakis (1,1,1,5,5,5-hexafluoro-2,4-pentanedionato)yttrate(III).-

This product was prepared by a procedure similar to those previously reported in the literature (32,48) for other β-diketonates.

To a boiling solution of 50 ml of 95% ethanol, 7.80 g of 1,1,1,5,5,5-hexafluoro-2,4-pentanedione (32 mmoles), and 3.16 ml of piperidine (0.86 g/ml; 32 mmoles) was added a 30 ml aqueous solution of yttrium(III) chloride hexahydrate (2.43 g, 8 mmoles). The mixture was stirred while refluxing for 0.5 hr and the solvent was evaporated (ca. 30 ml) by heating over a hot plate for a further 0.5 hr; this evaporation resulted in the formation of an oil which did not crystallize even after standing in the cold (0^{o}) for one day. The oily lower layer was separated and dissolved in ca. 20 ml of dichloromethane and 5 ml of hexane. This solution was concentrated by passing a gentle stream of nitrogen over the surface of the solution until the first appearance of crystals. The product was allowed to crystallize in the cold (0^{o}) for 2 days. The crystals were filtered, washed twice with 20 ml portions of hexane, and dried in vacuo in a drying pistol (70^{o}) for 8 hr. The yield was 1.3 g (16% of theoretical); in another preparation the yield was 12% of theoretical. Mp 130-132^{o}.

Anal. Calcd. for $C_5H_{12}NY(C_5HF_6O_2)_4$: C, 29.92; H, 1.60; N, 1.39; F, 45.44; Y, 8.86. Found: C, 29.89; H, 1.55; N, 1.49; F, 45.63; Y, 9.05.

6. Piperidinium Tetrakis(1,1,1-trifluoro-2,4-pentanedionato)yttrate(III).-

This compound was prepared in a manner similar to that previously reported in the literature (32,46). Thus

to a boiling solution of 80 ml of 95% ethanol, 8.0 ml of 1,1,1-trifluoro-2,4-pentanedione (density = 1.23 g/ml; 64 mmoles), and 6.32 ml of piperidine (0.86 g/ml; 64 mmoles) was added a 50 ml aqueous solution of yttrium(III) chloride hexahydrate (4.86 g, 16 mmoles). The mixture was stirred while refluxing for 2 hr and the solvent was evaporated to half the original volume by heating over a hot plate for a further 0.5 hr. The flask was then stoppered and kept in the refrigerator (0^{o}) for 12 hr. An oil resulted from which a yellow solid crystallized out when the flask was vigorously shaken. The mother liquor was decanted and the yellow solid dissolved in a minimum quantity of dichloromethane. Hexane was added dropwise till the solution turned cloudy. The compound was allowed to crystallize at 0^{o} for 12 hr. The white crystals were filtered, washed with hexane and dried in vacuo for 24 hr. The yield after recrystallization was 3.80 g (29% of theoretical). Mp 105.5-107.5^{o}. Lit., (32,46) mp 106-108^{o}.

Anal.Calcd. for $C_5H_{12}NY(C_5H_4F_3O_2)_4$: C, 38.13; H, 3.58; F, 28.97; Y, 11.29. Found: C, 38.03; H, 3.53; N, 1.78; F, 28.81; Y, 11.42.

7. Piperidinium Tetrakis(1-phenyl-1,3-butanedionato)-yttrate(III).

This compound was prepared by the same procedure as that used for the corresponding trifluoroacetylacetonate and as previously described (32). Mp 120-122^{o}. Lit. (32,46)

mp 120-122°.

8. Piperidinium Tetrakis(1,3-diphenyl-1,3-propanedionato)yttrate(III).-

This complex was prepared in near quanitative yield by a procedure similar to that of the corresponding trifluoroacetylacetonate. To a solution of 7.18 g of dibenzoylmethane (32 mmoles) in 70 ml of 95% ethanol was added 3.16 ml piperidine (0.86 g/ml ; 32 mmoles). The solution was heated and while hot 2.43 g of yttrium(III) chloride hexahydrate (8 mmoles) in 25 ml H_2O was added while stirring. The mixture was refluxed for 2 hr and subsequently allowed to cool to room temperature. The yellow product was filtered, washed once with a 50 ml portion of hexane and then dried *in vacuo* overnight. Mp 186-188°.

Anal.Calcd. for $C_5H_{12}NY(C_{15}H_{11}O_2)_4$: C, 73.09; H, 5.28; N, 1.31; Y, 8.32. Found: C, 72.96; H, 5.27; N, 1.38; Y, 8.44.

9. Piperidinium Tetrakis(1,1,1,5,5,5-hexafluoro-2,4-pentanedionato)lanthanate(III).-

This product was synthesized by the same procedure as for the corresponding yttrium analogue. Mp 145-147°.

Anal.[#] Calcd. for $C_5H_{12}NLa(C_5HF_6O_2)_4$: C, 28.50; H, 1.53; N, 1.33: Found: C, 29.33; H, 2.31; N, 2.52. The purity of the product was further checked from its infrared

[#] These analyses were kindly performed by Professor R.T. Rye.

spectrum and from its nmr spectrum.

10. Piperidinium Tetrakis(1,1,1-trifluoro-2,4-pentanedionato)lanthanate(III).-

This compound was prepared by the same procedure as employed for the yttrium analogue. Mp 120-122°. Lit. (32,46) mp 122-124°. The purity of the product was further checked from its infrared and nmr spectra.

11. Piperidinium Tetrakis(1-phenyl-1,3-butanedionato)-lanthanate(III).-

This product was synthesized by the same procedure as reported earlier in the literature (32,46). Mp 119.5-121°. Lit. (32,46) mp 118-120°.

12. Piperidinium Tetrakis(1,3-diphenyl-1,3-propanedionato)lanthanum(III).-

This compound was prepared by the same procedure as the corresponding yttrium analogue. Mp 170-172°.

Anal. Calcd. for $C_5H_{12}NLa(C_{15}H_{11}O_2)_4$: C, 69.82; H, 5.04; N, 1.25; La, 12.42. Found: C, 69.90; H, 4.99; N, 1.36; La, 12.41.

13. Diphenylbis(2,4-pentanedionato)tin(IV).-

This product was synthesized in a manner similar to that described in the literature (47,48) by reacting diphenyltin dichloride, $(C_6H_5)_2SnCl_2$, with sodium acetylacetonate, Na(acac), in dry dichloromethane. The desired

white crystals were recrystallized from dry dichloromethane-hexane solutions, and dried *in vacuo*. Mp 124-126°. Lit., (47) mp 125°. Lit. (48) mp 125-126°. The purity of the product was further ascertained from its infrared and nmr spectra.

14. Dimethylbis(2,4-pentanedionato)tin(IV).-

The preparation of this compound has been previously reported (49). Dimethyltin dichloride, $(CH_3)_2SnCl_2$, was reacted with sodium acetylacetonate, Na(acac), in dry dichloromethane. The desired product was recrystallized from dichloromethane-hexane solutions and dried *in vacuo* for 3 hr. Mp 179-180°. Lit., (49) mp 177-178°. The purity of this compound was further checked from its infrared and nmr spectra.

B. Preparation of Solutions

1. Solvents

Deuteriochloroform was prepared by a modified method of Paulsen and Cooke (50). Hexachloro-2-propanone was reacted with deuterium oxide in the presence of pyridine at *ca.* 0°. The mixture was distilled, and the distillate (below 100°) was collected in a cold flask over ice-water. The two-phase distillate was cooled to *ca.* -4° and the deuterated product was filtered through glass wool. The product was dried by refluxing over calcium hydride overnight and purified by distillation collecting only the

portion at 61-63°. Deuteriochloroform was transferred into septem-sealed bottles containing molecular sieves (type 4A), and subsequently, enough tetramethylsilane (TMS) was added to give a 10% v/v TMS-$CDCl_3$ solution. The purity of the deuterated product was ascertained from its nmr spectrum.

Bromoform (Canlab Chemicals) was purified by distillation over molecular sieves (type 4A) just prior to use.

Benzene, chlorobenzene, 1,2-dichloroethane, nitromethane, and acetonitrile were all reagent grade and used fresh as received from the supplier.

2. Solutions

a) Eight-Coordinate Complexes

Before solutions of mixtures could be prepared for the ligand exchange studies, preliminary work was first undertaken to determine which possible system would be suitable for quantitative studies.

An equimolar mixture of 10% (g/100 ml solvent) of [pip][$Y(bzac)_4$] and 10% [pip] [$Y(tfac)_4$] in benzene was made up in a 9-in nmr tube which was subsequently sealed in vacuo while immersed in liquid nitrogen. After standing for one week at ambient temperatures, an nmr spectrum was recorded. No observable exchange was apparent compared to the nmr spectrum of a freshly prepared solution. It is possible that equilibrium was extremely slow to be reached.

Here it was decided to speed up attainment of equilibrium by heating the sample overnight in refluxing water. The color of the sample darkened. The nmr spectrum (room temperature) revealed a multiplicity of resonances (8 as expected-see Section III) in the methyl region (ca. -2ppm from TMS). The same results were obtained in chlorobenzene. However, because of the darkening of the solution, possible decomposition was suspected. To test the latter possibility, two nmr samples were prepared one containing a 10% benzene solution of [pip] [$Y(bzac)_4$] (very pale yellow) and the other containing a 10% benzene solution of [pip][$Y(tfac)_4$](colorless). The nmr spectra of these revealed one CH_3 resonance, one -CH= (ring proton) resonance and two broad resonances close to the methyl resonances and attributable to the piperidinium cation. After a heating period of 4 hr in refluxing benzene (~80°), the recorded nmr spectra showed one CH_3, one -CH=, and two pip resonances for [pip] [$Y(tfac)_4$] (colorless) but the onset of additional resonances was observed in the CH_3 region for [pip][$Y(bzac)_4$] (yellow). Upon further heating for an additional 48 hr, the nmr spectrum of [pip][$Y(tfac)_4$] (colorless) revealed no extraneous resonances while that of [pip][$Y(bzac)_4$] (deep dark yellow) revealed a total of five sharp resonances in the methyl proton nmr region. Similar results were obtained when such tests were performed in chlorobenzene solutions of the benzoylacetonate and trifluoroacetylacetonate complexes.

A mixture of 0.187M in [pip][$Y(bzac)_4$] and

0.179M in [pip][Y(tfac)$_4$] in deuteriochloroform-TMS was prepared to check the suitability of $CDCl_3$ as a possible solvent. The room temperature nmr spectrum of the mixture revealed two methyl resonances sitting on the two very broad piperidinium proton resonances, and two ring proton resonances. Since such a spectrum could be the result of fast ligand exchange between the two complexes (see section III and ref. 35), nmr spectra were recorded at low temperatures in the hope that the exchange might be slowed down sufficiently to observe the five complexes possible in such mixtures (see Section III A2). Heating the mixture over refluxing acetone (~58°) for about 20 hr induced some decomposition as indicated by the nmr spectrum.

For the system [pip][Y(bzbz)$_4$]-[pip][Y(hfac)$_4$], an equimolar mixture was prepared in benzene and also in chlorobenzene. The two nmr samples were warmed slightly to get the complexes into solution. The nmr spectra revealed no apparent ligand exchange between these two complexes. In addition, since the ring proton -CH= was the probe, benzene and chlorobenzene were not suitable solvents because sidebands of the solvent resonance seriously interfered with -CH= proton resonance lines (in the region of -6.0 to -6.5 ppm from TMS). The solvents 1,2-dichloroethane, nitromethane, and acetonitrile were found unsuitable for ligand exchange studies in the dibenzoylmethanate-hexafluoroacetylacetonate system for two reasons: (a) low solubility of the mixture in nitromethane and acetonitrile,

and (b) sidebands from 1,2-dichloroethane interfered with the ring proton lines of the two complexes.

The methyl proton region of the nmr spectrum of an equimolar mixture of $[pip][Y(bzac)_4]$- $[pip][Y(hfac)_4]$ in a benzene solution showed no observable exchange even at 9°. This sample was not heated prior to recording the spectra to avoid decomposition.

An equimolar mixture of $[pip][Y(hfac)_4]$-$[pip]$-$[Y(tfac)_4]$ in deuteriochloroform yielded two, somewhat broad, ring proton resonance lines in the room temperature nmr spectrum. The low temperature spectrum revealed more than two such resonances indicative of the presence of the mixed complexes in the above system. Thenceforth, ligand exchange studies were pursued on deuteriochloroform solutions of systems of the type $[pip][M(hfac)_4]$-$[pip][M(tfac)_4]$ where M is Y(III) or La(III).

Samples of the $[pip][Y(hfac)_4]$-$[pip]$ $[Y(tfac)_4]$ mixture were prepared by weighing the appropriate amount of the compounds in a 1.00-ml volumetric flask and then adding deuteriochloroform (with 10% v/v of tetramethylsilane) to the 1.00-ml mark. The concentrations and mole fractions, $X_{[Y(dik)_4^-]} = \frac{[Y(dik)_4^-]}{[Y(dik)_4^-]+[Y(dik')_4^-]}$ of the various solutions are summarized in Table I. The solutions were shaken vigorously for ca. 10-15 min to enhance dissolution of the complexes. The solutions were transferred to 9-in nmr precision tubes and sealed in vacuo. Fourteen

Table I.- Molar Concentrations and Mole Fractions of [pip][Y(dik)$_4$] in Deuteriochloroform Solutions[a]

No.	Concentrations, M		Mole Fractions	
	[pip][Y(hfac)$_4$]	[pip][Y(tfac)$_4$]	[pip][Y(hfac)$_4$]	[pip][Y(tfac)$_4$]
2[b]	0.0215	0.3561	0.0569	0.9430
3	0.0391	0.3323	0.1052	0.8947
4	0.0599	0.3064	0.1635	0.8364
5	0.0813	0.2802	0.2248	0.7751
6	0.1027	0.2559	0.2863	0.7136
7	0.1189	0.2300	0.3420	0.6579
8	0.1430	0.1993	0.4177	0.5822
9	0.1645	0.1770	0.4816	0.5183
10	0.1832	0.1533	0.5444	0.4555
11	0.2026	0.1273	0.6141	0.3958
12	0.2165	0.0983	0.6877	0.3123
13	0.2419	0.0813	0.7485	0.2515
14	0.2615	0.0525	0.8329	0.1671
15	0.2806	0.0275	0.9107	0.0893

[a] Range of total weight of mixture: 0.2946-0.3067 g. [b] Solution number 1 and 16 consisted of the pure complexes.

solutions were thus prepared each one of which differed from the preceding and subsequent solution by 0.02 g in each of the complexes, while the total weight of the mixtures was kept constant at 0.30 g. Before running nmr spectra, the solutions richest in [pip][Y(hfac)$_4$] were tested for solubility at low temperatures to insure that a particular solution did not change concentration at temperatures at which spectra were run. Samples number 10, 11, 12 and 13 were placed in a tetrachloroethane-dry ice slush bath (-43.8°) and periodically taken out to see whether or not a precipitate was present. At this temperature, in solutions 11, 12, and 13 a precipitate was observed immediately, while a precipitate in solution 10 was observed only after 35 min. At -35.6° (1,2-dichloroethane-dry ice slush bath) a precipitate was observed immediately in samples 12 and 13 but only after 2-3 min in sample 11. At -22.9° (carbon tetrachloride-dry ice) a precipitate was immediately observed for solutions 12 and 13; in solution 11 it was observed after 10 min. Thus the three samples richest in [pip][Y(hfac)$_4$], nos. 13, 14 and 15, were not used for variable temperature nmr work because this complex is but slightly soluble at low temperature.

To check how fast equilibrium is achieved at the low temperatures, a sample 0.48 mole fraction in [pip]-[Y(hfac)$_4$] was prepared by weighing 0.145 g of [pip][Y(hfac)$_4$] in an nmr tube and adding 0.70 ml of deuteriochloroform; the mixture was frozen by placing the nmr tube in liquid

nitrogen. To this frozen mixture was added 0.124 g of [pip][Y(tfac)$_4$] dissolved in 0.30 ml of deuteriochloroform. The nmr tube was sealed in vacuo and transferred to a N,N-dimethylformamide-dry ice bath (-61°). The contents of the tube were shaken vigorously at -61°, but even after 15 min the mixture did not dissolve. The tube was taken out of the cold bath and the contents were vigorously shaken for ca. 10-15 sec until a solution was obtained; the sample was then quickly inserted into the variable temperature nmr probe (already at -58°). The spectrum was recorded 1 min after insertion of the sample.

Solutions of similar concentrations were prepared for the [pip][La(hfac)$_4$]- [pip][La(tfac)$_4$] system; unfortunately, the mixtures were barely soluble in deuteriochloroform even at ambient temperatures. Reducing the concentration of the solution by a factor of two did not eradicate the solubility problem. Hence ligand exchange studies were not carried out with this system.

b) Six-Coordinate Complexes

Because of possible hydrolysis (47) of $(C_6H_5)_2Sn(acac)_2$ and $(CH_3)_2Sn(acac)_2$ complexes, these were handled and the solutions prepared entirely under anhydrous conditions in a dry nitrogen atmosphere in a glove bag. Dimethylbis(2,4-pentanedionato)tin(IV) was weighed (0.035050 g, 0.10101 mmoles) in a 1.00-ml volumetric flask (previously dried in an oven and cooled under nitrogen in

a glove bag). To this flask was added 0.048357g (0.10264 mmoles) of diphenylbis(2,4-pentanedionato)-tin(IV) and enough deuteriochloroform-10% v/v TMS solvent to yield a 1.00-ml solution. The solution was transferred to a dry 9-in nmr precision tube which was subsequently sealed in vacuo. A similar 1.00-ml solution of 0.034714 g (0.10005 M) of $(CH_3)_2Sn(acac)_2$ and 0.046493 g (0.09869 M) of $(C_6H_5)_2Sn(acac)_2$ was prepared in bromoform-10% v/v TMS solvent.

For the concentration dependence studies, solutions were prepared in the same manner as described above; the concentrations are tabulated in Table II.

C. Nuclear Magnetic Resonance Spectra

1. General

Variable temperature proton magnetic resonance spectra were obtained with a Varian HA-100 high-resolution spectrometer operating at 100.00 MHz. The spectrometer was equipped with a variable temperature probe accessory, Model V-4333, and a temperature controller accessory, Model V-6040. The spectra were recorded in the frequency sweep mode in the temperature range +50 to -58° (ligand exchange equilibria), -32 to 59° (kinetics of ligand exchange in $CDCl_3$), and 36 to 102° (kinetics of ligand exchange in $CHBr_3$).

Room temperature and variable temperature chemical shifts (^1H) were measured with the HA-100 and A-60A spectro-

Table II.- Molar Concentrations of Mixtures of $(CH_3)_2Sn(acac)_2$ and $(C_6H_5)_2Sn(acac)_2$ Complexes in Bromoform-TMS.

Solution	$[(CH_3)_2Sn(acac)_2]$	$[(C_6H_5)_2Sn(acac)_2]$
B1	0.09772	0.16129
B2	0.10036	0.13728
B3	0.09817	0.11939
B4	0.10005	0.09869
B5	0.09661	0.08217
A1	0.15305	0.10052
A2	0.13405	0.10028
A3	0.11540	0.09999
A4	0.10005	0.09869
A6	0.06047	0.09807

meters. The magnetic field sweep of the spectrometers at room temperature was checked against a chloroform-TMS reference sample (Varian Part No 943346-07), a method in agreement with the sideband technique (51). Room temperature shifts are believed accurate to ±0.01 ppm, variable temperature shifts to ±0.02 ppm.

Temperatures below room temperature were measured from the chemical shift difference of the CH_3 and OH proton

resonances of CH_3OH. High temperatures were determined from chemical shift differences between the OH and CH_2 resonance signals of $OHCH_2CH_2OH$. All temperatures reported in this work are based on the standard curves supplied by Varian Associates in the Instruction Manuals for the HA-100 and A-60A nmr spectrometers.

2. Errors Involved in the Variable Temperature Nmr Method

a) Solvents

Both chloroform (bp 61.7°, mp -63.5°) and bromoform (bp 149.5°, mp 8.3°), used in this work possess a wide enough liquid range such that nmr line shapes can be determined over a wide temperature range. Jones (52) has indicated that the boiling point of the solvent limits the highest temperature at which spectra can be obtained. There are several reasons for this limit: (1) when the solution boils, the passage of bubbles through the liquid reduces the resolution of the spectrum and, (2) bumping in the solution can cause the nmr tube to move in the teflon spinner because the fit is no longer tight due to unequal rates of thermal expansion. Such changes in the position of the sample relative to the heater of the probe in turn cause fluctuations in the temperature of the sample.

b) Temperature Control

In variable temperature nmr studies it is essential to insure a minimum of temperature fluctuations at any one

temperature setting. This is especially true around the coalescence temperature where the rate of exchange is most sensitive to temperature changes. Gutowsky, Meinzer and Jones (53) have attributed the temperature fluctuations in the probe to variation in heater current and/or in the flow rate of gas. Temperature fluctuations affect the resolution which in turn affects the line shapes. The above workers (53) observed a 1^{o} difference in temperature between a spinning and a non-spinning sample. For this reason special care was taken to insure a constant spinning rate at any one temperature. This was achieved by maintaining a constant flow of nitrogen, by maintaining the pressure cap screw in approximately the same position, and by maintaining the liquid nitrogen level in the dewar at approximately the same level when spectra were recorded at low temperature.

c) Magnetic Field Inhomogeneities

In order to maintain the same maximum resolution, the magnetic field homogeneity was optimized at each temperature. This was done by adjusting the Y gradient and curvature controls of the instrument for maximum amplitude of the TMS lock signal on the oscilloscope. This procedure is essential since loss of resolution alters the line shapes of the proton resonances. Saturation of the resonances, caused by too high rf power affects the transverse relaxation time T_2 and the line shapes. Care was taken to keep rf magnitudes below saturation levels.

3. Measurement of Signal Intensities

Proton resonance signals were obtained under conditions of low radiofrequency fields, H_1, such that differences in the product T_1T_2 for the various signals could be neglected (54).

Signal areas (accurate to ±3%) used in calculating equilibrium quotients were determined using a compensating polar planimeter. In general, five spectra were recorded for each sample at each temperature to reduce errors caused by changes in magnetic field sweep. Each signal was integrated 10 times and the results were averaged. Because of some overlap between resonance signals, the spectra were resolved manually. This manual resolution was checked by resolving and integrating a set of spectra with the Dupont 310 Curve Resolver. Equilibrium quotients calculated by planimetric and electronic integration agreed within experimental error.

When hfac and tfac -CH= proton resonances of the complex $[pip][Y(hfac)_2(tfac)_2]$, the tfac ring proton resonance of $[pip][Y(hfac)_3(tfac)]$, and the hfac -CH= proton resonance of $[pip][Y(hfac)(tfac)_3]$ could not be resolved manually because of serious overlap, the total area under these resonance signals was obtained. This area was then subdivided into the area of the appropriate resonance signals since the area for the tfac -CH= proton resonance of $[pip][Y(hfac)_3(tfac)]$ and for the hfac -CH= proton resonance of $[pip][Y(hfac)(tfac)_3]$ are known from integration

of $(hfac)_3$ and $(tfac)_3$ ring proton resonances, respectively.

4. Processing of Nmr Spectra

a) Ligand Exchange Equilibria

To obtain equilibrium quotients from the nmr data, the concentration of the complexes in the equilibrium reaction must be known. To get the concentration of each of the complexes the following procedure was employed. The areas of the resonance lines of each complex were determined as described above (Section II C 3). Then, the concentration was determined using equation 2.

$$C_c = \left(\frac{C_p \times q}{A_t}\right) \times \left(\frac{A_m}{m}\right) \qquad 2$$

where C_c = concentration of the particular complex.

C_p = concentration of the parent complex.

q = number of bidentate ligands bound to the metal (in this case 4).

A_t = total area of resonance signals of all like ligands from all the complexes.

A_m = area under the particular resonance signal being used.

m = number of like ligands in the complex.

For example, if the concentration of $[pip][Y(hfac)(tfac)_3]$ is required, we have a choice of either using the hfac resonance or the tfac resonance of this complex. Suppose we use the latter, then C_p is the molar concentration of the parent compound $[pip][Y(tfac)_4]$, q is 4, A_t is the total

area under all tfac resonance signals, A_m is the area under the tfac resonance line of $[pip][Y(hfac)(tfac)_3]$, and m is 3, the number of tfac ligands in the complex.

In certain instances, however, depending on how the equilibria are defined (see Section III A 3), it is not necessary to determine the concentrations of the complexes. If the equilibrium constant sought is that of reaction 3, it can be calculated

$$[pip][Y(tfac)_4] + [pip][Y(hfac)_2(tfac)_2] \xrightleftharpoons{K_{eq}} 2[pip][Y(hfac)(tfac)_3] \qquad 3$$

as outlined in equations 4-6.

$$K_{eq} = \frac{\{[pip][Y(hfac)(tfac)_3]\}^2}{\{[pip][Y(tfac)_4]\}\{[pip][Y(hfac)_2(tfac)_2]\}} \qquad 4$$

which by substitution of equation 2 into 4 yields

$$K_{eq} = \frac{\left(\left(\frac{C_p \times q}{A_t}\right)\left(\frac{A_3}{3}\right)\right)^2}{\left(\left(\frac{C_p \times q}{A_t}\right)\left(\frac{A_4}{4}\right)\right)\left(\left(\frac{C_p \times q}{A_t}\right)\left(\frac{A_2}{2}\right)\right)} \qquad 5$$

whence

$$K_{eq} = \frac{\left(\frac{A_3}{3}\right)^2}{\left(\frac{A_4}{4}\right)\left(\frac{A_2}{2}\right)} \qquad 6$$

b) Kinetics of Ligand Exchange

The rate of exchange of chemically equivalent nuclei between two nonequivalent, uncoupled sites, may be determined by calculating τ_i, the mean lifetime of a nucleus on site i. Such τ can be calculated by solving the line shape function corresponding to the Bloch phenomenological equations as modified for exchange (54,55). However, even for the simplest of line shapes, solution of the Bloch equations is an extremely tedious and time consuming process. For this reason approximate solutions have been developed (53) in order to simplify the calculations. However, these calculations can in many cases result in serious errors in the values of the first order rate constants and activation parameters (53). With the availability of large digital computers, programs have been developed to analyse the experimental nmr spectra by means of a point by point comparison with a calculated line shape. This Complete Line Shape Analysis of nmr spectra to determine rates of exchange has been found to be the most satisfactory of all the available methods (53,56,57). This was the method used in this work to process the nmr data. The procedure is presently described.

Before nmr spectra could be subjected to computer fitting, they have to be converted into digital form. Digitization of the spectra was achieved with the aid of a Hewlett-Packard 2114A Computer, an Analog/Digital converter, a Moseley Autograph Model 7001AM X-Y Recorder, a Hewlett-

Packard G-2B Null Detector, and a Hewlett-Packard Type F-3B Line Follower.

The basic function of the F-3B Line Follower is to produce an electrical signal representing a graphic tracing (58). It consists of an optical pick-up head assembly and a control unit which provides the power and function controls. To be prepared for tracing, a spectrum is placed on the 7001AM X-Y Recorder with the base line parallel to the Recorder edge. In the pick-up head assembly, which replaces the pen of the Recorder, a light illuminates the paper in the vicinity of the spectrum line. Light which is reflected from the line is directed and focussed on two photo-diodes through a semi-cylindrical lens. The photo-diodes are mounted close together and are connected in a balanced voltage circuit. When the illumination reaching them is equal, a null condition exists; but if tracking is not exact, the photo-diode pair produces an error signal. This signal is applied to the servo system of the recorder through an amplifier. Balancing action of the servo tends to return the pick-up assembly to a position directly over the line and cancel the error signal.

Signals from the Line Follower are converted into digital form by the Analog/Digital converter as a series of points of an X-Y plot (intensity vs. frequency in Hz.). These points are then recorded on punched paper tape. A program LINDI has been written (59,60) for the Hewlett-

Packard 2114A Computer in order to sychronize and coordinate the whole operation of digitizing a set of spectra.

The digitized spectra must then be transferred from paper tape to magnetic tape. This operation was simply effected with the aid of a Hewlett-Packard 2114A Computer, a Hewlett-Packard Model 2020 Digital Tape Unit and a Hewlett-Packard Model 2737A Punched Tape Reader together with a program TAPGH (59,60), written for the purpose. The computer fitting program NLINGH requires that initial trial values of τ_a, the lifetime of a nucleus on site a; τ_b, the lifetime on site b; the chemical shift, with respect to some arbitrary zero, of the nucleus at site a and that of the nucleus at site b; the linewidth in the absence of exchange; and finally a scaling factor (given the value 1500). TAPGH provides for introducing initial guesses of the above parameters with the option of keeping any combination of them fixed for each spectrum. Linewidths at $\frac{1}{2}$ height of the acetylacetonate methyl resonances of $(CH_3)_2Sn(acac)_2$ were used as the standard for values of the linewidth in the absence of exchange at each temperature; this parameter was kept as a fixed parameter. These linewidths of acac methyl resonances in deuteriochloroform and bromoform are plotted against temperature in Figure 1, and are tabulated in Table III. All the other parameters in program TAPGH and NLINGH were, unless indicated otherwise, allowed to vary.

Once on magnetic tape, the spectra are ready for

computer fitting. This operation was executed with program NLINGH (59,60) adapted for the Sir George Williams University CDC 6400 Computer. This program looks for the best combination of the variable parameters such that the corresponding line shape plot deviates by the sum of least squares of its points from that of the experimental plot. After a best fit has been determined, the computer prints out the resulting calculated line shape together with the experimental spectrum. If the initial guesses of the τ_a and τ_b parameters are too far off the "true" values, either a bad fit is obtained or the iteration limit is exceeded and the run for that spectrum is terminated. In such cases more appropriate values had to be entered and the process repeated until an acceptable fit was obtained.

Some serious problems were encountered when NLINGH attempted to fit spectra above coalescence where only one resonance line exists. Although the computer fit of the experimental and calculated spectra was good, in some cases exceptional, the τ_a and τ_b values from the print out varied by a factor sometimes as high as 100, even though the population in the two sites is experimentally equal; in addition, the difference in the chemical shifts of sites a and b deviated markedly from the averaged difference obtained from computer fit of spectra below coalescence. In order to obtain more meaningful values of τ_a and τ_b, the chemical shifts of sites a and b were kept fixed in TAPGH and NLINGH for spectra above coalescence such that the

Table III.- Linewidths at ½ Height of acac-CH_3 Resonances for $(CH_3)_2Sn(acac)_2$

Temp., [a] (°C)	$CDCl_3$	Temp., [a] (°C)	$CHBr_3$
-53.5	1.66 ± 0.05 [b]	15	1.39 ± 0.04 [b]
-45	1.55 ± 0.04	19	1.39 ± 0.05
-30	1.33 ± 0.02	24	1.28 ± 0.02
-21.5	1.27 ± 0.05	29.5	1.19 ± 0.05
-12.5	1.16 ± 0.03	40.5	1.03 ± 0.04
3.5	1.04 ± 0.04	48.5	1.07 ± 0.02
14.5	0.97 ± 0.04	56	1.00 ± 0.04
33	0.97 ± 0.03	64.5	0.92 ± 0.03
40.5	0.91 ± 0.02	71.5	0.87 ± 0.03
		81.5	0.88 ± 0.02

[a] Temperatures were determined by first measuring the chemical shift difference between the nonequivalent protons of methanol and then reading the values off the Varian calibrated graph provided with the instrument. [b] One standard deviation; Hz.

difference, $\delta\nu$, was equal to the average $\delta\nu$ obtained from below coalescence spectral fits.

D. Thermogravimetric Analysis

All thermogravimetric analytical data were obtained with a Dupont Model No 950 Thermogravimetric Analyzer. The atmosphere over the sample was nitrogen gas. The nitrogen gas flow rate was ~10 ml/min for all experiments and the sample heating rate was 15°C/min. The weight of the samples ranged from 7.8 to 9.2 mg.

Figure 1. - Temperature dependence of the linewidths at one-half maximum amplitude for acetylacetonate methyl proton signals in deuteriochloroform and bromoform. Bars represent one standard deviation based on five spectral runs at each temperature.

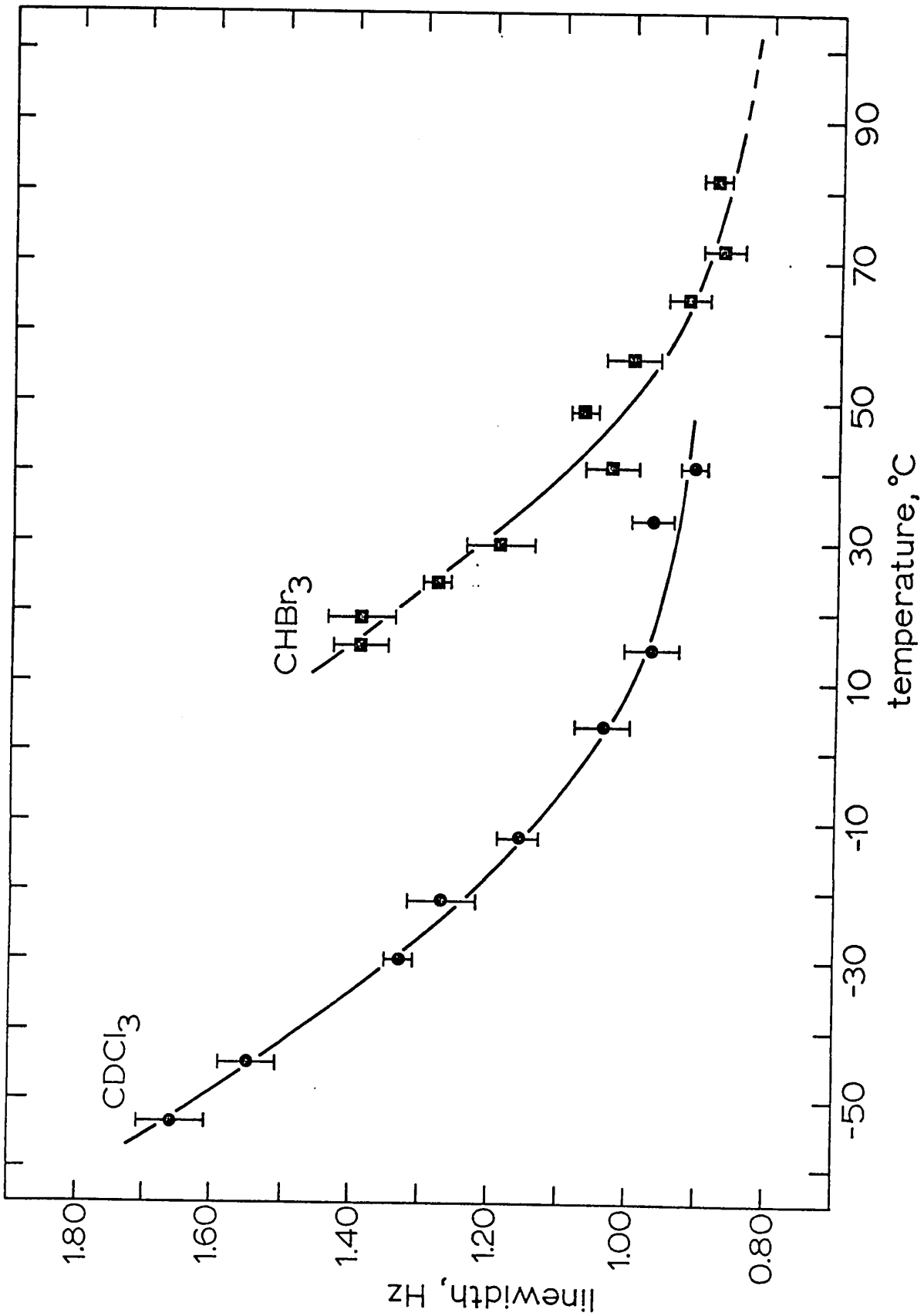
1.80
1.60
1.40
1.20
1.00
0.80
linewidth, Hz
-50
-30
-10
10
30
50
70
90
temperature, °C
$CDCl_3$
$CHBr_3$

III. RESULTS AND DISCUSSION

A. Ligand Exchange Equilibria

1. Dissociation and Thermal Stabilities

As mentioned earlier, nmr spectra of heated solutions of $[pip][Y(bzac)_4]$ in benzene and chlorobenzene reveal a multiplicity of resonances in the methyl proton region. This multiplicity of signals has been attributed to a possible decomposition (Section II B 2) of the piperidinium tetrakis-β-diketonate complex. In fact, this decomposition may well be a dissociation process of the complex into complexes of lower coordination number. These tetrakis-β-diketonate chelates, $[pip][Y(dik)_4]$, have two most probable ways of dissociation in solution (61).

$$[pip][M(dik)_4] \rightleftharpoons [M(dik)_3] + [pip][dik] \quad \text{(homolytic)}$$

$$[pip][M(dik)_4] \rightleftharpoons [M(dik)_4]^- + [pip]^+ \quad \text{(heterolytic)}$$

Homolytic dissociation of $[pip][Y(bzac)_4]$ would thus yield both <u>cis</u>-$Y(bzac)_3$ and <u>trans</u>-$Y(bzac)_3$ since the benzoylacetonate ligand is an unsymmetrical bidentate ligand ($C_6H_5COCHCOCH_3^-$), and (pip)(bzac). The nmr spectrum of a mixture of these compounds should show one CH_3 proton resonance for (pip)(bzac), one CH_3 resonance for <u>cis</u>-$Y(bzac)_3$ (point group C_3), and three CH_3 signals for <u>trans</u>-$Y(bzac)_3$ (point group C_1); a total of five methyl resonance lines consistent with experimental observations on $[pip][Y(bzac)_4]$ spectra. Heterolytic dissociation yields the two free ions $[pip]^+$ and $[Y(bzac)_4]^-$; only one methyl resonance should be

observed assuming of course rapid intramolecular exchange. This is indeed observed for the trifluoroacetylacetonate complex and for all unheated solutions. In a study designed to characterize rare earth β-diketonate chelate molecules in solution because of their paramount importance in liquid lasers, Filipescu, Hurt, and McAvoy (61) determined that piperidinium tetrakis(β-diketonato)europate-(III) complexes dissociate heterolytically in polar solvents such as acetonitrile, N,N-dimethylformamide, and chloroform; but homolytic dissociation predominates in non-polar solvents such as benzene. The following results were obtained (61): [pip][Eu(bzbz)$_4$], 80% in C_6H_6, 100% in $CHCl_3$, and 96% in CH_3CN; [pip][Eu(bzac)$_4$], 100% in C_6H_6, $CHCl_3$, and CH_3CN; [pip][Eu(bztf)$_4$], 1% in C_6H_6, 5% in $CHCl_3$, and 100% in CH_3CN (however, see also references 62, 63 and 64). These heterolytic dissociations were later confirmed by fluorescence studies (65, 66, 67) and by electrolytic conductance studies (25). The results from the latter studies did not preclude some ion-pairing (67), a configuration energetically more favourable in non-polar solvents (66). It should be noted, however, that the electrolytic conductance studies (0.005 M), fluorescence emission studies (10^{-2}-10^{-6} M), and molecular weight determinations (0.005 to 0.02 M) were carried out at solution concentrations about ten times more dilute than those used here (ca. 0.02 to 0.36 M). Although the extent of dissociation of the trifluoroacetylacetonate and hexafluoroacetylacetonate complexes

of yttrium(III) in deuteriochloroform investigated in this work is not known, these complexes are either undissociated or at best are probably only slightly heterolytically dissociated (cf. the fluorinated benzoyltrifluoroacetonate, bztf, complex above). The species involved in the ligand exchange are therefore believed to be undissociated $[pip][Y(dik)_4]$ with some $[Y(dik)_4]^-$. Unfortunately, the data presented here do not distinguish between these two species.

Thermogravimetric curves for the complexes $[pip][Y(dik)_4]$, where dik is hfac, tfac, bzac, or bzbz, were obtained to determine the volatility and heat stability of the compounds. These thermograms are pictured in Figure 2. The hexafluoroacetylacetonate complex (mp 130-132°) volatilizes at temperatures of 200-270° with 100% weight loss, probably as the ion-pair. This is consistent with earlier work on other hexafluoroacetylacetonate compounds, eg. $M(hfac)_3$ where M is aluminum (27) or chromium (27), and $[(C_2H_5)_3NH][Eu(hfac)_4]$ (28), but is not in keeping with the work on $Cs[Y(hfac)_4]$ which apparently sublimes at temperatures between 180 and 230° and which can exist in the gas phase as a stable ion-pair (24). The trifluoroacetylacetonate complex (mp 106-108°) is stable up to ca 140° and then decomposes with possible loss (about 70%) of the tris chelate $Y(tfac)_3$. The benzoylacetonate compound begins to decompose at the melting point (120-122°) while the corresponding dibenzoylmethanate analogue starts

Figure 2. - Thermogravimetric curves of [pip][$Y(dik)_4$] complexes where dik is hfac, tfac, bzac, or bzbz. The arrows indicate the melting points of the respective complexes.

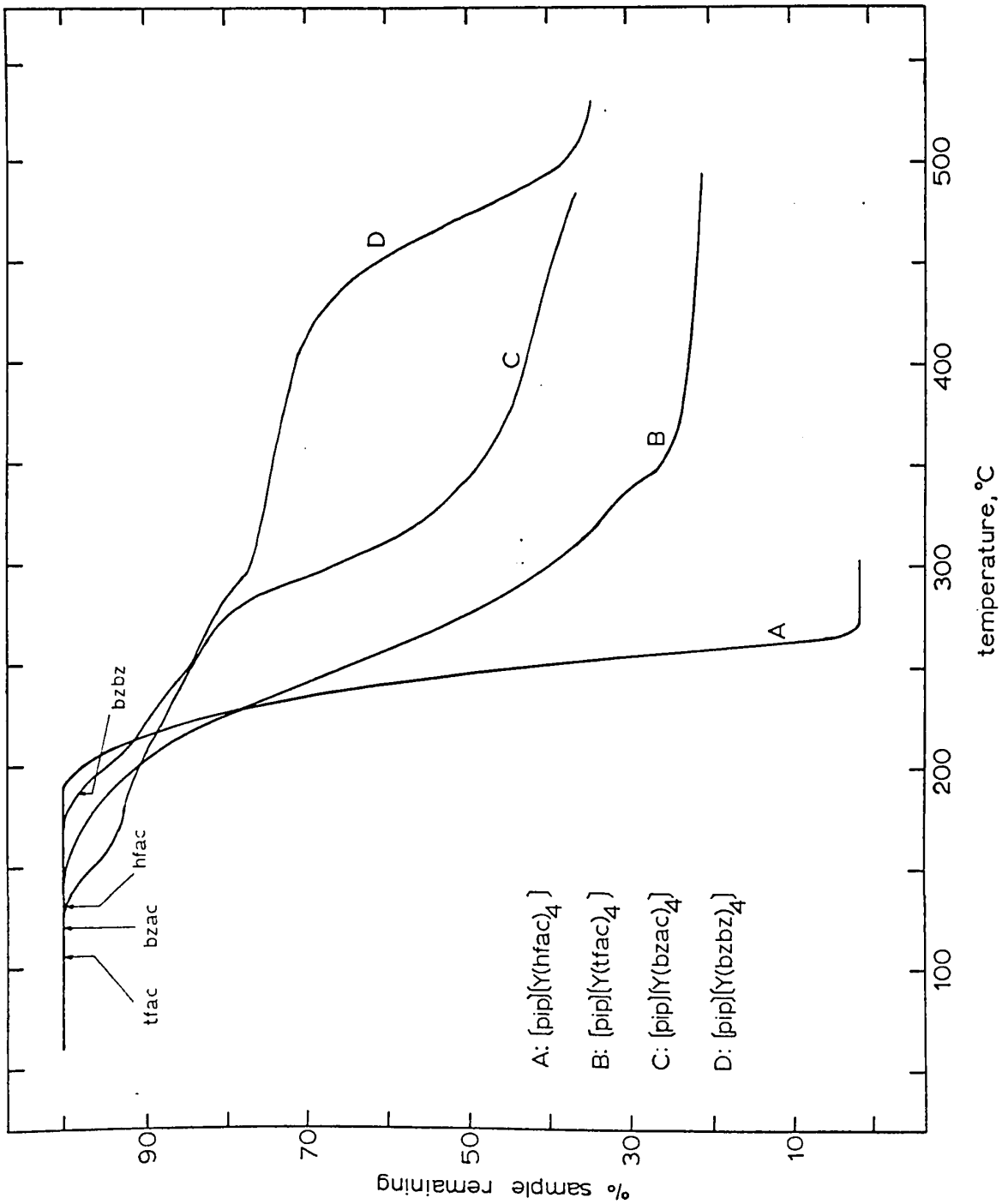
% sample remaining
90
70
50
30
10
100
200
300
400
500
temperature, °C
A
B
C
D
A: [pip][Y(thfac)4]
B: [pip][Y(tfac)4]
C: [pip][Y(bzac)4]
D: [pip][Y(bzbz)4]
tfac
bzac
hfac
bzbz

decomposing at 160° (mp 186-188°). The greater thermal stability of the hexafluoroacetylacetonate complex is rationalized (24) in terms of a sheath of fluorine atoms in the anion which tightly bind the cation $[C_5H_{12}N]^+$. In addition, the thermogravimetric curves indicate that volatility increases with the number of fluorocarbon substituents in the coordination sphere (cf. refs 27,28, and 68).

2. Proton NMR Spectra

Random distribution of ligands in equilibrium mixtures of $[pip][Y(dik)_4]$ and $[pip][Y(dik')_4]$ should give rise to five compounds having the general formula $[pip][Y(dik)_n(dik')_{4-n}]$ where n = 0, 1, 2, 3, or 4, and dik and dik' are hfac, tfac, bzac, or bzbz. When n = 0 or 4, the proton nmr spectrum should show one ring proton (-CH=) and one CH_3 resonance for each of the parent complexes; and for n = 2, the mixed complex $[pip][Y(dik)_2(dik')_2]$ should give rise to two equally intense -CH= and two equally intense CH_3 resonance signals, one each for the dik and dik' ligands. Spectra of the mixed complexes $[pip][Y(dik)(dik')_3]$ and $[pip][Y(dik)_3(dik')]$ when n = 1 or 3, respectively, should reveal a total of four -CH= resonances and four CH_3 resonances. In the former complex, the -CH= or CH_3 signal for the dik' ligand is expected to be three times more intense than that of the dik ligand; for the latter mixed complex, the dik proton resonances are expected to be three times more intense than those of dik'.

Therfore, the nmr spectrum of an equilibrium mixture containing all five complexes should reveal a maximum of eight -CH= signals and eight CH_3 proton resonances for the [pip][Y(tfac)$_4$]-[pip][Y(bzac)$_4$] mixture; eight -CH= resonances for the [pip][Y(hfac)$_4$]- [pip][Y(bzbz)$_4$] system; and eight -CH= proton resonances and four CH_3 resonances for the [pip][Y(hfac)$_4$]-[pip][Y(tfac)$_4$] mixture. To investigate ligand exchange equilibria in these mixtures, -CH= protons were chosen as probes rather than CH_3 protons. The methyl resonances were poorly resolved. The use of the ring protons necessitated more concentrated solutions (0.34 M) than would have been required had methyl protons been used as probes.

The methylene region in the variable temperature spectra of an equimolar mixture of [pip][Y(tfac)$_4$]-[pip][Y(bzac)$_4$] reveals only two -CH= proton resonances; linewidths at one-half maximum amplitude are 1.9 Hz (tfac) and 1.4 Hz (bzac) at 38°, 2.4 Hz (tfac) and 2.1 Hz (bzac) at -31.5°, and 3.5 Hz (tfac) and 3.0 Hz (bzac) at -57.5°. Spectra of a mixture of [pip][Y(hfac)$_4$] and [pip][Y(bzbz)$_4$] reveal two -CH= proton signals at 37° (linewidth 2.7 Hz for hfac and 3.2 Hz for bzbz), but a broad -CH= resonance doublet (hfac, linewidth ca. 8 Hz) and a very broad -CH= proton doublet (bzbz, linewidth ca. 11 Hz) at -58.5°. Temperature dependent broadening of ring proton resonances is consistent with ligands exchanging between all five complexes in the equilibrium mixture. Unfortunately, the

above two mixtures were unsuitable for quantitative studies. It appears that intermolecular ligand exchange in these two systems is rapid enough, even at ca. -58°, so as to average the chemical environment of the individual protons.

Ring proton resonance spectra (temperature is -58°) for equilibrium mixtures of $[pip][Y(hfac)_4]$ and $[pip][Y(tfac)_4]$ in deuteriochloroform solution at various values of mole fraction of $[pip][Y(hfac)_4]$ are presented in Figure 3. Six -CH= proton resonance signals are observed; the seventh resonance is masked by one of the more intense signals (vide infra). The $[Y(hfac)_4]^-$ ring proton resonance is not observed[#] at values of mole fractions shown in Figure 3. These spectra are consistent with the presence of $[pip][Y(tfac)_4]$ and the three mixed complexes (n = 1, 2, or 3). The two equally intense resonances at δ-5.99 ppm and -5.88 ppm are respectively assigned to hexafluoroacetylacetonate and trifluoroacetylacetonate protons of $[pip][Y(hfac)_2(tfac)_2]$. The -CH= signal at δ -5.72 ppm is

---

[#] The -CH= proton resonance of $[(C_6H_5)_4As][Y(hfac)_4]$ was clearly observed by Cotton and coworkers (35) but not that of $[(C_6H_5)_4As][Y(tfac)_4]$at values of mole fraction > 0.29. However, at a mole fraction of 0.17 in $[Y(hfac)_4]^-$, the ring proton signal of $[Y(tfac)_4]^-$ was observed at -5.68 ppm (-40°) [S.J. Lippard, private communication, January, 1971]. The difference between observations reported here and those reported earlier (35) is probably due to slight changes in chemical shifts for the $[pip]^+$ versus the $[(C_6H_5)_4As]^+$ salts because of ion pairing, and diamagnetic anisotropic effects of the phenyl groups in the latter salts which tend to shift proton resonances upfield (cf. ref 34).

Figure 3. - Ring proton resonance spectra for equilibrium mixtures of [pip][Y(hfac)$_4$] and [pip][Y(tfac)$_4$] in deuteriochloroform solution at -58.0°; total solute molarity is 0.34 M. The resonances are ascribed to [pip][Y(hfac)$_n$(tfac)$_{4-n}$] complexes were n = 0, 1, 2, or 3.

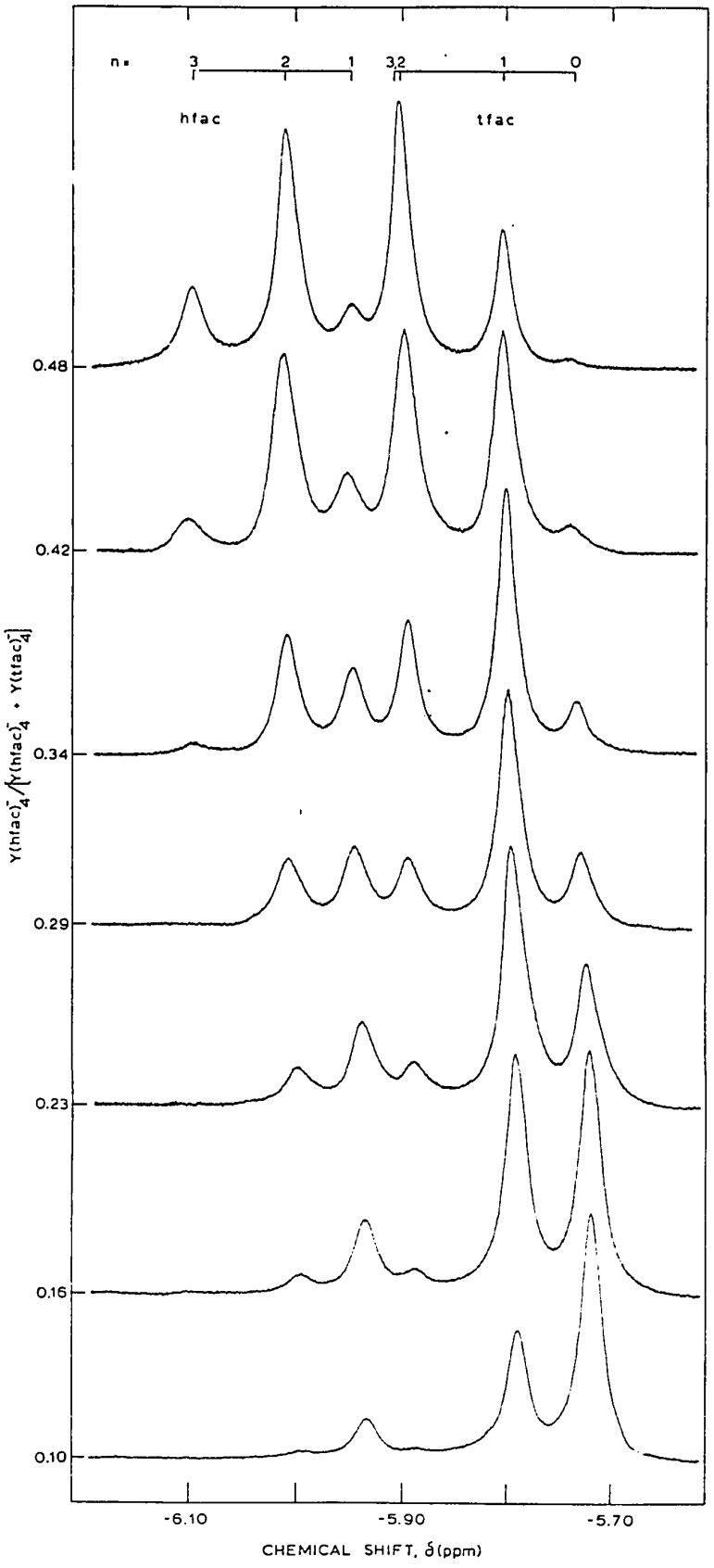
n=
3
2
1
3,2
1
0
hfac
tfac
0.48
0.42
0.34
0.29
0.23
0.16
0.10
Y(hfac)$_4^-$/[Y(hfac)$_4^-$ + Y(tfac)$_4^-$]
-6.10
-5.90
-5.70
CHEMICAL SHIFT, δ(ppm)

assigned to [pip][Y(tfac)$_4$]; the chemical shift of the ring proton resonance in a pure sample of [pip][Y(tfac)$_4$] is -5.72 ppm at -58°. The two resonances at -5.92 and -5.78 ppm are ascribed to the -CH= protons of hfac and tfac, respectively, of the [pip][Y(hfac)(tfac)$_3$] mixed complex. The proton signal at -6.07 ppm is assigned to the hexafluoroacetylacetonate ring proton of [pip][Y(hfac)$_3$(tfac)]; the corresponding -CH= resonance for the trifluoroacetylacetonate ligand in this mixed complex is masked by the more intense resonances of the [pip][Y(hfac)$_2$(tfac)$_2$] complex. However, inspection of Figure 3 reveals that the -CH= (tfac) resonance of [pip][Y(hfac)$_2$(tfac)$_2$] is slightly more intense than the corresponding hfac -CH= resonance; it is probable that the ring proton resonance of the trifluoroacetylacetonate ligand in [pip][Y(hfac)$_3$(tfac)] occurs at -5.88 ppm. This resonance is clearly observed at -5.82 ppm (-16°) in Figure 4 which presents ring proton spectra at higher values of mole fraction of [pip][Y(hfac)$_4$]. The temperature dependence of the tfac -CH= proton chemical shifts (see below) allows the tfac ring proton resonance for [pip][Y(hfac)$_3$-(tfac)] to be identified. The [Y(hfac)$_4$]$^-$ ring proton resonance (mole fraction = 0.69) is barely discernible on the lowfield side of the [pip][Y(hfac)$_3$(tfac)] hexafluoroacetylacetonate proton resonance.

Figure 5 shows the temperature dependent ring proton resonance spectra for [pip][Y(hfac)$_n$(tfac)$_{4-n}$] complexes. In the low temperature region (-28.5 to -58°),

Figure 4. - Ring proton resonance spectra for equilibrium mixtures of [pip][$Y(hfac)_4$] and [pip][$Y(tfac)_4$] in deuteriochloroform solution at -16.0°; total solute molarity is 0.34 M. The resonances are ascribed to [pip][$Y(hfac)_n(tfac)_{4-n}$] complexes where n = 0, 1, 2, 3, or 4.

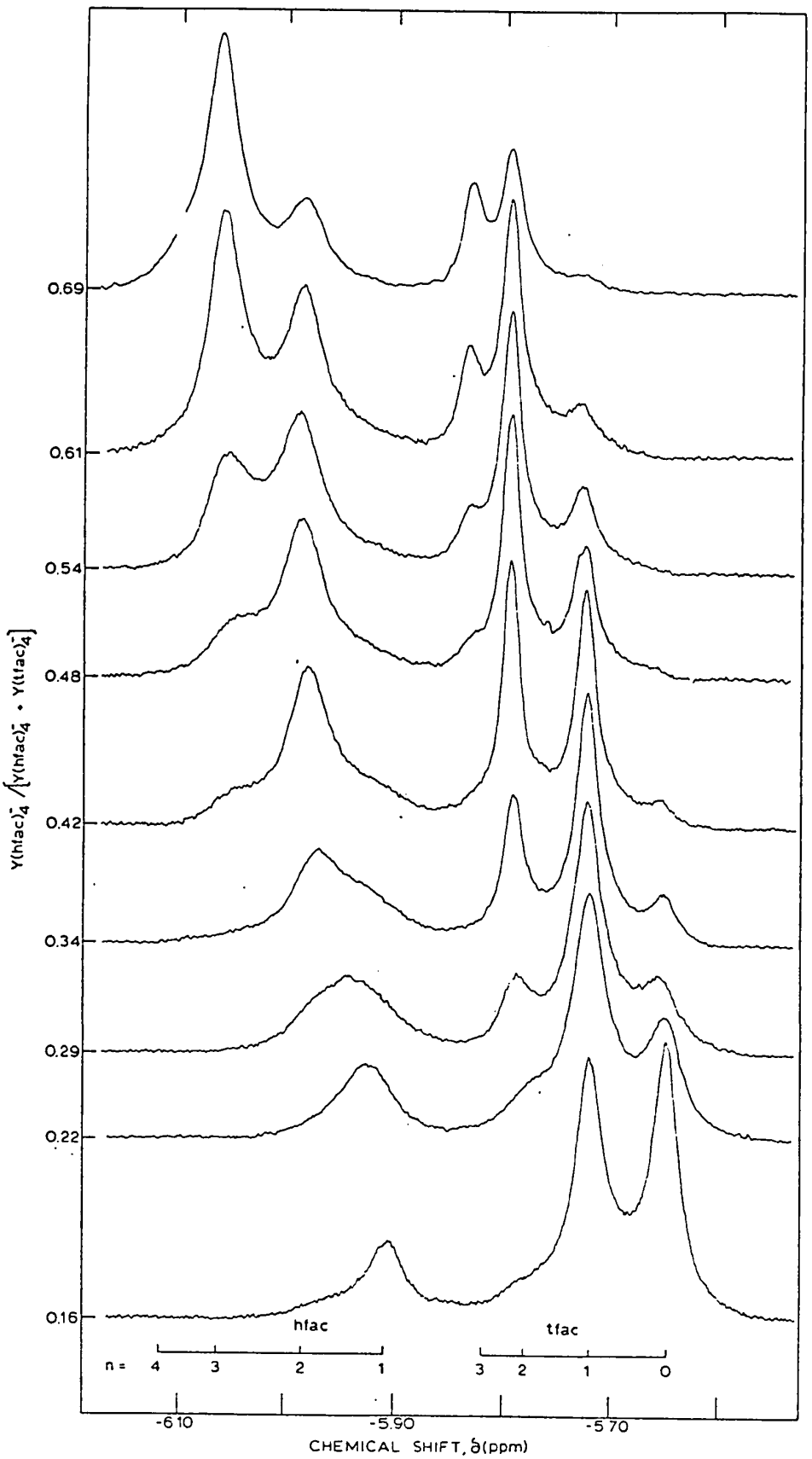
0.69
0.61
0.54
0.48
0.42
0.34
0.29
0.22
0.16
Y(hfac)$_4^-$ /[Y(hfac)$_4^-$ + Y(tfac)$_4^-$]
hfac
tfac
n = 4 3 2 1
3 2 1 0
-6.10
-5.90
-5.70
CHEMICAL SHIFT, δ(ppm)

Figure 5. - Temperature dependence of the methylene (-CH=) proton nmr spectra for an equilibrium mixture of [pip][Y(hfac)$_4$] and [pip][Y(tfac)$_4$] in deuteriochloroform; mole fraction in [pip][Y(hfac)$_4$] is 0.48.

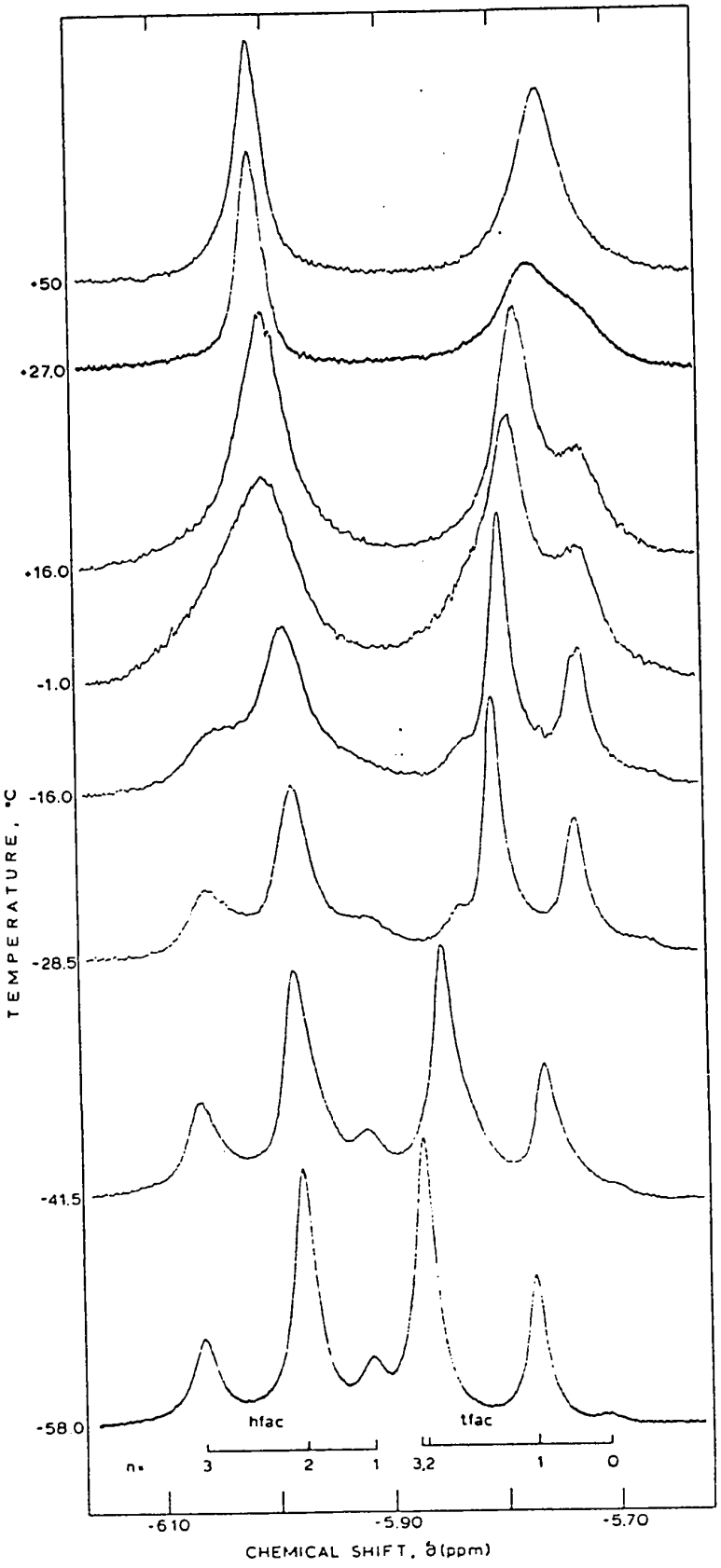
+50
+27.0
+16.0
-1.0
-16.0
-28.5
-41.5
-58.0
TEMPERATURE, °C
hfac
tfac
n•
3
2
1
3,2
1
0
-6.10
-5.90
-5.70
CHEMICAL SHIFT, δ(ppm)

seven ring proton resonances are observed consistent with the presence of the complexes for n = 0, 1, 2, and 3. As the temperature is increased the -CH= resonances for the individual complexes coalesce until only one hexafluoroacetylacetonate (lowfield line) and one trifluoroacetylacetonate peak (highfield line) are observed in the high temperature limit. This coalescence is attributed to a rapid intermolecular ligand exchange process which averages the magnetic environment of the individual protons. Similar observations have been reported by others (33-35).

Attempts to observe geometrical isomers of the mixed complexes (n = 1, 2, or 3) were not successful. The rate of the intramolecular exchange process is rapid enough that only the time-averaged chemical shifts of the methylene protons of each of the five compounds are observed.

Of significance are the relative rates of hexafluoroacetylacetonate and trifluoroacetylacetonate ligand exchange amongst the five compounds in the equilibrium mixture. Two types of ligand exchange can take place (33); these are shown in reactions 7 and 8, and reactions 9 and 10. First, as described in reactions 7 and 8, a hfac

$$[pip][Y(hfac)_3(tfac)] + [pip][Y(hfac)(tfac)_3] \rightleftarrows 2[pip][Y(hfac)_2(tfac)_2] \qquad 7$$

$$[pip][Y(hfac)(tfac)_3] + [pip][Y(hfac)_2(tfac)_2] \rightleftarrows [pip][Y(hfac)_2(tfac)_2] + [pip][Y(hfac)(tfac)_3] \quad 8$$

$$[pip][Y(hfac)(tfac)_2(\underline{tfac})] + [pip][Y(hfac)_2(tfac)_2] \rightleftarrows [pip][Y(hfac)(tfac)_3] + [pip][Y(hfac)_2(tfac)(\underline{tfac})] \quad 9$$

$$[pip][Y(hfac)(\underline{hfac})(tfac)_2] + [pip][Y(hfac)_3(tfac)] \rightleftarrows [pip][Y(hfac)_2(tfac)_2] + [pip][Y(hfac)_2(\underline{hfac})(tfac)] \quad 10$$

ligand from one complex can intermolecularly exchange a tfac ligand of another complex. In reaction 7, a hfac ligand in $[pip][Y(hfac)_3(tfac)]$ exchanges with a tfac ligand in $[pip][Y(hfac)(tfac)_3]$, the result of which is to shift a hfac ligand from $[pip][Y(hfac)_3(tfac)]$ to $[pip][Y(hfac)_2(tfac)_2]$, and a tfac ligand from $[pip][Y(hfac)(tfac)_3]$ to $[pip][Y(hfac)_2(tfac)_2]$. In the back reaction 7, a hfac and a tfac ligand exchange between the two $[pip][Y(hfac)_2(tfac)_2]$ resulting in a shift of a hfac from $[pip][Y(hfac)_2(tfac)_2]$ to $[pip][Y(hfac)_3(tfac)]$ and a tfac ligand from $[pip][Y(hfac)_2(tfac)_2]$ to $[pip][Y(hfac)(tfac)_3]$. This intermolecular exchange process should be observed as coalescence of the hfac methylene proton resonances, and coalescence of the tfac $-CH=$ resonances in all three complexes involved in reaction 7. If the separations between the resonances in the absence of exchange are equal and the ring proton resonances coalesce at the same temperature, then the rates

of exchange of hfac and tfac ligands are the same. In reaction 8, the hfac and tfac ligands exchange between [pip][Y(hfac)(tfac)$_3$] and [pip][Y(hfac)$_2$(tfac)$_2$], a process which should lead to coalescence of hfac and tfac -CH= proton resonances in these two complexes. Other reactions of this type which occur at the same time as reaction 7 and 8 exchange hfac and tfac ligands into [pip][Y(hfac)$_4$] and [pip][Y(tfac)$_4$], respectively. Thus exchange of ligands can occur amongst all possible sites.

The second type of ligand exchange (reactions 9 and 10) involves exchanging a hfac ligand of one complex with another hfac ligand of another complex, and exchanging tfac ligands also between two complexes. In reaction 9, the tfac ligand in [pip][Y(hfac)(tfac)$_3$]exchanges with a tfac ligand of [pip][Y(hfac)$_2$(tfac)$_2$], a process which should manifest itself in the coalescence of the tfac -CH= proton resonances. In reaction 10, the hfac in [pip][Y(hfac)$_2$-(tfac)$_2$] exchanges with a hfac ligand of [pip][Y(hfac)$_3$-(tfac)]; this process should be observed as a coalescence of the hfac methylene proton resonances of these two complexes. Relative rates of ligand exchange can be obtained from the temperature dependence of the methylene proton resonances (Figure 5).

Figure 5 reveals that at -58.0^o the [pip]-[Y(hfac)$_3$(tfac)] and [pip][Y(hfac)$_2$(tfac)$_2$] hexafluoro-acetylacetonate -CH= proton resonance separation is 8.9 Hz while the separation is 9.7 Hz for the trifluoroacetyl-

acetonate -CH= proton resonances of $[pip][Y(hfac)_2(tfac)_2]$ and $[pip][Y(hfac)(tfac)_3]$; at -16.0° the separation is 6.3 Hz (hfac) and 6.7 Hz (tfac). The coalescence temperatures of the -CH= proton resonances are -1.0° (hfac) and ca. 30° (tfac). These data and other hfac and tfac -CH= resonance separations, as well as the higher coalescence temperatures of tfac ring proton resonances (Figure 5), suggest that the hexafluoroacetylacetonate ligands intermolecularly exchange faster than the trifluoroacetylacetonate ligands. This is in contrast to reports (8) that in the $[(C_6H_5)_4As][Y(hfac)_4]$-$[(C_6H_5)_4As][Y(tfac)_4]$ system the two different ligands exchange at the same rate. In the $Hf(acac)_4$-$Hf(tfac)_4$ system the temperature dependence of certain line separations in the proton spectra indicated that whatever the mechanism of exchange, the acetylacetonate and trifluoroacetylacetonate ligands also exchange at the same rate (33).

The available data presented here do not afford speculations on a possible mechanism; however, the piperidinium cation probably plays an important role in any mechanism since the two reacting species are anionic.

3. Ligand Exchange Equilibria in $[pip][Y(hfac)_4]$-$[pip][Y(tfac)_4]$ System

Ligand exchange equilibria for the $[pip][Y(hfac)_4]$-$[pip][Y(tfac)_4]$ system (Type III exchange) have been quantitatively characterized in deuteriochloroform solution. To describe these ligand exchange equilibria three independent

equilibrium quotients defined by the reaction 11-13 must be specified:

$$[pip][Y(hfac)_4] + [pip][Y(hfac)_2(tfac)_2] \underset{}{\overset{K_1}{\rightleftharpoons}} 2[pip][Y(hfac)_3(tfac)] \quad 11$$

$$[pip][Y(hfac)_3(tfac)] + [pip][Y(hfac)(tfac)_3] \overset{K_2}{\rightleftharpoons} 2[pip][Y(hfac)_2(tfac)_2] \quad 12$$

$$[pip][Y(hfac)_2(tfac)_2] + [pip][Y(tfac)_4] \overset{K_3}{\rightleftharpoons} 2[pip][Y(hfac)(tfac)_3] \quad 13$$

Quotients K_2 and K_3 were computed from the relative intensities of the trifluoroacetylacetonate methylene proton resonances. Failure to observe the hexafluoroacetylacetonate -CH= resonance for $[pip][Y(hfac)_4]$ at values of mole fraction < 0.69 precluded calculation of K_1. In a more dilute solution (total solute concentration = 0.026 M) and at a mole fraction of 0.91, $[pip][Y(hfac)_4]$ is insufficently soluble in deuteriochloroform at temperatures below 0° to permit observation of the hfac ring proton resonance and thus calculation of the equilibrium quotient, K_1, of reaction 11.

The dependence of equilibrium molar fractions of total solute, defined by

$$f_{[pip][Y(hfac)_n(tfac)_{4-n}]} = \frac{[pip][Y(hfac)_n(tfac)_{4-n}]}{\sum_{n=0}^{4} [pip][Y(hfac)_n(tfac)_{4-n}]} \quad 14$$

on the molar fraction of total ligand as hfac, f_{hfac}, in deuteriochloroform solution at -58.0° (open circles), -37.5° (solid circles), and -16.0° (open rhombi) is presented in Figure 6. Statistical curves yielding computed values of $f_{[pip][Y(hfac)_n(tfac)_{4-n}]}$ assuming a completely random distribution of ligands are also included. These curves were calculated using the relation (6,34).

$$f_{[pip][Y(hfac)_n(tfac)_{4-n}]} = (f_{hfac})^n(1 - f_{hfac})^{4-n}\frac{4!}{n!(4-n)!}\frac{15}{}$$

Comparison of calculated and experimental curves indicates that the mixed complexes $[pip][Y(hfac)_n(tfac)_{4-n}]$ (n = 1, 2, 3) are favoured at the expense of the parent complexes (n = 0 and 4).

Values of the equilibrium quotients K_2 and K_3 are, within experimental error, independent of ligand composition, f_{hfac}, and total solute concentration. The data, reported in Tables IV and V, demonstrate that the values of K_2 and K_3 are 3 to 5 times larger than those expected assuming a random ligand distribution. The independence of K_2 and K_3 on ligand composition and total solute concentration suggests that the quotients of activity coefficients are constant in the range of concentrations used*.

---

* Although activity coefficients for the five complexes of reactions 11-13 are unknown, they are probably close in value since the complexes are very similar. Under these conditions, the quotient of activity coefficients will be close to unity and the equilibrium quotients will approximately equal the thermodynamic equilibrium constant.

Figure 6. - Equilibrium distribution of [pip][Y(hfac)$_n$-(tfac)$_{4-n}$] complexes as a function of molar fraction of total ligand in deuteriochloroform solution at -58.0° (open circles), -37.5° (closed circles), and -16.0° (open rhombi). Total solute molarity is 0.34 M. Solid lines, experimental curves (-37.5°); dashed lines, theoretical curves assuming a random distribution of ligands

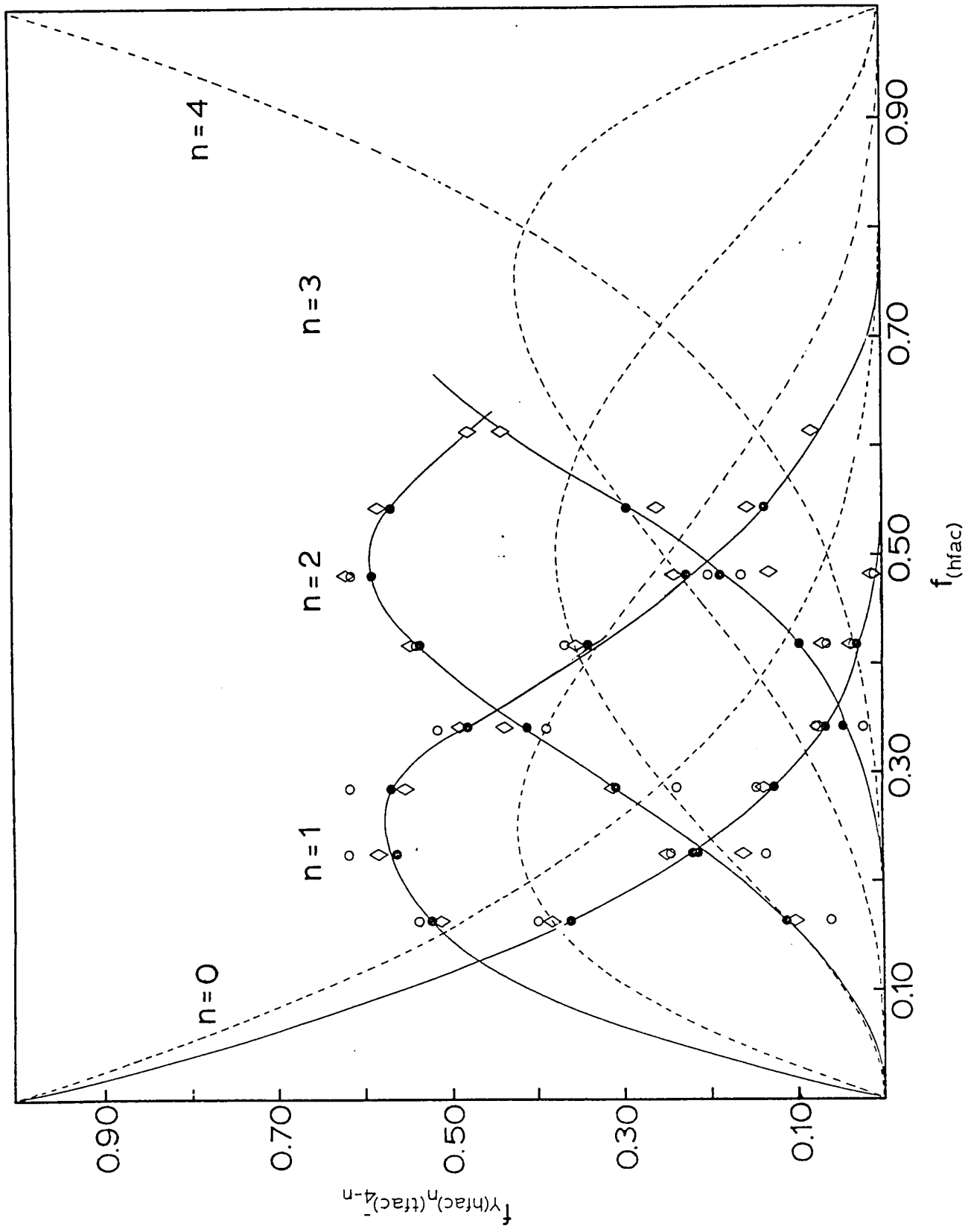
n=0
n=1
n=2
n=3
n=4
0.10
0.30
0.50
0.70
0.90
$f_{(hfac)}$
$f_{Y(hfac)_n(tfac)_{4-n}}$

Table IV.- Dependence of Equilibrium Quotients for the $[pip][Y(hfac)_4]$- $[pip][Y(tfac)_4]$ System on Solute Composition[a] at -16.0°

f_{hfac}	K_2[b]	K_3[b]
0.164	-	6.8 ± 0.3[c]
0.225	-	8.4 ± 1.6
0.286	-	7.2 ± 0.7
0.342	-	7.5 ± 0.4
0.418	-	7.1 ± 1.6
0.482	-	7.0 ± 1.4
0.544	8.4 ± 0.5	-
0.614	6.4 ± 0.4	-
Mean of all spectral measurements	7.4 ± 0.8	7.3 ± 0.3
Statistical equilibrium quotients	2.25	2.67

[a] Solvent is deuteriochloroform; total solute molarity is 0.34 M. [b] Average of five spectral measurements. [c] All errors are estimated at the 95% confidence level.

Table V.- Dependence of Equilibrium Quotients for the $[pip][Y(hfac)_4]$- $[pip][Y(tfac)_4]$ System on Total Solute Composition[a] at -60°

Total Molarity	K_2[b]	K_3[b]
0.342	11.9 ± 0.9[c]	8.4 ± 0.5
0.314	10.6[d] ± 3.2	6.8[d] ± 1.8
0.245	10.1 ± 0.9	7.8 ± 0.4
0.199	9.9 ± 1.1	7.8 ± 0.8
Mean of all spectral measurements	10.6 ± 0.6	7.8 ± 0.8
Statistical equilibrium quotients	2.25	2.67

[a] Deuteriochloroform solution; ± 2°; f_{hfac} = 0.418. [b] Average of five spectral measurements. [c] All errors are estimated at the 95% confidence level. [d] Average of three spectral measurements.

To investigate whether enthalpy or entropy changes are the driving force in these Type III ligand exchange reactions, the equilibrium quotients were studied as a function of temperature, data for which are presented in Table VI. Equilibrium in these ligand exchange reactions is established very rapidly within the time required for

Table VI.- Temperature Dependence of Equilibrium Quotients for the [pip][Y(hfac)$_4$]- [pip][Y(tfac)$_4$] System in Deuteriochloroform

Temperature, (^{o}C)	K_2[a]	K_3[a]
-58.0	11.4 ± 0.6[b]	10.4 ± 0.6
-50.5	9.5 ± 0.3	7.5 ± 0.4
-41.5	8.3[c] ± 0.7	6.7 ± 0.4
-37.5	8.2 ± 0.3	7.6 ± 0.4
-28.5	7.7 ± 0.8	6.5 ± 0.3
-16.0	7.4 ± 0.8	7.3 ± 0.3

[a] Mean of all spectralmeasurements; total solute molarity is 0.34 M. [b] All errors are estimated at the 95% confidence level. [c] Lit.,(35) 4.0 ± 0.5 at -40^{o}.

temperature equilibration of the sample (ca. 10 min) at the prevailing temperature of the nmr probe. In an experiment designed to test this, K_2 = 9.96 in fair agreement with the value of 10.6 ± 0.6 of Table V. Enthalpy and entropy changes at 25^{o} were calculated from the slope and intercept, respectively, of a plot of log K versus 1/T. The data of Table VI were treated by least-squares analysis including about 10-20 data points (K_2) and about 20-30 data points (K_3) at each temperature. These thermodynamic parameters, along with the free energy changes and the calculated entropy

changes assuming statistical behaviour, are summarized in Table VII.

Table VII.- Thermodynamic Data for the $[pip][Y(hfac)_4]$-$[pip][Y(tfac)_4]$ System in Deuteriochloroform Solution at 25°

Reaction	ΔH kcal/mole	ΔG kcal/mole	ΔS eu	Statistical ΔS eu
11	-	-	-	1.95
12	-1.14 ±0.27[a]	-0.95 ±0.48	-0.61 ±1.32	1.61
13	-0.79 ±0.22	-0.98 ±0.40	0.61 ±1.11	1.95

[a] All errors are estimated at the 95% confidence level.

Experimental entropy changes are less than statistical even at the upper 95% confidence limit, and are nearly zero or zero within experimental error. Deviations from statistical behaviour cannot be accounted for by these entropy changes. The important driving force in these Type III ligand exchange reactions is the exothermic enthalpy changes. It appears then that enthalpy changes can also effect deviations from statistical behaviour in ligand exchange reactions where values of equilibrium quotients are less than one order of magnitude larger than the expected statistical values. Further studies on other hfac-tfac systems should be carried out to verify this hypothesis.

It is also instructive to examine these ligand exchange equilibria in terms of thermodynamic parameters for the formation of mixed ligand complexes from the parent complexes (37-39) $[pip][Y(hfac)_4]$ and $[pip][Y(tfac)_4]$

according to reactions 16-18 (also see footnote in Section I, p 4).

$$\tfrac{3}{4}[pip][Y(hfac)_4] + \tfrac{1}{4}[pip][Y(tfac)_4] \xrightleftharpoons{K_{f1}} [pip][Y(hfac)_3(tfac)] \quad 16$$

$$\tfrac{1}{2}[pip][Y(hfac)_4] + \tfrac{1}{2}[pip][Y(tfac)_4] \xrightleftharpoons{K_{f2}} [pip][Y(hfac)_2(tfac)_2] \quad 17$$

$$\tfrac{1}{4}[pip][Y(hfac)_4] + \tfrac{3}{4}[pip][Y(tfac)_4] \xrightleftharpoons{K_{f3}} [pip][Y(hfac)(tfac)_3] \quad 18$$

where

$$K_{f1} = K_1^{\frac{3}{4}} K_2^{\frac{1}{2}} K_3^{\frac{1}{4}} = K_2^{\frac{1}{2}} K_3 \quad 19$$

$$K_{f2} = K_1^{\frac{1}{2}} K_2 K_3^{\frac{1}{2}} = K_2 K_3 \quad 20$$

$$K_{f3} = K_1^{\frac{1}{4}} K_2^{\frac{1}{2}} K_3^{\frac{3}{4}} = K_2^{\frac{1}{2}} K_3 \quad 21$$

assuming K_1 values parallel values of K_3. This is not an unreasonable assumption in view of reports on the $Zr(acac)_4$-$Zr(tfac)_4$ system (33,34) which indicate that the random distribution of acetylacetonate and trifluoroacetylacetonate ligands in the $Zr(tfac)_n(acac)_{4-n}$ complexes (n = 3, 4) closely parallels the random ligand distribution in the n = 1 and 0 complexes. Under these conditions, the values of the quotients K_3 (reaction 13) and K_1 (reaction 11) are also expected to be similar at the same temperatures.

Table VIII summarizes values of K_f, enthalpy, and entropy changes at 25° computed from least squares analysis of values of K_f at the different temperatures; a total of six data points were included in this analysis. Statistical

Table VIII.- Thermodynamic Data for the $[pip][Y(hfac)_4]$-$[pip][Y(tfac)_4]$ System in Deuteriochloroform Solution at 25°

Reaction	$10^{-1}K_f$	ΔH (kcal/mole)	ΔS (eu)	Statistical K_f	Statistical ΔS(eu)
16,18	1.18±0.71[a]	-1.4 ± 1.5	0.3±6.9	4.00	2.75
17	2.69±0.84	-1.9 ± 1.7	0.1±8.1	6.00	3.56

[a] All errors are estimated at the 95% confidence level.

values of K_f and entropy are also presented in Table VIII for comparison.

The equilibrium quotients of formation of the mixed ligand complexes at 25° are 3 to 5 times larger than statistical. These deviations from a completely statistical distribution of ligands cannot be ascribed to entropy changes since these are zero or nearly zero. Again, the small exothermic enthalpy changes are the prime driving force in these Type III exchange reactions.

In a related study on zirconium(IV) complexes, Pinnavaia, Mocella, Averill, and Woodward (39) observed that exchange in acac-bzbz and acac-β-isopropyltropolonate systems (Type I exchange) exhibits values of K_{fi} (see Appendix) which are slightly less than those expected for random exchange. However, in the exchange between acac and hfac on zirconium(IV) (Type II exchange), the mixed complexes were favoured over the parent complexes and K_{fi} values were 3 to 4 orders of magnitude larger than the statistical

values. Even larger values of K_{fi} were obtained for the mixed dpm-hfac complexes (39). Deviations from statistical scrambling in the $Zr(acac)_4$-$Zr(hfac)_4$ system were attributed mainly to enthalpy changes in the range -3.32 to -5.45 kcal/mole (39). In an earlier study (34,39) on the $Zr(acac)_4$-$Zr(tfac)_4$ system (Type III exchange), Pinnavaia and Fay (34) found values of K_{fi} at 25° to be 4 to 6 times greater than the statistical values, and in addition, deviations from random scrambling were attributed to entropy effects. Deviations of comparable magnitude on values of equilibrium quotients also have been reported for acac-tfac exchange on Hf(IV) (33,34), Th(IV) (34), and Ce(IV) (34).

Thus it appears that Type I exchange reactions yield values of K_{fi} equal to or slightly less than values expected for random scrambling, while deviation from randomness is ascribable to small enthalpy and/or entropy effects (39). Type II exchange reactions give values of K_{fi} which are about 10^2-10^5 times larger than statistical ; deviation from randomness is attributable to substantial exothermic enthalpy changes (-1.2 to -5.5 kcal/mole) and to entropies which are somewhat larger (1.5-4.8 eu) than values from random exchange (39). On the other hand, in Type III reactions values of K_{fi} are only slightly larger than statistical, while deviations from random exchange are due to entropy effects in one case [$Zr(acac)_4$-$Zr(tfac)_4$ system (34)] and to small enthalpy effects in the [pip][$Y(hfac)_4$]-[pip][$Y(tfac)_4$] system.

In a recent review, Fay (6) has pointed out that when ligands differ in electronic structure, equilibrium quotients for formation of mixed complexes will probably be appreciably larger than statistical. In addition, electrostatic effects may also contribute to the stability of mixed complexes when these contain both fluorinated and non-fluorinated diketonate ligands because the inductive effect of the fluorine atoms causes the charges on the donor oxygen atoms to differ. In the present system studied here, there is a fluorinated [$CF_3COCHCOCF_3^-$] and a partially fluorinated [$CF_3COCHCOCH_3^-$] diketonate ligand. Using a point charge model, the stabilization energy for the dodecahedral (18) [pip][$Y(hfac)_2(tfac)_2$] mixed complex relative to the parent complexes is given by $(e' - e")^2/r$ (69), where (e' - e") is the difference in charge between the donor oxygen atoms of hfac and tfac ligands, and r (= 2.32 Å) is the yttrium-oxygen (18) distance. To attain a stabilization energy of 1 kcal/mole the difference in charge between the donor atoms need only be ca. 0.08 electron charge units. Although electrostatic effects may have some stabilizing influence on the mixed complexes, especially [pip][$Y(hfac)_2(tfac)_2$], the enthalpy changes cannot be solely attributed to these effects.

Preferential solvation of the mixed complexes by deuteriochloroform over the parent complexes can also contribute to the stability of the mixed species. Figure 5, for example, reveals that the resonances of the trifluoro-

acetylacetonate -CH= protons are shifted markedly to low-field with decreasing temperature (see below) suggesting increased solvent-solute interactions preferentially at the tfac ends of the mixed species. This increased solvation at the lower temperatures stabilizes the mixed ligand complexes. Although enthalpies and entropies of solvation for these $[pip][Y(hfac)_n(tfac)_{4-n}]$ complexes in deuterio-chloroform are unknown, it appears that the former make some contribution to the ΔH of the ligand exchange reactions [cf. $Zr(acac)_4$-$Zr(tfac)_4$ system (34), and $Ga(acac)_3$-$Ga(bzbz)_3$ and $Ga(acac)_3$-$Ga(hfac)_3$ systems (37)].

In a study to test the importance of electrostatic effects versus solvation enthalpy effects, Pinnavaia and coworkers (39) very astutely investigated the $Al(acac)_3$-$Al(hfac)_3$ system in solvents with a dielectric constant ranging from 2.2 to 34.8. No appreciable solvent dependence was observed for the exchange enthalpies (-1.39 to 1.98 kcal/mole). It was therefore speculated (39) that although solvation effects may contribute to the somewhat larger than statistical values of ΔH for Type II exchange reactions, non-additive bond energies probably play a greater role in deciding the magnitudes of the enthalpy changes.

4. Proton Chemical Shifts

It has been shown previously (32) that the charge on a cationic or anionic β-diketonate complex gives rise to an electric field which will alter the chemical shifts of the proton resonances. The chemical shift $\Delta\sigma$ due to the

electric field is given theoretically by the relation(70,71)

$$\Delta\sigma = -2.9 \times 10^{-12} E_z - 7.38 \times 10^{-19} E^2 \qquad 22$$

where E_z is the electric field component along the C-H bond direction, and E is the absolute magnitude of the electric field, both evaluated at the proton. The electric field at the -CH= proton is given by $\underset{\sim}{E} = q \underset{\sim}{r} / r^3$ where q is the charge on the ion, $\underset{\sim}{r}$ is the vector extending from the metal to the proton, and r is the metal-proton distance. To estimate $\Delta\sigma$ for $[Y(bzbz)_4]^-$ and $[Y(hfac)_4]^-$ the same model as that reported earlier (32) was used; the bond lengths and bond angles were obtained from recent X-ray structural data (18) on $Cs[Y(hfac)_4]$. Bond distances and bond angles were taken equal to the average of the values reported by Bennett and coworkers (18). Bond distances are: Y-O, 2.323 Å; $O-C_1$, 1.263 Å; C_1-C_2, 1.386 Å; C_2-H, 1.084 Å the distance in benzene. Bond angles are: O-Y-O, 73.2°; $Y-O-C_1$, 134.9°; $O-C_1-C_2$, 127.5°; $C_1-C_2-C_3$, 121°.

Calculated and observed chemical shifts are listed in Table IX wherein the $[Y(hfac)_4]^-$ -CH= proton shifts are compared with the methylene proton chemical shifts of hexafluoroacetylacetone, and the chemical shifts of the ring proton resonance of $[Y(bzbz)_4]^-$ with those of dibenzoylmethane and $Al(bzbz)_3$ (-6.86 ± 0.05 ppm) (72), in addition, those shifts of $[M(bzac)_4]^-$ and $[M(tfac)_4]^-$ where M is Y(III) or La(III) are also given. Comparison of calculated and observed values of $\Delta\sigma$ reveals that the

Table IX.- Chemical Shifts of β-Diketonate Compounds in Deuteriochloroform at 37°

Complex	$\delta_{-CH=}$ (ppm)	Δσ (ppm) calcd	Δσ (ppm) obsd	Ref
$[Y(hfac)_4]^{-a}$	-6.11[b] (-6.10)[c]	0.56	0.28	this work
Hhfac	-6.39[d]	-	-	this work
$[Y(bzbz)_4]^{a}$	-6.57	0.56	0.29	this work
Hbzbz	-6.82	-	-	72
$Al(bzbz)_3$	-6.91	-	-	72
$[Y(bzaz)_4]^{-a}$	-6.02	0.56	0.20	32
$[La(bzac)_4]^{-e}$	-5.91	0.50	0.31	32
$Al(bzac)_3$	-6.22	-	-	73
$[Y(tfac)_4]^{-a}$	-5.63	0.56	0.34	32
$[La(tfac)_4]^{-e}$	-5.64	0.50	0.33	32
$M(tfac)_n$[f]	-5.97[g]	-	-	34,74

[a] r is 4.88 Å; E is -2.02×10^5 statcoul/cm; E_z is -2.02×10^5 statcoul/cm. [b] ±0.01 ppm; against an internal standard reference of tetramethylsilane; saturated solution. [c] Saturated solution in carbon tetrachloride. [d] Temperature is ca. 27°. [e] r is 5.14 Å; E and E_z are -1.82×10^5 statcoul/cm. [f] Mean chemical shift for nine neutral metal trifluoroacetylacetonates; n = 3 or 4. [g] ± 0.07 ppm.

electric field model predicts the correct sign of Δσ and that this model overestimates the values of Δσ by about 50%. This overestimation is not unreasonable in view of the crudeness of the model used in these calculations which places the negative charge at the central metal ion (32). The general effects of these electric fields on the proton

resonances of anionic β-diketonate complexes are to shift proton resonances upfield relative to resonance signals of analogous neutral β-diketonate compounds.

It was implied earlier, and shown in Figure 5, that ring proton resonances of $[pip][Y(hfac)_n(tfac)_{4-n}]$ complexes are temperature dependent. The dependence of -CH= proton chemical shifts (tabulated in Table X) on temperature is pictured in Figure 7 which also shows the temperature dependent ring proton frequencies of $Co(acac)_3$ and $Ti(acac)_2Br_2$ in dichloromethane (75). Evidently, proton nmr frequencies shift downfield with decreasing temperature, a trend which appears to be general for β-diketonate complexes and which has been attributed to increased solvent-solute interaction via hydrogen bonding (35) at the lower temperatures (75). The greater temperature dependence of the tfac proton frequencies of $[pip][Y(hfac)_2(tfac)_2]$ allows the tfac ring proton resonance of $[pip][Y(hfac)_3(tfac)]$ to be observed at the higher temperatures. It is also apparent that the temperature dependence of the trifluoroacetylacetonate proton resonances is more pronounced than that of the hexafluoroacetylacetonate ligands. This would imply that solvent-solute interactions are more effective at the tfac ends of the complexes. This view is supported by chemical shift data in deuteriochloroform and in an "inert" solvent such as carbon tetrachloride. The hexafluoroacetylacetonate ring proton frequencies of $[pip][Y(hfac)_4]$ are -6.11 ppm

Table X.- Temperature Dependence of the -CH= Proton Chemical Shifts for the [pip][Y(hfac)$_4$]-[pip][Y(tfac)$_4$] System

Temp., °C	δ [a] (ppm)							
	(hfac)$_4$	(hfac)$_3$	(hfac)$_2$	(hfac)	(tfac)	(tfac)$_2$	(tfac)$_3$	(tfac)$_4$
-58.0	-	-6.070	-5.985	-5.923	(-5.877)	-5.877	-5.873	-5.717
-50.5	-	-6.056	-5.977	-5.917	(-5.850)	-5.850	-5.764	-5.696
-41.5	-	-6.067	-5.983	-5.922	(-5.845)	-5.845	-5.762	-5.698
-37.5	-	-6.053	-5.976	-5.914	(-5.827)	-5.827	-5.751	-5.677
-28.5	-	-6.036	-5.965	-5.900	-5.820	-5.793	-5.726	-5.656
-16.0	-	-6.033	-5.958	-5.898	-5.817	-5.780	-5.716	-5.648
-1.0	-	-6.025	-5.966	-	-5.807	-5.763	-5.704	-5.625
16.0	-	-6.013	-5.960	-	-	-5.760	-5.705	-
27	-6.120[b]	-	-	-	-	-	-	-5.63[c]

[a] In deuteriochloroform solution; against an internal standard reference of tetramethylsilane (10% v/v); ± 0.003 ppm. [b] δ of -CH= proton of [pip][Y(hfac)$_4$] in deuteriochloroform. [c] Temperature is 37° (ref 32).

Figure 7.- Variable temperature chemical shifts in deuteriochloroform solution of the ring proton resonances of: (a) $Co(acac)_3$ in dichloromethane (75); (b) [pip][Y(tfac)$_4$]; (c) [pip][Y(hfac)-(tfac)$_3$]; (d) [pip][Y(hfac)$_2$(tfac)$_2$]; (e) [pip]-[Y(hfac)$_3$(tfac)]; (f) [pip][Y(hfac)(tfac)$_3$]; (g) [pip][Y(hfac)$_2$(tfac)$_2$]; (h) [pip][Y(hfac)$_3$-(tfac)]; (i) $Ti(acac)_2Br_2$ in dichloromethane (75); (j) pure sample of [pip][Y(tfac)$_4$]; (k) pure sample of [pip][Y(hfac)$_4$].

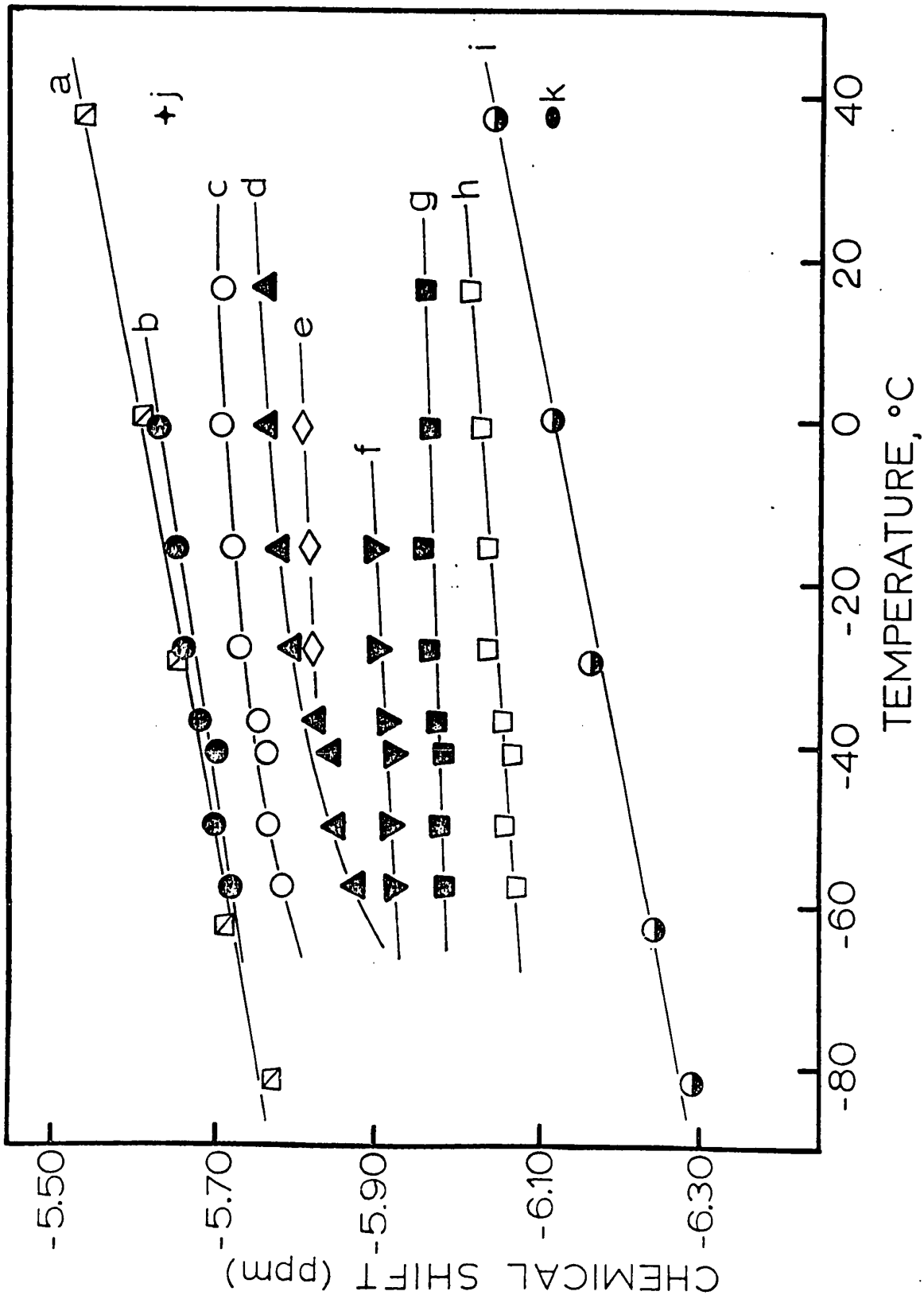
a
b
c
d
e
f
g
h
i
j
k
-5.50
-5.70
-5.90
-6.10
-6.30
CHEMICAL SHIFT (ppm)
-80
-60
-40
-20
0
20
40
TEMPERATURE, °C

($CDCl_3$) and -6.10 ppm (CCl_4); the trifluoroacetylacetonate -CH= proton chemical shifts of [pip][Y(tfac)$_4$] are -5.63 ppm ($CDCl_3$) (32) and -5.57 ppm (CCl_4).

For an assumed 1:1 complex, for example between a Y(tfac) ring and $CDCl_3$, Abraham (76) has put forth a method by which the equilibrium constant K for the reaction solvent + solute $\rightleftarrows$ complex, and the enthalpy and entropy of formation can be evaluated from the temperature dependent chemical shift data. If f is the fraction of complexed solute, the equilibrium constant is given by

$$K = \frac{f}{1 - f} = \exp\left(\frac{-\Delta H^o}{RT}\right) \exp\left(\frac{\Delta S^o}{R}\right) \qquad 23$$

The value of f at any temperature is taken equal to $(\delta_t - \delta_o)/(\delta_c - \delta_o)$ where δ_t and δ_c are the observed chemical shifts at temperature t, and the proton resonance frequency in the pure complex at 0^oK, respectively; the proton chemical shift in an "inert" solvent such as carbon tetrachloride is taken to give δ_o. From the slope of a plot of log K against 1/T, the enthalpy of complex formation can be estimated. To calculate these thermodynamic parameters, the temperature dependent ring proton frequencies (δ_t) of [pip][Y(tfac)$_4$]* in the equilibrium mixture (Figure 7) were

*It would have been useful to perform similar calculations for the mixed complexes [pip][Y(hfac)$_n$(tfac)$_{4-n}$] (n = 1, 2, or 3) and for [pip][Y(hfac)$_4$] in order to obtain a quantitative estimate of the solvent effect (in terms of ΔH of complex formation) on these compounds. Unfortunately, a value of δ_o cannot be obtained for the mixed complexes because these cannot be isolated, and for the parent complex [pip][Y(hfac)4] because the -CH= resonance of this compound was not observed (cf. Figure 3 and 4).

used to get δ_c (-6.057 ppm); δ_o was taken as -5.570 ppm, the chemical shift of [pip][Y(tfac)$_4$] -CH= resonance in carbon tetrachloride. The data are tabulated in Table XI. The intercept and the slope of the log K versus 1/T plot (Figure 8) produced an entropy of formation of -12.9 ±2.5 eu and an enthalpy of formation of -2.5 ± 0.6 kcal/mole, a value similar to the value of -2.7 ± 0.5 kcal/mole reported for a 1:1 complex between chloroform and acetone (77), in which complex formation occurs via hydrogen bonding between the $CHCl_3$ proton and the carbonyl oxygen of acetone. It is tempting to suggest that hydrogen bonding occurs between $CDCl_3$ deuterium and the carbonyl oxygen atoms of the β-diketonate ligand in these metal diketonate complexes (46,78). However, the values of entropy and enthalpy of formation should be taken with caution in view of the assumptions (76) for and the criticisms (79) of this model.

The two main assumptions made in Abraham's model are that (1) the temperature dependence of the chemical shifts is not an intramolecular effect but is one of association, and (2) that there is a 1:1 stoicheiometry in this association. An additional assumption was made in this work that the 1:1 stoicheiometry prevails between one Y(tfac) heterochelate ring (the solute) and $CDCl_3$ (the solvent). The low solubility of [pip][Y(tfac)$_4$] in carbon tetrachloride precluded experiments to verify the validity of assumption (1). Two further assumptions, implicit in the model, which have been criticized (79) concern δ_o and δ_c. The concentration

Table XI.- Chemical Shift Data of tfac -CH= Proton Resonances for the $[Y(tfac)_4]^-$ Anion in the Mixture $[pip][Y(hfac)_4]$-$[pip][Y(tfac)_4]$[a]

Temp., [b] °C	1/T x 10^3	δ_t [c] (ppm)	$\lvert\delta_t-\delta_o\rvert$ [d] (ppm)	$\lvert\delta_c-\delta_o\rvert$ [d] (ppm)	f	1-f	K	log K
-58.0	4.65	-5.717	0.147	0.487	0.302	0.698	0.433	-0.3638
-50.5	4.49	-5.696	0.126	0.487	0.259	0.741	0.349	-0.4565
-41.5	4.32	-5.698	0.128	0.487	0.263	0.737	0.357	-0.4475
-37.5	4.24	-5.677	0.107	0.487	0.220	0.780	0.282	-0.5497
-28.5	4.09	-5.656	0.086	0.487	0.177	0.823	0.215	-0.6674
-16.0	3.89	-5.648	0.078	0.487	0.160	0.840	0.190	-0.7202
-1.0	3.67	-5.625	0.055	0.487	0.113	0.887	0.127	-0.8948

[a] For the meaning of symbols used, see text. [b] Varian temperatures, ± 1.0. [c] Average of the chemical shifts for different mole fraction of $[pip][Y(hfac)_4]$; with respect to an internal standard of tetramethylsilane 10% v/v. [d] δ_o = -5.570 ppm, chemical shift of -CH= protons of $[pip][Y(tfac)_4]$ in CCl_4; δ_c = -6.057 ppm, the extrapolated chemical shift of $[pip][Y(tfac)_4]$ -CH= protons at 0^oK.

Figure 8.- Plot of log K *versus* $1/T \times 10^3$ for the equilibrium constants of the *solvent* + *solute* $\rightleftarrows$ *complex* reaction.

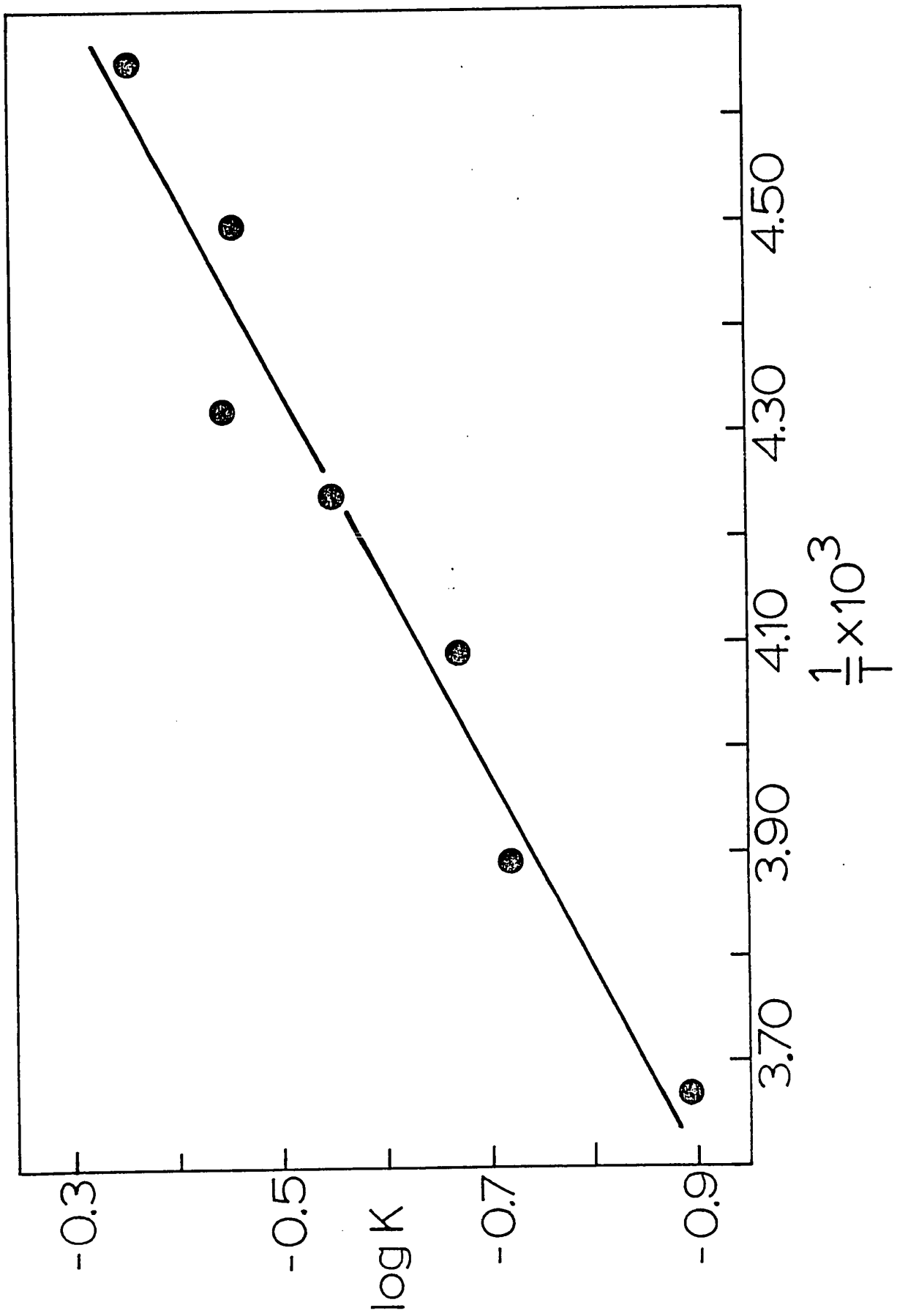
-0.3
-0.5
-0.7
-0.9
log K
3.70
3.90
4.10
4.30
4.50
1/T x10^3

dependence of the chemical shift in the "inert" solvent makes it necessary to use 1-2 mole % solutions (79), and to check that in this concentration range the dilution shift is less than the error in the extrapolation of δ_t at $0^{\circ}K$. The error in the extrapolation is ±0.039 ppm (one standard deviation). Once again, the low solubility of [pip]-[$Y(tfac)_4$] in carbon tetrachloride precluded experiments on the concentration dependence of the -CH= proton chemical shift. However, for the isoelectronic $Zr(tfac)_4$ complex, concentration dependence studies (80) reveal a dilution shift of only 0.01 ppm for the -CH= proton resonance in chloroform and in benzene (solvents which can cause solvent induced shifts; cf. ref 79) in the 0.2-1.2 mole % range. For [pip][$Y(tfac)_4$] the following chemical shifts in $CDCl_3$ were observed for the -CH= ring proton: δ -5.62 ppm (concentration is 9.53 g/100 ml), -5.63 ppm (8.90 g/100 ml), -5.62 ppm (6.08 g/100 ml), -5.63 ppm (4.04 g/100 ml), and -5.62 ppm (2.12 g/100 ml); hence a dilution shift of $\leq$0.01 ppm is also observed for this compound in the 0.2-1 mole % range. If anything, dilution shifts would be expected to be $<$ 0.01 ppm in an inert solvent. As for the extrapolated shift δ_c in the pure complex, the good straight line obtained is shown in Figure 7(b). The value of -2.5 ± 0.6 kcal/mole for the enthalpy of formation is to be regarded only as an order of magnitude, since there may well be several possible perturbing phenomena as for example the simultaneous occurrence of 1:1, 1:2, etc...., complexes.

In addition, there may also be temperature shifts associated with dispersion (Van der Waals type) forces which may be unequal for the tetramethylsilane reference and the temperature dependent resonances followed. The interactions are in any event very weak. Also, from the extrapolated equilibrium constant (ca. 0.05 M^{-1} at 25°) it is seen that only a minority of molecules is complexed at ambient temperatures. Finally, it may well be that the enthalpy of formation does not reflect a 1:1 complex formation but may instead indicate a much looser, more long range type of interaction (79,81).

B. Kinetics of Ligand Exchange

1. Introduction

Ever since the pioneering work of Gutowsky and coworkers, the nuclear magnetic resonance technique has proven to be of great value in studies of numerous rapid inter- and intramolecular exchange processes in both organic and inorganic complexes. Although the nmr techniques have been very effective in studies of intramolecular configurational rearrangement phenomena (1) in transition metal and organometallic complexes, little attention has been given to these techniques, except until recently (82), to systems involving intermolecular exchange processes. Where it can be applied, nuclear magnetic resonance can prove to be a powerful tool indeed in observing kinetics of intermolecular ligand exchange particularly, as

is the case in this work, in organometallic systems. There are three principal advantages to be had with the nuclear magnetic resonance method: (a) it can be used to follow the kinetics of exchange reactions which are too fast for conventional kinetic techniques; (b) it permits the study of systems which are in a state of chemical equilibrium; and (c) because the system can be studied at variable temperature while it is enclosed in a sealed sample nmr tube - systems which are thermally unstable and/or reactive towards oxygen and water can be studied. Furthermore, in studies of intermolecular ligand exchange reactions, the relative populations of the sites between which exchange occurs can be varied so as to provide data from which an expression for the rate equation can be deduced for the particular system under investigation. This is in contrast to studies of intramolecular exchange processes where the relative populations at the sites undergoing exchange are usually fixed by the system. For the $(C_6H_5)_2Sn(acac)_2$-$(CH_3)_2Sn(acac)_2$ system studied in this work, advantage was taken of concentration dependent rates to obtain a rate expression for the exchange process.

In general, the nuclear magnetic resonance experiment can provide access to the mean lifetime, τ_i, of an absorbing nucleus at the site giving rise to the ith resonance absorption (83). The reciprocal of the mean lifetime, $1/\tau_i$, is the first-order rate constant for transfer of the resonating nucleus out of the ith site.

Several methods (53,84,85) have been put foward to determine the quantity $1/\tau_i$ from the experimental line-shape data. For the case of an uncoupled two-site exchange system, as is the case here, one such method involves calculating the over-all line shape as a function of τ. This method will be presently described.

2. Total Line-Shape Method

A reliable method for evaluating exchange rates from the nmr spectral data consists in matching the observed spectra with a series of calculated spectra in which the exchange rate is varied. In the system under investigation it is possible to assign values of $1/T_2$, $\delta\omega$, P_A, and P_B at each temperature, and thus to calculate a realistic line shape as a function of the exchange rate. The line-shape function is given (86) by suitable modifications of the Block phenomenological equations as developed by Gutowsky and Holm (55), but retaining terms involving the transverse relaxation times.

$$v = \frac{\left(P\left[1+\tau\left(\frac{P_B}{T_{2A}}+\frac{P_A}{T_{2B}}\right)\right] + Q\left[R+\tau\left(\frac{1}{T_{2B}}-\frac{1}{T_{2A}}\right)\frac{\delta\omega}{2}\right]\right)\omega_1 M_0}{P^2 + R^2 + \tau^2\left(\frac{1}{T_{2B}}-\frac{1}{T_{2A}}\right)^2\left(\frac{\delta\omega}{2}\right)^2 + 2R\left(\frac{1}{T_{2B}}-\frac{1}{T_{2A}}\right)\frac{\delta\omega}{2}} \quad 24$$

where

$$P = \tau\left[\frac{1}{T_{2A}T_{2B}} - \Delta\omega^2 + \left(\frac{\Delta\omega}{2}\right)^2\right] + \frac{P_A}{T_{2A}} + \frac{P_B}{T_{2B}}$$

$$Q = \tau\left[\Delta\omega - \frac{\delta\omega}{2}\quad (P_A - P_B)\right]$$

$$R = \Delta\omega\left[1 + \frac{\tau}{T_{2A}} + \frac{\tau}{T_{2B}}\right] + \frac{\delta\omega}{2}\ (P_A - P_B)$$

and $\tau = \dfrac{\tau_A \tau_B}{\tau_A + \tau_B}$ 25

The notations employed in these expressions have their usual denotations: v, the transverse component of the resultant magnetic moment perpendicular to the rotating field H_1, which is proportional to the absorption intensity; ω_1, the applied rotating radiofrequency field; $\Delta\omega$, the difference in frequencies (radians/sec) of the applied radiofrequency and the frequency center of the two resonance components; $\delta\omega$, the difference of the resonance frequencies (radians/sec) corresponding to the states A and B; τ_A and τ_B the mean lifetimes for a stay on A and B sites; P_A and P_B, the fractional populations of A and B sites; T_2, the transverse relaxation times in the absence of exchange; M_0, the equilibrium value of the z component of the resultant magnetic moment.

A Fortran program has been written (87) to compute a normalized lineshape function over the frequency range of interest, for a given set of input parameters. The modified version (88) of this program requires as input parameters for each temperature a value of $\pi\delta\nu$ where $\delta\nu$ is the chemical

shift separation (in Hz) in the absence of exchange between the two resonance components of the exchanging system, a value for the fractional population at sites A and B, viz., P_A and P_B, and a value for T_{2A} and T_{2B} [$=1/\pi$ (linewidth)], the transverse relaxation times at sites A and B in the absence of exchange. For the system $(C_6H_5)_2Sn(acac)_2$-$(CH_3)_2Sn(acac)_2$ under study, values for P_A and P_B can be obtained experimentally by making up an equimolar concentrated solution; for T_{2A} and T_{2B}, the full linewidth (in the absence of exchange) at one-half maximum amplitude can be obtained from spectra of the pure components. However, since linewidths of $(CH_3)_2Sn(acac)_2$ were used for the intramolecular exchange studies on $(C_6H_5)_2Sn(acac)_2$ (44), these were used for the intermolecular ligand exchange studies reported here. The linewidths have been summarized in Table III and plotted as a function of temperature in Figure 1. Finally, $\delta\nu$ in the absence of exchange can be obtained from the very slow exchange limit or from a plot (89) of $\delta\nu$ vs temperature in which the linear portion in the slow exchange region is extrapolated in the intermediate and fast exchange regions. Early investigators of restricted rotation in N,N-disubstituted amides often assumed that $\delta\nu$ remained constant throughout the exchange region. This assumption resulted in serious systematic errors in the activation energy (53), since $\delta\nu$ often varies with temperature because of changes in the degree of molecular association (90).

Values of the chemical shift separations, $\delta\nu_e$, during exchange are tabulated in Table XII and plotted as a function of temperature in Figure 9 for both deuteriochloroform and bromoform solutions. Inspection of Figure 9 indicates that the slow exchange region was not attained - this precluded acquisition of $\delta\nu$ values in the absence of exchange, thus precluding the use of the computer program (87,88) to obtain mean lifetimes for the exchange process.

Table XII.- Temperature Dependence of the CH_3 Proton Resonance Separation in a Mixture of $(C_6H_5)_2Sn(acac)_2$ and $(CH_3)_2Sn(acac)_2$ in Deuteriochloroform and Bromoform

Temp., (^oC)	$\delta\nu$, (Hz)	Temp., (^oC)	$\delta\nu$, Hz)
		20	(3.41)
-23.5	3.07 ± 0.04	36	3.21 ± 0.04
-15	2.97 ± 0.05	42	3.21 ± 0.03
- 6	2.92 ± 0.07	51	3.10 ± 0.04
- 1	2.75 ± 0.04	57	3.07 ± 0.04
7.5	2.66 ± 0.06	64	2.91 ± 0.05
17.5	2.28 ± 0.06	68	2.83 ± 0.07
20	2.22 ± 0.09	75	2.65 ± 0.06
30	2.02 ± 0.14	83	2.40 ± 0.04
32.5	1.38 ± 0.03	87.5	2.22 ± 0.04
		92	2.07 ± 0.07
		94.5	1.85 ± 0.03
		99	1.61 ± 0.05

Figure 9.- Temperature dependence of the methyl nmr resonance peak separations in the ligand exchange reaction between $(C_6H_5)_2Sn(acac)_2$ and $(CH_3)_2Sn(acac)_2$.

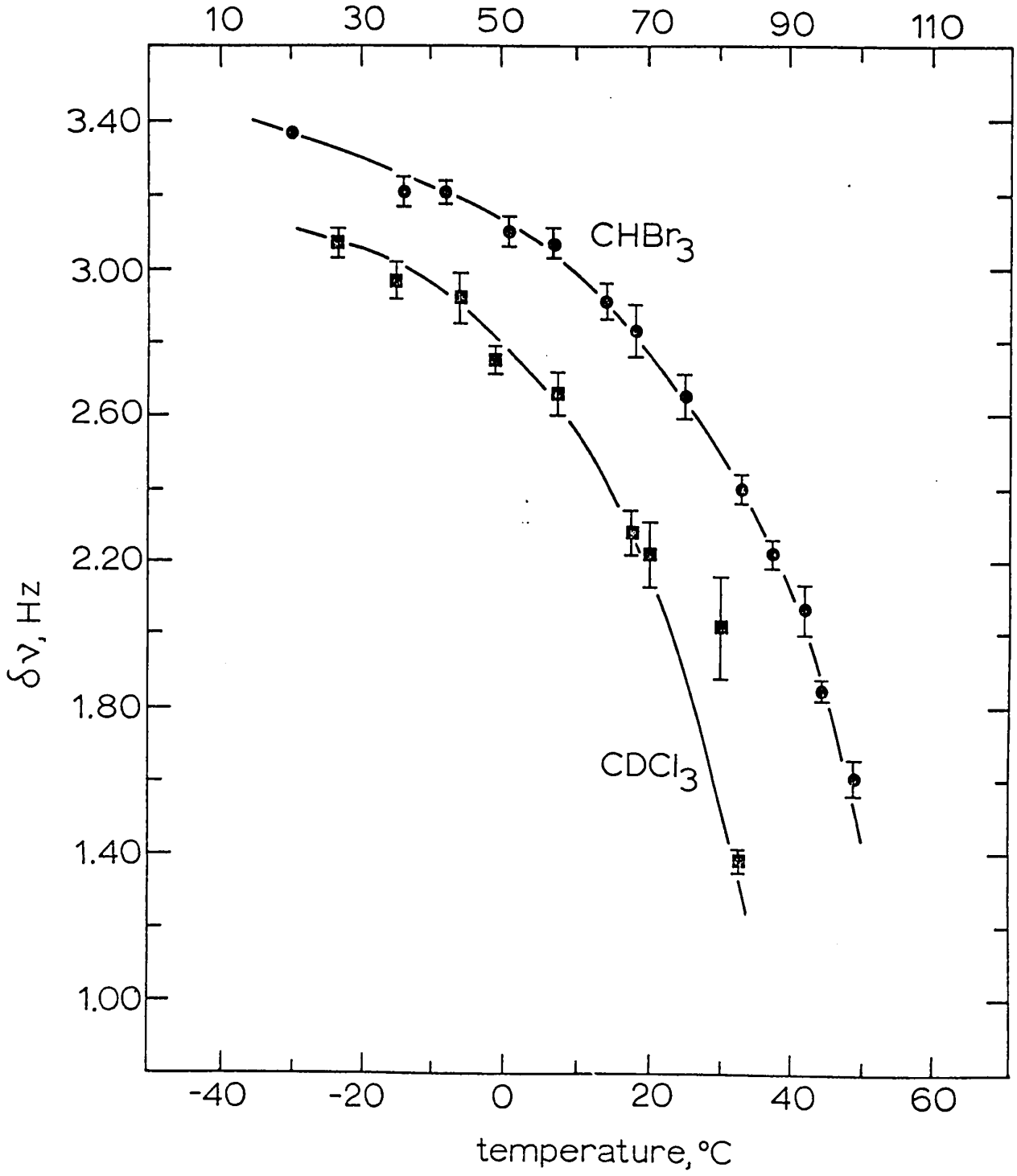
10
30
50
70
90
110
3.40
3.00
2.60
2.20
1.80
1.40
1.00
δν, Hz
CHBr3
CDCl3
-40
-20
0
20
40
60
temperature, °C

3. Approximate Methods

Although the model chosen for an uncoupled two-site exchange process may be appropriate, problems can still arise in its application to the data for the exchanging system because line-shape equations derived from such a model might be sufficiently complicated that a computer is required to extract the exchange rates. Thus it would be useful to have equations which relate some readily calculated parameters to those of the experimental spectrum. Even such equations might still require use of a computer, however. Therefore what is needed is to reduce these complicated equations to simpler ones by making some appropriate approximations. The accuracy of such approximations depends upon the relative values of the exchange rates $1/2\tau$ (or $1/\tau a$) as compared to values of the chemical shift separation, $\delta\nu$, and the natural (full) linewidth $1/\pi T_2^{o}$ in the absence of exchange. Neglect of such dependence may well lead to appreciable, systematic errors in the kinetic data (53). In using approximate equations, the range of their validity should be understood and tested numerically for the case under study. In addition, the validity of the equations should never be exceeded beyond their usefulness.

For an equally populated uncoupled two-site exchange, approximate equations result (53) if

$$1/\tau \text{ and } \delta\nu >> (1/\pi T_2'') \equiv W'' \qquad 26$$

where

$$\frac{1}{T_2''} = \frac{1}{T_2^{o}} + \frac{1}{T_2'} \qquad 27$$

and $1/T_2'$ represents contributions to W", the effective full linewidth in the absence of exchange, from inhomogeneity, instability, and other such instrumental limitations (cf. Section II C 2). Conditions of equation 26 on the exchange rates can be met (53) for many systems by careful adjustment of the temperature and/or concentrations of the reactants; the chemical shift separation, however, is less adjustable, control being limited to solvent effects and increasing the magnetic field (53). For very small chemical shifts, as may probably be the case in the presently investigated system, the approximate equations may not be valid. In cases where they have failed, graphical methods have been employed to extract exchange rates (55,91,92). Nevertheless, it is instructive to test for the present case these approximate equations.

a) Below Coalescence

Under conditions of slow exchange, where exchange rates are too slow to coalesce the AB doublet to a single resonance line, the experimentally observed resonance peak separation $\delta\nu_e$ (in Hz) has been used (55) in the following approximation

$$\frac{1}{2\tau} = \frac{1}{\tau_A} = \frac{\pi}{\sqrt{2}}\left(\delta\nu_o^{\,2} - \delta\nu_e^{\,2}\right)^{\frac{1}{2}} \qquad 28$$

where $\delta\nu_o$ is the peak separation in the absence of exchange. As has already been pointed out by Gutowsky and Holm (55), the major change in peak separation with exchange rate

occurs over a rather narrow range, $0.45 \leq 2\tau\delta\nu_o \leq 2$; and $\delta\nu_e$ becomes decreasingly sensitive to rate for slower rates - that is, for $2\tau\delta\nu > 2$ (53). At very slow rates, the errors in determining $\delta\nu_e$ may well exceed the errors involved in using equation 28; in this case, both types of errors become comparable to the exchange rate itself (55,93) and the peak separation should then not be used under these conditions (53). It has also been shown (53) that the effect of T_2^o on the percent error for a particular pair of $\delta\nu$ and $1/2\tau$ values is inversely proportional to $\delta\nu$- that is, the percent error increases the smaller the values of $\delta\nu$. In a theoretical treatment to test the validity and to find the magnitude of errors, Allerhand and coworkers (53) contend that the error introduced in $1/2\tau$ values obtained from equation 28 does not exceed 10% in systems for which $2\tau\delta\nu \leq 5$. It should be pointed out, however, that in the theoretical calculations, instrumental broadening of the resonance lines was neglected. Inclusion of such broadening effects which are not negligible, especially when $\delta\nu_e$ are small, would yield a higher percent error in exchange rates. On the other hand, use of the complete line-shape numerical methods will minimize errors in $1/2\tau$ because these generally include the instrumental broadening as a convolution function. Another possible source of error in equation 28 is the narrow temperature range accessible for some systems so that systematic errors in the exchange rates and/or temperatures can produce quite large

errors in the apparent enthalpy and entropy of activation.

b) At Coalescence

When the fractional populations on sites A and B are the same, $P_A = P_B$, and when equation 26 holds, the exchange rate at the coalescence temperature T_c is given (55) by

$$\frac{1}{2\tau} = \frac{\pi\delta\nu_o}{\sqrt{2}} \qquad 29$$

c) Above Coalescence

Because of the narrow temperature range generally accessible below coalescence, it is desirable, in fact it is essential to extend this range so as to minimize the errors discussed above. To do so requires an analysis of the line-shape above the coalescence temperature T_c, where only a single resonance line is observed. The parameter most likely to be used is the observed linewidths W* of the resonance line at one-half maximum amplitude.

$$W^* = \frac{1}{\pi T_2^*} = \left(\frac{1}{\pi T_2}\right)_{exch.} + \frac{1}{\pi T_2''} \qquad 30$$

where $(1/\pi T_2)_{exch}$ is the exchange contribution to the linewidth. For the uncoupled two-site exchange model, Piette and Anderson (94) have derived the relationship

$$\frac{1}{2\tau} = \frac{1}{\tau_A} = \frac{2\pi P_A P_B (\delta\nu_o)^2}{(W^* - W'')} \qquad 31$$

where W" has been defined by equations 26 and 27 as the effective linewidth in the absence of exchange. Equation 31 holds under conditions of very fast exchange - that is, when

$$\frac{1}{2\tau} \quad >> \quad \delta\nu_o \qquad 32$$

Allerhand and coworkers (53) have questioned the validity of the Piette-Anderson equation. They have shown by computer line-shape calculations that equation 31 leads to large errors in the exchange rate unless the rate is sufficiently larger than the coalescence value such that equation 32 applies. In addition to this, they contend that for small $\delta\nu_o$ values, the contribution to W* from exchange becomes so small that (W* - W") approaches the experimental error in W*, and the error in the exchange rate $1/2\tau$ becomes very large. This error is a systematic error (decreasing with increasing rate), and if equation 31 is used to extract exchange rates it generally leads (53) to (a) low rates, (b) too large $\Delta H^{\neq}$ values, and (c) to more positive values of $\Delta S^{\neq}$.

A more valid expression was derived (53) on condition that equation 26 holds. Expression 33 reduces

$$\frac{1}{2\tau} = \frac{\pi\delta\nu_o}{2}\left(\frac{\frac{W"}{\delta\nu_o} + \frac{W^*}{\delta\nu_o}\sqrt{1 + 2\left(\frac{W^*}{\delta\nu_o}\right)^2 - \left(\frac{W^*}{\delta\nu_o}\right)^4}}{\left(\frac{W^*}{\delta\nu_o}\right)^2 - \left(\frac{W"}{\delta\nu_o}\right)^2}\right) \qquad 33$$

to the Piette-Anderson (94) relationship 31 when the exchange rate is sufficiently fast that $W^*/\delta\nu_o << 1$ with P_A and $P_B = 0.5$ (53). Furthermore, if the conditions of the exchanging system are such that the exchange contribution to the linewidth is much greater than W" - that is, if

W* >> W", then equation 33 leads to expression 34 (53).

$$\frac{1}{2\tau} = \frac{\pi\delta\nu_o}{2}\sqrt{\left(\frac{\delta\nu_o}{W^*}\right)^2 - \left(\frac{W^*}{\delta\nu_o}\right)^2 + 2} \qquad 34$$

This last expression has been shown to be valid at and above coalescence when equation 26 holds. It is also valid below coalescence (53) if W* is more generally defined as the width of the spectrum at the point where it possesses an amplitude one-half of the central intensity (95). Notwithstanding this, if equation 26 holds, the linewidth W* at the coalescence temperature is equal to the chemical shift $\delta\nu_o$ and in addition $W^* > \delta\nu_o$ below T_c and $W^* < \delta\nu_o$ above T_c (53). These results provide a means of estimating $\delta\nu_o$ without going to the very low temperatures where exchange is "frozen out".

In the region of very fast exchange, errors from the approximation to equations 31 and 33 have been shown to be comparable and negligible - but as the exchange rate decreases toward the rate at coalescence, the former expression yields very large negative errors while the latter is accurate up to $\delta\nu 2\tau \approx 1.0$ (53). As a general rule then (53), if the errors in using the approximate Piette-Anderson relationship 31 are to be kept to < 5%, then it should be used only for rates for which $\delta\nu 2\tau \leq 0.2$. In addition, it was also demonstrated (53) that the approximate expression 34 yields errors of less than 5% in the range $1.0 > \delta\nu 2\tau \geq 0.04$; however, its range of

applicability is strongly dependent on $\delta\nu_o$ and T_2^o (the transverse relaxation time in the absence of exchange), and in fact for small values of these two parameters its use is limited (53).

4. Total Line Shape Digitization Method

In the total line shape method none of the aforementioned approximations are made. Instead, the line shapes can be calculated - requires the use of a computer - given certain characteristic line-shape parameters as for example $\delta\nu_o$ in the absence of exchange, T_{2A} and T_{2B} in the absence of exchange and P_A and P_B. Then, for certain values of (as defined by equation 25), the calculated line-shape parameters, $\delta\nu_e$ (peak separation during exchange), r (the ratio between the maximum to the central minimum intensity (93)), $W^*_{1/4}$, $W^*_{1/2}$, and $W^*_{3/4}$ (the linewidths of the resonance signals at 1/4, 1/2, and 3/4 of the maximum amplitude, respectively) can be compared to the same experimentally determined line-shape parameters in order to obtain an appropriate value of the relaxation time, τ. Unfortunately, as has already been mentioned earlier, for the system $(C_6H_5)_2Sn(acac)_2$-$(CH_3)_2Sn(acac)_2$ investigated here, the problem of not being able to obtain $\delta\nu_o$ in the absence of exchange precluded the use of such method. Rather, the nmr spectra can be digitized point by point as intensity vs. frequency (Hz). The digitized spectrum, then, can be fed to a computer using an appropriate program (eg. NLINGH used here) which will look for the best

combination of the variable line-shape parameters such that the corresponding calculated spectrum deviates by the sum of least squares of its points from that of the experimental spectrum. The latter total line-shape method has already been described earlier in Section II C 4 b.

5. Nuclear Magnetic Resonance Spectra and Kinetics of Ligand Exchange

a) Total Line-Shape Calculations

The variable temperature acetylacetonate methyl proton nuclear magnetic resonance spectra for an equimolar mixture of $(C_6H_5)_2Sn(acac)_2$ and $(CH_3)_2Sn(acac)_2$ in deuteriochloroform are presented in Figure 10a. In Figure 10b are compared the calculated spectra and the experimental spectra along with the residence times in site a, the site in $(C_6H_5)_2Sn(acac)_2$, and in site b, the site in $(CH_3)_2Sn(acac)_2$; solid circles represent experimental points, solid triangles represent calculated points, open circles denote both the calculated and experimental points. The methyl region in the variable temperature nuclear magnetic resonance spectra for an equimolar mixture of $(C_6H_5)_2Sn(acac)_2$ and $(CH_3)_2Sn(acac)_2$ in bromoform solution is shown in Figure 11a; the calculated and experimental spectra are shown in Figure 11b along with the calculated residence times τ_A and τ_B.

Downfield from the acetylacetonate methyl resonances of $(C_6H_5)_2Sn(acac)_2$ and $(CH_3)_2Sn(acac)_2$ (Figure 11a) appears a very small resonance which increases

Figure 10.- Nmr spectra for the acetylacetonate methyl proton region as a function of temperature in the ligand exchange between $(C_6H_5)_2Sn(acac)_2$ and $(CH_3)_2Sn(acac)_2$ in deuteriochloroform; (a) experimental spectra; (b) comparison of experimental and calculated nmr spectra, solid circles represent experimental points, solid triangles calculated points and open circles denote a perfect fit of experimental and calculated points.

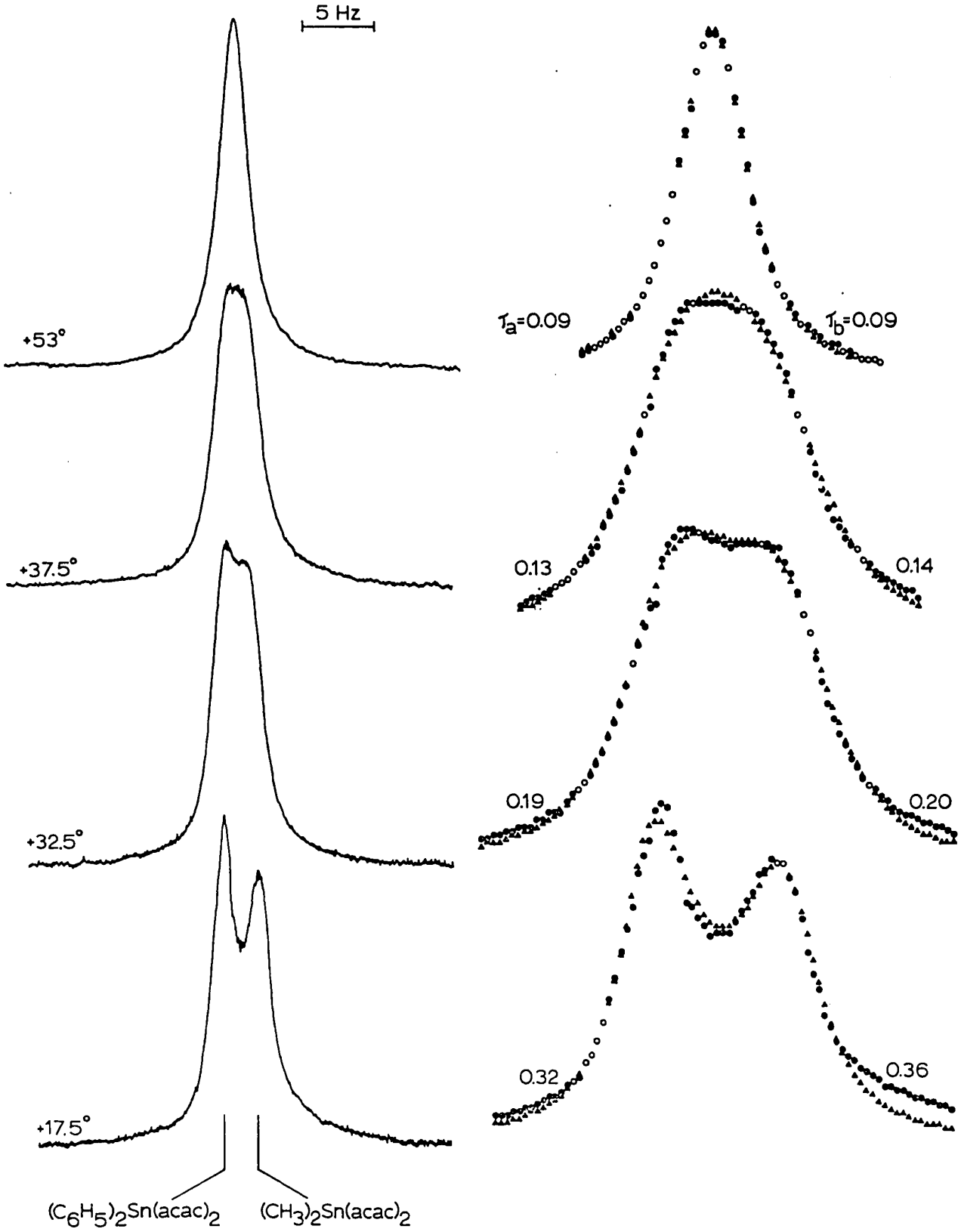
5 Hz
+53°
+37.5°
+32.5°
+17.5°
$(C_6H_5)_2Sn(acac)_2$
$(CH_3)_2Sn(acac)_2$
τ_a=0.09
τ_b=0.09
0.13
0.14
0.19
0.20
0.32
0.36
(a)
(b)

Figure 11.- Nmr spectra for the acetylacetonate methyl proton region as a function of temperature in the ligand exchange between $(C_6H_5)_2Sn(acac)_2$ and $(CH_3)_2Sn(acac)_2$ in bromoform; (a) experimental spectra; (b) comparison of experimental and calculated nmr spectra, solid circles represent experimental points, solid triangles calculated points and open circles denote a perfect fit of experimental and calculated points.

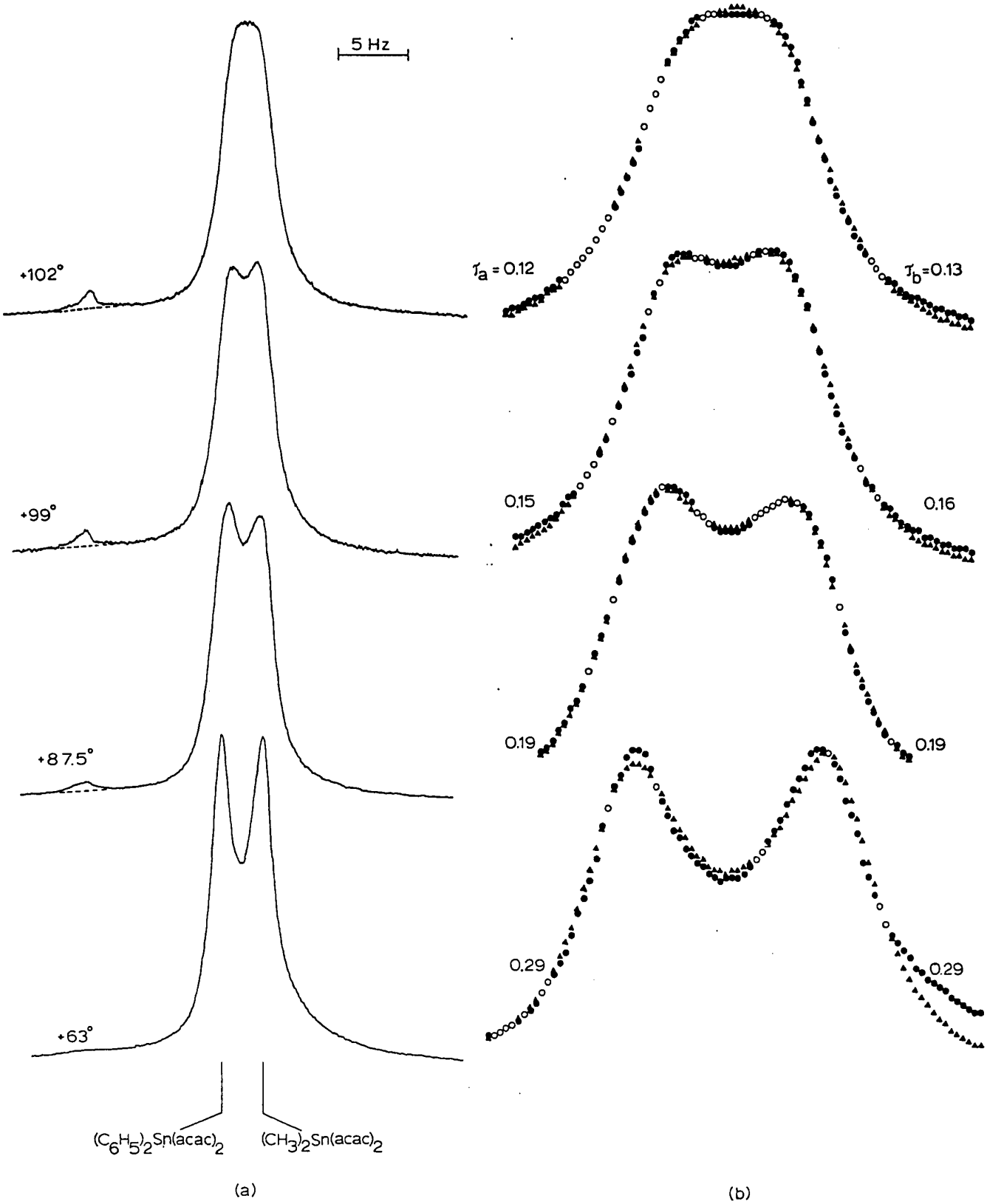
5 Hz
+102°
+99°
+87.5°
+63°
$(C_6H_5)_2Sn(acac)_2$
$(CH_3)_2Sn(acac)_2$
(a)
τ_a = 0.12
τ_b=0.13
0.15
0.16
0.19
0.19
0.29
0.29
(b)

in intensity as the temperature is increased. The room temperature nmr spectrum of the solution taken after the 102° nmr spectral run, also revealed the small resonance signal. This resonance is attributed to a small decomposition impurity from $(C_6H_5)_2Sn(acac)_2$ which decomposes to an extent < 1% at and above ca. 80°. Variable temperature nmr spectra of separate bromoform solutions containing the diphenyltin and the dimethyltin complexes indicated that slight decomposition occurs only in the diphenyltin acetylacetonate sample.

Two features are worth noting in Figures 10 and 11. First, as the temperature is increased, the methyl proton resonance signal of $(C_6H_5)_2Sn(acac)_2$ and the acetylacetonate methyl proton signal of $(CH_3)_2Sn(acac)_2$ broaden, and then coalesce into a single broad line (T_c = 37.5° and W* = 3.37 Hz in $CDCl_3$; T_c = 102° and W* = 4.19 Hz in $CHBr_3$), which in the high temperature limit changes to a single, sharp line (Figure 10). Second, the calculated and experimental nmr spectra (Figures 10b and 11b) deviate sometimes markedly, at the upfield tail end of the dimethyltin acetylacetonate resonance signal (cf. the 17.5° spectrum in Figure 10 and the 63° spectrum in Figure 11). This deviation arises from an inherent reference phase-baseline problem on the HA-100 spectrometer. If the reference phase correction is adjusted such that a horizontal baseline is maintained between the downfield and upfield ends of a resonance line, the resonance signal is skewed at the upfield tail end. But

if the reference phase is adjusted so as to remove this skewedness to obtain a symmetrical signal, the downfield and upfield baselines no longer match. When nmr spectra were run in this work (those shown in Figure 10a and 11a) the reference phase was adjusted such as to achieve an acceptable compromise between a symmetrical resonance signal and a matching baseline. The calculated spectra on the other hand, are perfectly symmetrical about the resonance maxima.

The coalescence behaviour of the diphenyltin- and the dimethyltin acetylacetonate methyl proton resonance signals is attributed to a rapid intermolecular exchange process which exchanges acetylacetonate groups between the two complexes, $(C_6H_5)_2Sn(acac)_2$ and $(CH_3)_2Sn(acac)_2$. However, it could also be construed that the coalescence behaviour of the acetylacetonate methyl resonances arise, wholly or in part, from differing temperature dependences of the acetylacetonate methyl proton chemical shifts in the diphenyltin and the dimethyltin complexes. To test the latter possibility, chemical shifts for the acetylacetonate methyl protons of $(C_6H_5)_2Sn(acac)_2$ and $(CH_3)_2Sn(acac)_2$ were determined in deuteriochloroform and bromoform at variable temperatures. The shifts are tabulated in Table XIII and plotted as a function of temperature in Figure 12. This plot clearly reveals that for the deuteriochloroform solution, the difference in chemical shifts is constant, within experimental error, in the temperature range studied, while the difference for the bromoform sample increases with increase

Table XIII.- Temperature Dependence of the Methyl Proton Chemical Shifts[a] for $(C_6H_5)_2Sn(acac)_2$ and $(CH_3)_2Sn(acac)_2$ in Deuteriochloroform and Bromoform

Temp., (°C)	δ(ppm)[b]		Temp., (°C)	δ(ppm)[e]	
	$(C_6H_5)_2Sn(acac)_2$[c]	$(CH_3)_2Sn(acac)_2$[d]		$(C_6H_5)_2Sn(acac)_2$[f]	$(CH_3)_2Sn(acac)_2$[g]
			37	-	-1.99
-17.5	-	-1.99[c]	43	-2.01	-1.99
- 7	-2.02	-1.98	54.5	-2.00	-
2	-	-1.97	60.5	-	-1.97
7.5	-	-1.96	65.5	-1.99	-
8	-2.01	-	69	-	-1.96
16	-2.01	-	75	-1.99	-
28	-	-1.95	80.5	-	-1.96
32.5	-1.99	-1.95	86	-1.98	-
38	-1.98	-	88	-	-1.95
48	-	-1.94	95	-1.98	-
59	-	-1.93	95.5	-	-1.95

[a] ±0.01 ppm (Varian A-60A nmr spectrometer). [b] Solvent is deuteriochloroform. [c] 0.101 M. [d] 0.103 M. [e] Solvent is bromoform. [f] 0.099 M. [g] 0.098 M.

Figure 12.- Temperature dependence of the acetylacetonate methyl proton chemical shifts of the pure complexes in deuteriochloroform (open) and bromoform (solid). Circles and triangles refer to $(C_6H_5)_2Sn(acac)_2$.

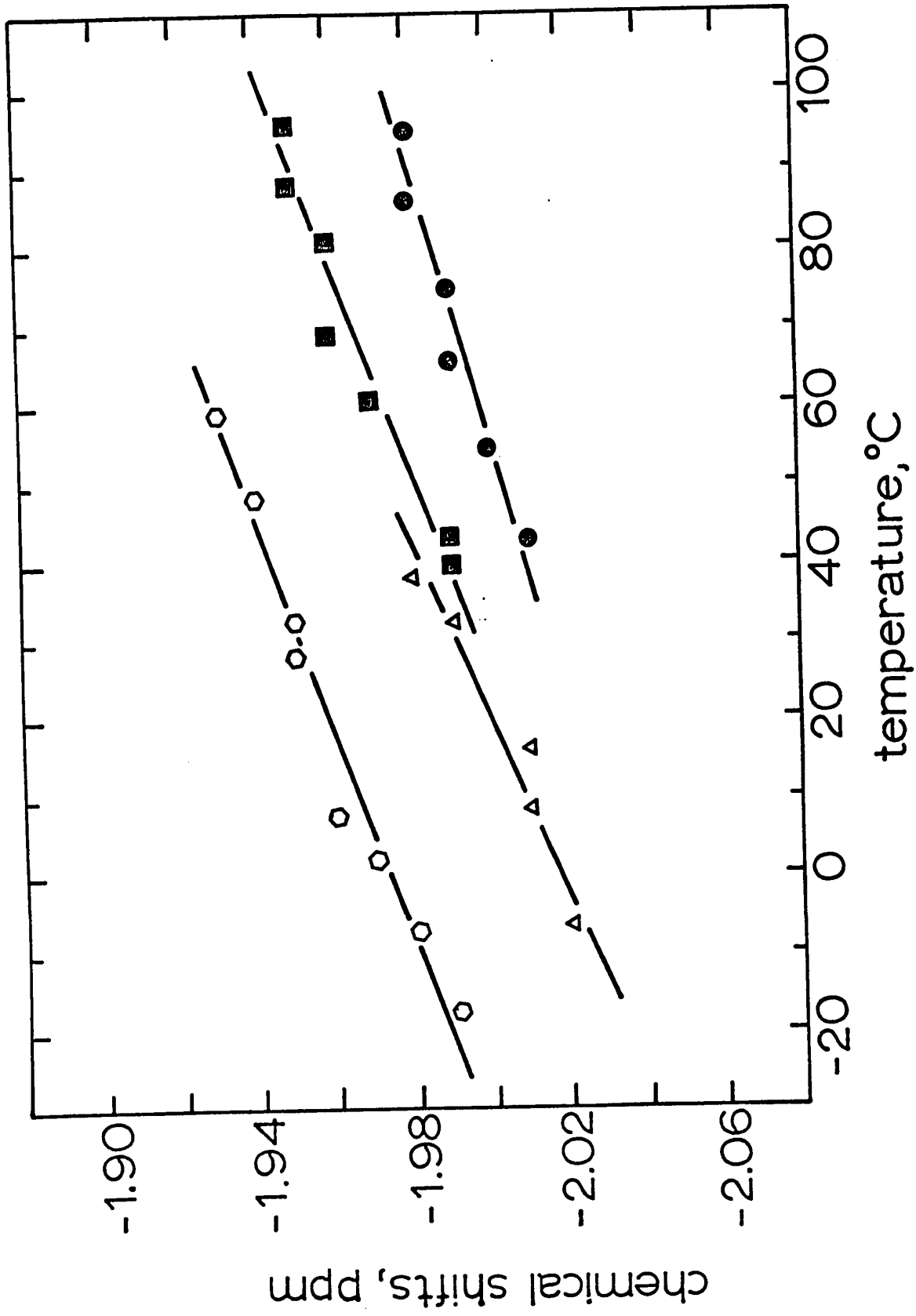
chemical shifts, ppm
-1.90
-1.94
-1.98
-2.02
-2.06
-20
0
20
40
60
80
100
temperature, °C

in temperature. Hence, coalescence of the resonance signals cannot be ascribed to the latter possibility, ie. to differences in the temperature dependences of the methyl proton chemical shifts, but to an intermolecular exchange process.

Values of the residence times τ_a and τ_b for an acetylacetonate methyl group in $(C_6H_5)_2Sn(acac)_2$ and $(CH_3)_2Sn(acac)_2$, respectively, along with the chemical shifts, $\delta\nu$, were obtained from a computer-fitting of the experimental spectra (Figures 10 and 11). These parameters, as well as the mean residence times (as 2τ) are tabulated in Table XIV for the deuteriochloroform sample, and are summarized in Table XV for the bromoform solution. The mean residence times (as 2τ) at 58.5 and 55° for the deuteriochloroform sample (Table XIV) were calculated from the Piette-Anderson expression 31 using the average $\delta\nu_o$ (=3.08 Hz) from the computer-fitted spectra, the fractional populations at site a (p_A = 0.496) and at site b (p_B = 0.504), and the linewidth at one-half maximum amplitude during exchange (W* = 1.92 Hz) and in the absence of exchange (W" = 0.89 Hz).

Kinetic data for the intermolecular ligand exchange between $(C_6H_5)_2Sn(acac)_2$ and $(CH_3)_2Sn(acac)_2$ were collected in the temperature range 17.5-58.5° ($CDCl_3$) and 57-102° ($CHBr_3$). Arrhenius activation energies, E_a, and frequency factors, A, were obtained from the least-squares straight line of log k vs. 1/T plots (Figure 13), where $k = (2\tau)^{-1}$ is the pseudo first-order rate constant for

Table XIV.- Temperature Dependence of Mean Residence Times for Exchange of Acetylacetonate Groups Between $(C_6H_5)_2Sn(acac)_2$ and $(CH_3)_2Sn(acac)_2$ in Deuteriochloroform[a] from Computer-fitted Spectra

Temp., (°C)	1/T x 10^3	τ_A[b] (sec)	τ_B[b] (sec)	2τ (sec)	k(=1/2τ)[c] (sec^{-1})	log k	$\delta\nu_o$ (Hz)
58.5	3.01	-	-	0.069[d]	14	1.159	3.08[e]
55	3.05	-	-	0.089[d]	11	1.046	3.08[e]
53	3.07	0.096	0.089	0.092	11	1.036	3.02
42	3.17	0.10	0.12	0.11	9.0	0.953	3.24
37.5	3.22	0.13	0.14	0.14	6.9	0.841	3.19
35.5	3.24	0.17	0.17	0.17	5.9	0.774	3.03
32.5	3.27	0.19	0.20	0.19	5.2	0.716	2.95
30	3.30	0.26	0.28	0.27	3.7	0.564	3.05
17.5	3.44	0.32	0.36	0.34	3.0	0.473	Ave = $\frac{3.11}{3.08} \pm 0.09$

[a] $[(C_6H_5)_2Sn(acac)_2] = 0.103$ M; $[(CH_3)_2Sn(acac)_2] = 0.101$ M. [b] A ≡ $(C_6H_5)_2Sn(acac)_2$; B ≡ $(CH_3)_2Sn(acac)_2$; errors estimated to be about 10-15%. [c] $1/2\tau = 4.0$ sec^{-1} at 40° (43). [d] Calculated using equation 31 (see text). [e] Average of $\delta\nu$'s from computer-fitted spectra.

Table XV.- Temperature Dependence of Mean Residence Times for Exchange of Acetylacetonate Groups Between $(C_6H_5)_2Sn(acac)_2$ and $(CH_3)_2Sn(acac)_2$ in Bromoform[a] from Computer-fitted Spectra

Temp., (°C)	$1/T \times 10^3$	τ_A[b] (sec)	τ_B[b] (sec)	2τ (sec)	$k(=1/2\tau)$ (sec^{-1})	log k	$\delta\nu_o$ (Hz)
102	2.67	0.12	0.13	0.13	7.9	0.901	3.76
99	2.69	0.16	0.16	0.16	6.4	0.804	3.63
94.5	2.72	0.15	0.15	0.15	6.6	0.821	3.81
92	2.74	0.15	0.16	0.15	6.5	0.812	3.87
87.5	2.77	0.19	0.19	0.19	5.3	0.721	3.65
83	2.81	0.21	0.21	0.21	4.7	0.676	3.58
75	2.87	0.24	0.24	0.24	4.2	0.625	3.63
68	2.93	0.31	0.32	0.31	3.2	0.502	3.51
64	2.97	0.29	0.29	0.29	3.4	0.536	3.64
57	3.03	0.34	0.35	0.35	2.9	0.462	3.65
						Ave =	3.67 ± 0.11

[a] $[(C_6H_5)_2Sn(acac)_2] = 0.099$ M; $[(CH_3)_2Sn(acac)_2] = 0.100$ M. [b] A ≡ $(C_6H_5)_2Sn(acac)_2$; B ≡ $(CH_3)_2Sn(acac)_2$; errors estimated to be about 10-15%.

Figure 13.- Log k *vs* 1/T plots for acetylacetonate ligand exchange between $(C_6H_5)_2Sn(acac)_2$ and $(CH_3)_2Sn(acac)_2$ in deuteriochloroform and bromoform; $k = (2\tau)^{-1}$ is the first-order rate constant for the exchange process.

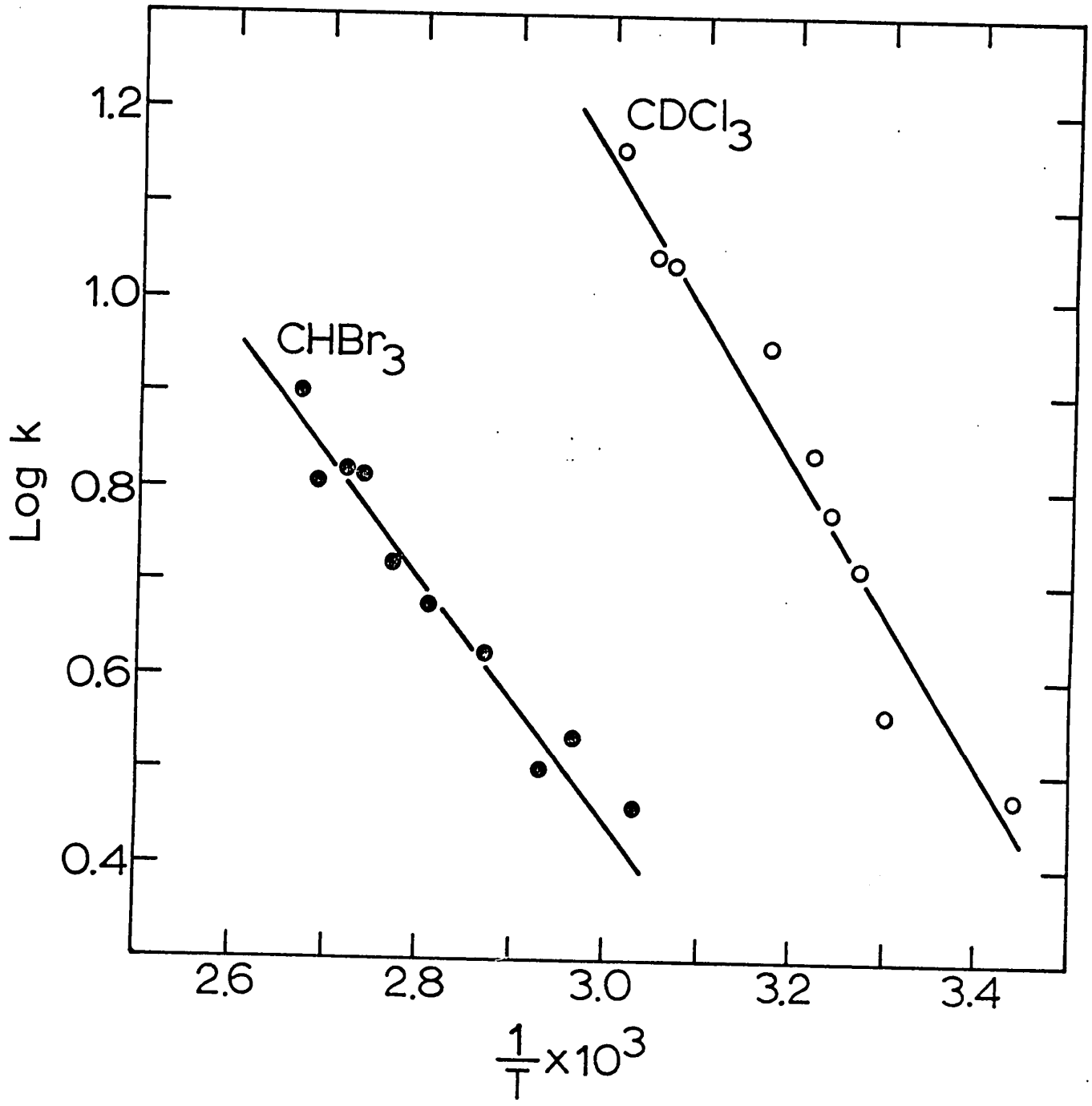
CDCl3
CHBr3
Log k
1.2
1.0
0.8
0.6
0.4
2.6
2.8
3.0
3.2
3.4
1/T x10^3

exchange. Activation entropies, $\Delta S^{\neq}$, at 25° and at T_c, were calculated from the relation 35:

$$\Delta S^{\neq} = R\left[\ln A - \ln\frac{RT}{Nh}\right] - R \qquad 35$$

where the symbols have their usual meaning. The activation enthalpies were obtained from $\Delta H^{\neq} = E_a - RT$ and the Gibb's free energy of activation was computed from $\Delta G^{\neq} = \Delta H^{\neq} - T\Delta S^{\neq}$. The activation parameters* are summarized in Table XV along with values of k at T_c and extrapolated values of k at 25°.

The results for the intermolecular ligand exchange are subject to some small systematic error because the linewidths in absence of exchange are temperature dependent (see Figure 1) throughout the temperature range in which spectra were recorded. The errors, estimated at the 95% confidence level and reported in Table XVI for the activation parameters, represent the scatter of the points from the least-squares straight lines; they do not include the small systematic errors from the estimation of the linewidths in absence of exchange. However, the linewidths in absence of exchange, W", differ only by about 0.10 Hz (0.89 to 0.99 Hz in $CDCl_3$ and 0.87 to 0.96 Hz in $CHBr_3$) in the temperature ranges studied so that the systematic errors are expected to be less than those reported in Table XVI. Further, errors propagated into E_a, $\Delta H^{\neq}$, and $\Delta S^{\neq}$ from the uncertainty

* These activation parameters were all obtained from the computer program ACTPAR written (59) for the CDC 6400 computer.

Table XVI.- Arrhenius and Eyring Activation Parameters for the Intermolecular Exchange of acac Groups Between $(C_6H_5)_2Sn(acac)_2$ and $(CH_3)_2Sn(acac)_2$

Parameters \ Solvent	Deuteriochloroform[a]	Bromoform[b]
E_a (kcal/mole)	7.5 ± 1.5[c]	5.4 ± 0.9[c]
log A	6.05 ± 1.08	4.02 ± 0.57
$\Delta H^{\neq}_{298}$ (kcal/mole)	6.9 ± 1.5	4.8 ± 0.9
$\Delta H^{\neq}_{T_c}$ (kcal/mole)	6.8 ± 1.5	4.7 ± 0.9
$\Delta S^{\neq}_{298}$ (eu)	-33 ± 5	-42 ± 3
$\Delta S^{\neq}_{T_c}$ (eu)	-33 ± 5	-43 ± 3
$\Delta G^{\neq}_{298}$ (kcal/mole)	16.65 ± 0.09	17.37 ± 0.15
$\Delta G^{\neq}_{T_c}$ (kcal/mole)	16.99 ± 0.07	20.63 ± 0.07
k_{298} (sec^{-1})	3.8 ± 0.6	1.1 ± 0.3
k_{T_c} (sec^{-1})	5.9 ± 0.6	7.4 ± 0.7

[a] Coalescence temperature is 37.5°. [b] Coalescence temperature is 102°. [c] Errors are estimated at the 95% confidence level.

in τ values amount to about 10 to 15% and are less than those reported in Table XVI. Jones and Fay (96) have observed that an overestimation of T_2'' (thus an underestimation of W") leads to lower E_a and $\Delta S^{\neq}$ values.

The rate of ligand exchange at 25° in $CDCl_3$ is about 3-4 times the rate in $CHBr_3$ although the activation energy is larger by 2 kcal/mol in deuteriochloroform than in bromoform. However, the entropy of activation is about 10 eu more positive in deuteriochloroform. Since a Sn-O

bond rupture is necessary in the ligand exchange process, the difference in the two activation energies may arise from several factors: (i) a more effective solvation of the ground state of the complexes by deuteriochloroform versus bromoform, the former being well known to hydrogen bond (46,97) to acetylacetonate chelate rings - the effect of this is to lower the ground state energy relative to the energy of the transition state; (ii) a solvent assisted rupture of a tin-oxygen bond to yield a five-coordinate trigonal bipyramidal intermediate or a square pyramidal intermediate with a dangling unidentate acetylacetonate ligand - if deuteriochloroform is more effective here it will increase the rate of ligand exchange consistent with experimental observation (Table XVI) and (iii) a transition state in which the sixth coordination site is occupied by a solvent molecule. Presumably process (iii) above is more favourable in deuteriochloroform. The difference in the entropies of activation is probably the result of a tighter, more compact transition state in $CHBr_3$. This is not unlikely in view of the larger size of $CHBr_3$. Whatever the effects of the solvent in the ground state of the complexes and on the transition state (or intermediate), they cannot simply be related to differences in dipole moments of the solvents (98) as these are nearly the same [1.01 Debyes ($CHCl_3$) and 0.99 Debye ($CHBr_3$)] nor to differences in the dielectric constants (98) of the solvents [4.806(20°) for $CHCl_3$; 4.39(20°) and 3.71(100°)

for $CHBr_3$] though chloroform has a slightly higher dielectric constant.

b) Calculations Using Approximate Methods

It is instructive to compare kinetic data obtained from approximate methods with those from total line-shape calculations so as to obtain an estimate of the differences in the activation parameters between the two methods. The line-shape parameters used in the approximate calculations are presented in Table XVII (deuteriochloroform solution) and in Table XVIII (bromoform solution). Results of the computations of rates for the exchange in deuteriochloroform using $\delta\nu_o$ = 3.08 Hz (the average value from the computer-fitted spectra) and $\delta\nu_o$ = 3.37 ($W^*_{1/2}$ at T_c, see Section III B 3c) along with equations 28, 29, 31, 33, and 34 as well as those from the total line shape method are compared in Table XIX. Those rates calculated for exchange in bromoform using $\delta\nu_o$ = 3.67 Hz (see Table XVII) and $\delta\nu_o$ = 4.19 Hz ($W^*_{1/2}$ at T_c) and equations 29 and 28 as well as those from the total line-shape calculations are tabulated in Table XX.

Inspection of Table XIX reveals that above coalescence, where rates at only two temperatures are compared with those from the total line-shape (TLS) method, rates from expression 31 and 34 compare favorably with those from the TLS method. Rates from equation 33 overestimate the TLS values by more than the estimated error of 10-15%.

Table XVII.- Line-shape Parameters for Intermolecular Exchange in the $(C_6H_5)_2Sn(acac)_2$-$(CH_3)_2Sn(acac)_2$ System in Deuteriochloroform[a]

Temperature, (^oC)	W*, (Hz)	W", (Hz)	$\delta\nu_e$, (Hz)
58.5	1.92	0.89	-
55	2.23	0.90	-
53	2.39	0.90	-
47.5	2.59	0.90	-
42	2.97	0.91	-
37.5 (T_c)	3.37	0.92	-
35.5	-	0.93	(1.0)[b]
32.5	-	0.93	1.38
30	-	0.94	(1.55)[b]
20	-	0.97	2.22
17.5	-	0.99	2.28

[a] $\delta\nu_o$ = 3.08 Hz, the average of the $\delta\nu$'s from the computer-fitted spectra; Also $\delta\nu_o$ = 3.37 Hz, the linewidth of the resonance line at coalescence (W*), see text. P_A = 0.496. P_B = 0.504. [b] Values read from plot of Figure 9.

Table XVIII.- Line-Shape Parameters for Intermolecular Exchange in the $(C_6H_5)_2Sn(acac)_2$-$(CH_3)_2Sn(acac)_2$ System in Bromoform[a]

Temperature, (^oC)	W*, (Hz)	W", (Hz)	$\delta\nu_e$, (Hz)
102 (T_c)	4.19	0.87	-
99	-	0.87	1.61
94.5	-	0.87	1.85
92	-	0.87	2.07
87.5	-	0.87	2.22
83	-	0.87	2.40
75	-	0.87	2.65
68	-	0.89	2.83
64	-	0.91	2.91
57	-	0.96	3.07

[a] $\delta\nu_o$ = 3.67 Hz, the average of the $\delta\nu$'s from the computer-fitted spectra; Also $\delta\nu_o$ was taken as 4.19 Hz, the line-width of the resonance line at coalescence (W*), see text.

Table XIX.- Comparison of Mean Residence Times[a] for the Intermolecular Ligand Exchange in $(C_6H_5)_2Sn(acac)_2$-$(CH_3)_2Sn(acac)_2$ in Deuteriochloroform Solution

Temp., (°C)	$1/2\tau$, (sec^{-1})										
	Eq. 28		Eq. 29		Eq. 31		Eq. 33		Eq. 34		Computer fit
	$\delta\nu_o$ = 3.08[b]	$\delta\nu_o$ = 3.37[c]	$\delta\nu_o$ = 3.08	$\delta\nu_o$ = 3.37	$\delta\nu_o$ = 3.08	$\delta\nu_o$ = 3.37	$\delta\nu_o$ = 3.08	$\delta\nu_o$ = 3.37	$\delta\nu_o$ = 3.08	$\delta\nu_o$ = 3.37	TLS
58.5	-	-	-	-	14	17	21	24	9.9	11	-
55	-	-	-	-	11	13	17	20	8.9	10	-
53	-	-	-	-	10	12	13	15	8.5	9.9	11
47.5	-	-	-	-	8 8	10	11	13	8.0	9.3	9.0
42	-	-	-	-	7.2	8.7	9.5	10	7.1	8.4	-
37.5(T_c)	-	-	6.8	7.5	-	-	-	-	-	-	6.9
35.5	(6.5)[d]	(7.2)[d]	-	-	-	-	-	-	-	-	5.9
32.5	6.1	6.8	-	-	-	-	-	-	-	-	5.2
30	5.2	6.0	-	-	-	-	-	-	-	-	3.7
20	4.7	5.6	-	-	-	-	-	-	-	-	-
17.5	4.6	5.5	-	-	-	-	-	-	-	-	3.0

[a] $1/2\tau$ = 4.0 sec^{-1} at 40° (43). [b] In Hz; average value from the computer-fitted spectra (see Table XVII). [c] Linewidth at one-half maximum amplitude, $W^*_{1/2}$, at the coalescence temperature (see Table XIV). [d] Estimated values using $\delta\nu_e$ = 1.0 Hz (see Table XVII).

Table XX.- Comparison of Mean Residence Times for the Intermolecular Ligand Exchange in $(C_6H_5)_2Sn(acac)_2$-$(CH_3)_2Sn(acac)_2$ in Bromoform Solution

Temperature, (°C)	1/2τ, (sec^{-1})				
	Eq. 29		Eq. 28		Computer-fit
	$\delta\nu_o$ = 3.67[a] (Hz)	$\delta\nu_o$ = 4.19[b] (Hz)	$\delta\nu_o$ = 3.67 (Hz)	$\delta\nu_o$ = 4.19 (Hz)	TLS
102 (T_c)	8.2	9.3	-	-	7.9
99	-	-	7.3	8.6	6.4
94.5	-	-	7.0	8.4	6.6
92	-	-	6.7	8.1	6.5
87.5	-	-	6.5	7.9	5.3
83	-	-	6.2	7.6	4.7
75	-	-	5.6	7.2	4.2
68	-	-	5.2	6.9	3.2
64	-	-	5.0	6.7	3.4
57	-	-	4.5	6.3	2.9

[a] Average value from computer-fitted spectra (see Table XV). [b] Linewidth at one half maximum amplitude, $W^*_{1/2}$, at the coalescence temperature (see Table XVIII).

In making these comparisons it should be remembered that the Piette-Anderson equation 31 holds for very fast exchange, ie. when $1/2\tau >> \pi\delta\nu_o$. In the present case, $1/2\tau \approx 10$ while $\pi\delta\nu_o \approx 10$, so that agreement in the rates is merely coincidental. Expression 34 holds if $1/\tau$ and $W^* >> W''$, where for this case $1/\tau \approx 20$ sec^{-1}, $W^* \approx 2.5$ Hz and $W'' \approx 0.90$ Hz (see Table XVII); so it would appear that this expression is applicable to the present problem (but see below). At coalescence, use of equation 29 leads to good agreement with the TLS rate for $\delta\nu_o = 3.08$ Hz. This is not too surprising since $\delta\nu_o$ was obtained from the average $\delta\nu$ values of the computer-fitted spectra. Below coalescence, the relationship 28 was employed to compute the rates of ligand exchange. In both cases where $\delta\nu_o = 3.08$ Hz and 3.37 Hz, the computed rates are slightly larger than those from the TLS method near coalescence (at 35.5 and 32.5°) but the overestimation increases the further one gets from coalescence. The increase in the difference in rates (equation 28 vs TLS) indicates that the resonance peak separation parameter is more sensitive to changes in rates of exchange near coalescence (see ref 55); indeed, as mentioned earlier, the major change in $\delta\nu_e$ occurs in the narrow range $0.45 \leq 2\tau\delta\nu_o \leq 2$ (55) [here $2\tau\delta\nu_o \approx 0.5$ to 1.0 in the temperature range 17.5-35.5° and for $\delta\nu_o = 3.08$ Hz]. Further, the format of expression 28 demonstrates that as $\delta\nu_e$ values approach $\delta\nu_o$, the percent error in the rates, $1/2\tau$, increases. Thus far, computed values of

$1/2\tau$ generally agree more with TLS values when $\delta\nu_o$ = 3.08 Hz.

Table XX shows that at coalescence the computed rate of 8.2 sec^{-1} using equation 29 and $\delta\nu_o$ = 3.67 Hz is in good agreement with the TLS value of 7.9 sec^{-1}. Below coalescence, the rates computed with the approximate expression 28 again overestimate those obtained with the TLS method; in this case, $2\tau\delta\nu_o \approx 0.6$ to 1.3 for $\delta\nu_o$ = 3.67 Hz in the temperature range 57-99°.

The effect of using approximate methods in computing rates of exchange and activation parameters is clearly pictured in Figure 14 ($CDCl_3$) and 15 ($CHBr_3$) where log k ($=1/2\tau$) is plotted against 1/T. The straight line plots from the total line shape method are also shown for comparison. The Arrhenius and Eyring activation parameters for intermolecular ligand exchange in deuteriochloroform and in bromoform are summarized in Table XXI and XXII, respectively. Below coalescence use of equation 28 yields low activation energies and low activation entropies vis-á-vis those from the TLS calculations by as much as 3 to 4 kcal/mol and 7 to 12 eu, respectively (Table XXI and XXII). Above coalescence, equation 34 leads to the same results as equation 28. Expression 31, however, yields values of the Arrhenius and Eyring activation parameters which are in good agreement, within experimental error, with the TLS values; use of equation 33, on the other hand, leads to large values of the activation energies and activation entropies compared to those of the TLS method

Figure 14.- Plots of log k versus 1/T for exchange of acac groups between $(C_6H_5)_2Sn(acac)_2$ and $(CH_3)_2Sn(acac)_2$ in deuteriochloroform solution. Plots a through f are compared with the plot from the TLS method (see text). Plot a from eqs 33, 29 and $\delta\nu_o$ = 3.37 Hz; plot b from eqs 33, 29 and $\delta\nu_o$ = 3.08 Hz; plot c from eqs 31, 29 and $\delta\nu_o$ = 3.37 Hz; plot d from eqs 31, 29 and $\delta\nu_o$ = 3.08 Hz; plot e from eqs 34, 29, 28 and $\delta\nu_o$ = 3.37 Hz; plot f from eqs 34, 29, 28 and $\delta\nu_o$ = 3.08 Hz.

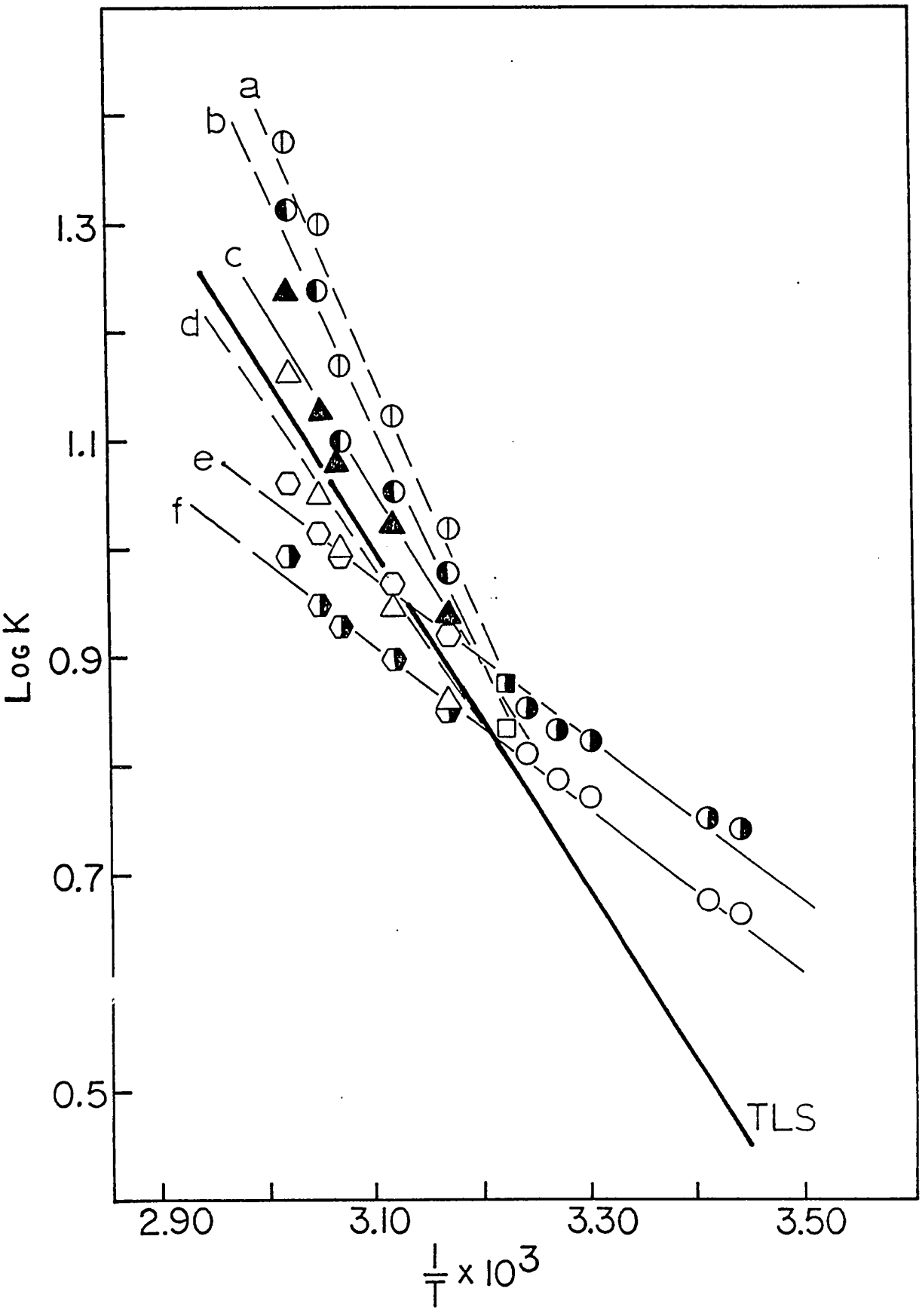
a
b
c
d
e
f
1.3
1.1
0.9
0.7
0.5
Log K
TLS
2.90
3.10
3.30
3.50
1/T x 10^3

Figure 15.- Plots of log k versus 1/T for exchange of acac groups between $(C_6H_5)_2Sn(acac)_2$ and $(CH_3)_2Sn(acac)_2$ in bromoform solution. Plots a and b are compared with the plot from the TLS method (see text). Plot a from eqs 28, 29 and $\delta\nu_o$ = 4.19 Hz; plot b from eqs 28, 29 and $\delta\nu_o$ = 3.67 Hz.

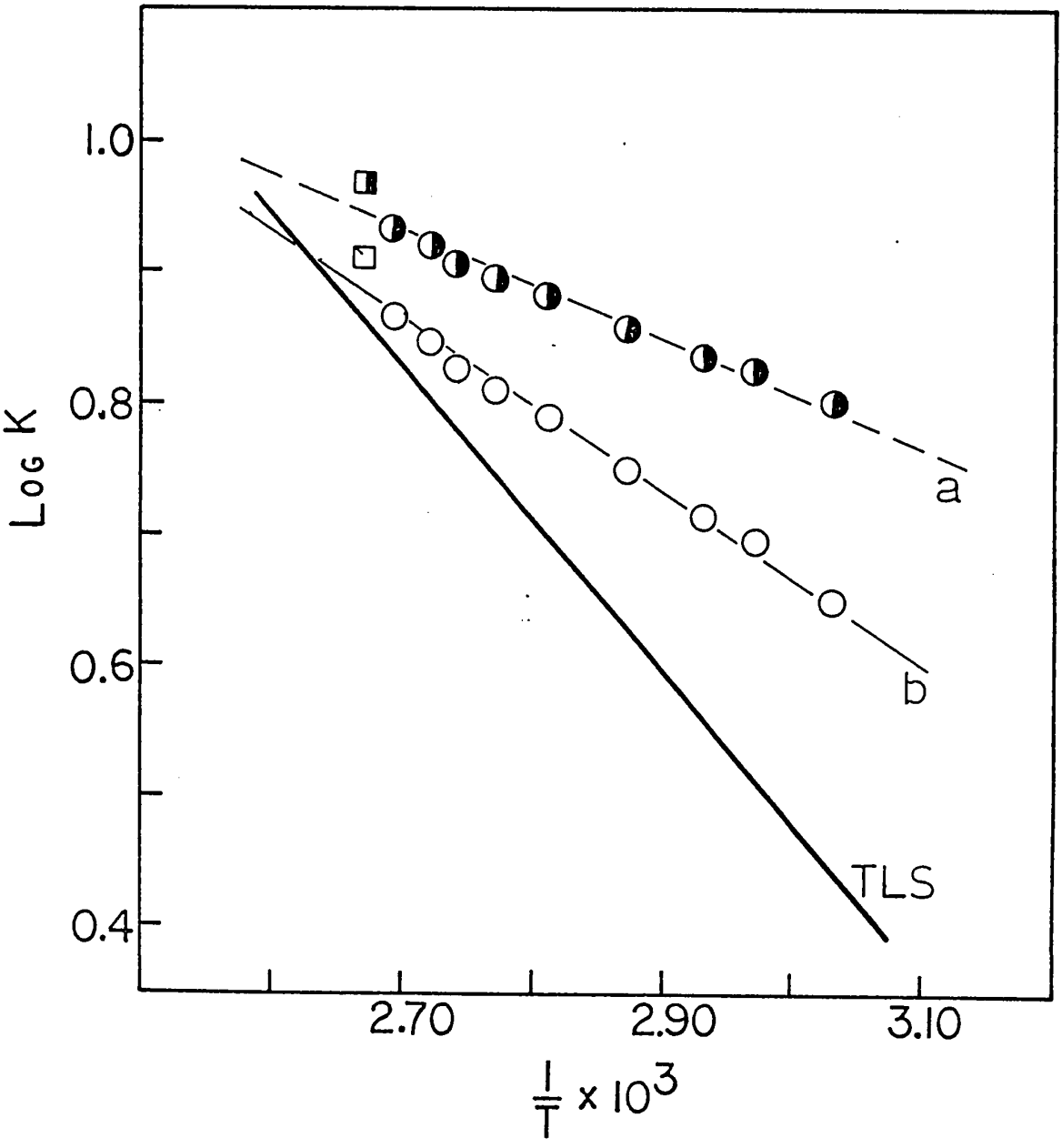
1.0
0.8
0.6
0.4
Log K
2.70
2.90
3.10
1/T x 10^3
a
b
TLS

Table XXI.- Comparison of Activation Parameters for $(C_6H_5)_2Sn(acac)_2$-$(CH_3)_2Sn(acac)_2$ Exchange in Deuteriochloroform Solution

Parameters refer to 298°K	Eq 28,29,34 $\delta\nu_o$=3.08[a]	Eq 28,29,34 $\delta\nu_o$=3.37	Eq 29,31 $\delta\nu_o$=3.08	Eq 29,31 $\delta\nu_o$=3.37	Eq 28,33 $\delta\nu_o$=3.08	Eq 28,33 $\delta\nu_o$=3.37	Total line Shape Method
E_A, (kcal/mole)	3.5 ± 0.2[b]	3.4±0.3	6.6±3.5	7.5±2.1	9.9±3.3	10.5±2.9	7.5±1.5
$\Delta H^{\neq}$, (kcal/mole)	2.9 ± 0.2	2.8±0.3	6.0±3.5	6.9±2.1	9.3±3.3	9.9±2.9	6.9±1.5
log A	3.27 ± 0.17	3.30±0.22	5.5±2.4	6.1±1.4	7.8±2.3	8.3±1.9	6.05±1.08
$\Delta S^{\neq}$, (eu)	-45 ± 1	-45±1	-36±11	-32±6	-25±10	-23±9	-33±5
$\Delta G^{\neq}$, (kcal/mole)	16.5 ± 0.0	16.4±0.0	16.6±0.3	16.6±0.2	16.7±0.3	16.7±0.2	16.7±0.1
k, (sec^{-1})	5.3 ± 0.2	6.1±0.2	4±2	4.4±1.2	4±2	4±2	3.8±0.6

[a] ± Hz. [b] ± All errors estimated at the 95% confidence level.

Table XXII.- Comparison of Activation Parameters for $(C_6H_5)_2Sn(acac)_2$-$(CH_3)_2Sn(acac)_2$ Exchange in Bromoform Solution

Parameters refer to 298°K	Eq 28, 29		Total Line Shape Method
	$\delta\nu_o$ = 3.67 Hz	$\delta\nu_o$ = 4.19 Hz	
E_A, (kcal/mole)	3.0 ± 0.3[a]	1.9 ± 0.3	5.4 ± 0.9
$\Delta H^{\neq}$, (kcal/mole)	2.4 ± 0.3	1.3 ± 0.3	4.8 ± 0.9
log A	2.63 ± 0.18	2.05 ± 0.16	4.02 ± 0.57
$\Delta S^{\neq}$, (eu)	-48 ± 1	-51 ± 1	-42 ± 3
$\Delta G^{\neq}$, (kcal/mole)	16.9 ± 0.0	16.5 ± 0.0	17.4 ± 0.2
k, (sec^{-1})	2.7 ± 0.2	4.6 ± 0.3	1.1 ± 0.3

[a] All errors estimated at the 95% confidence level.

by as much as 2.5 to 3 kcal/mol and about 9 eu, respectively.

6. Mechanisms of Ligand Exchange

(a) Previous Studies

The kinetics of intermolecular exchange between $M(tfac)_4$ [M=Zr or Hf] and the free ligand trifluoroacetylacetone in chlorobenzene and benzene as well as the kinetics of exchange between $M(acac)_4$ [M=Zr or Hf] and acetylacetone in chlorobenzene have been investigated by Adams and Larsen (30). These kinetics follow the rate law 36

$$\frac{[HL]_{enol}}{\tau_{HL}} = \frac{4[ML_4]}{\tau_{ML_4}} = k\,[ML_4][HL]_{enol} \qquad 36$$

Ligand exchange for $M(acac)_4$ [M=Zr or Hf] with acetylacetone in benzene has also been studied (30). The kinetics in benzene have been observed to follow the rate equation 37

$$\frac{[HL]_{enol}}{\tau_{HL}} = \frac{4[ML_4]}{\tau_{ML_4}} = k_1[ML_4] + k_2[ML_4][HL]_{enol} \qquad 37$$

Exchange was found to be faster for $Zr(acac)_4$ than for $Hf(acac)_4$, but when the ligand was trifluoroacetylacetone exchange rates for both zirconium and hafnium complexes were approximately the same. The proposed mechanism for the first order exchange in ML_4 and HL obeying rate law 36 is described in the scheme below, where step (1) involves a rapid breaking and reforming of one of the M-O bonds; this has already been proposed by several workers (cf. ref 1) to explain the intramolecular ligand exchange in

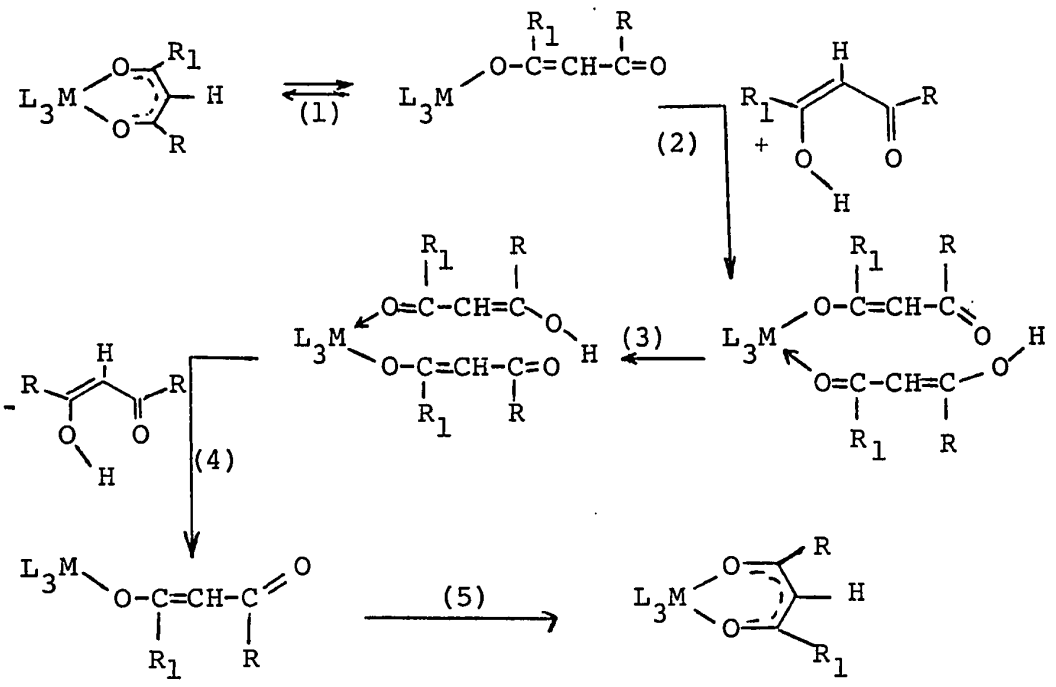

M(β-diketonato)$_3$ complexes. The rapid equilibrium probably explains (30)why geometric isomers have not been observed. Step (2) involves reactions of a seven-coordinate species with the free ligand, while in step (3) a hydrogen atom bonded to the oxygen exchanges with the leaving ligand bonded to the metal. In step (4), loss of a ligand leads to a seven-coordinate species; the eight-coordinate species is obtained by formation of a M-O bond in step (5). Because of the mass difference between Zr (91.22 amu) and Hf (178.49 amu) it was expected (30) that the exchange rate be faster for the Zr than for the Hf complexes, as was found experimentally. It was thus speculated (30) that step (4) is the rate-determining step for the acetylacetonate complexes in chlorobenzene. However, step (2) or step (3)

was suggested as being the slow step for the trifluoroacetylacetonate complexes since the rates were about equal when M was Zr or Hf. Hydrogen exchange, as in step (3), would be expected to be fast so that the rate-determining step is probably step (2). It was also observed that exchange in the trifluoroacetylacetonate complexes was faster than in the acetylacetonate complexes. This is consistent with the fact that a highly electronegative substituent, such as CF_3, on the β-diketonate ring increases the rate at which M-O bonds are broken in β-diketonate compounds (99). On this basis, it is expected that the slow step in the ligand exchange is breaking of a M-O bond in both $M(tfac)_4$ and $M(acac)_4$ complexes; thus, step (4) should not be precluded as a likely slow step in ligand exchange in $M(tfac)_4$ complexes. A bimolecular mechanism (shown below) involving attack by the free ligand on the eight-coordinate species to form a nine-coordinate species could not be ruled out (30).

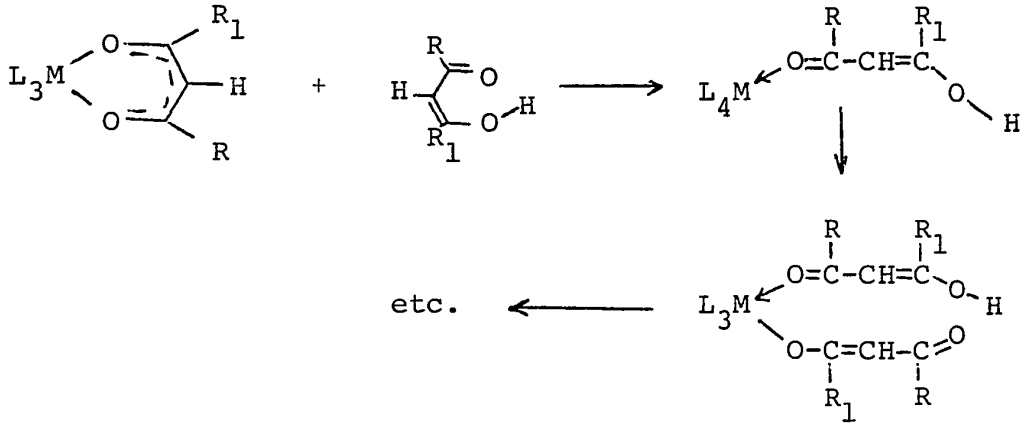

No mechanism was suggested for the k_1 path in the ligand exchange in $M(acac)_4$ complexes with acetylacetone in benzene

solutions.

Radioactive tracer studies to follow the exchange of ^{36}Cl with $Ti(acac)_2Cl_2$ have been undertaken (100). The kinetics follow the rate equation 38

$$\text{Rate} = k_2[Ti(acac)_2Cl_2][Et_4NCl] \qquad 38$$

where $k_2 = 1.8 \times 10^{-4} M^{-1} sec^{-1}$, $\Delta H^{\neq} = 13.6$ kcal/mol, and $\Delta S^{\neq} = -11.5$ eu; exchange was suggested as occurring via a bimolecular substitution at titanium.

The cis ⇄ trans isomerization in $Al(acac)_2(DMF)_2$ where DMF is dimethylformamide has also been investigated (101). The rate-determining step has been suggested as dissociation of a DMF ligand.

In a general study of ligand exchange kinetics in some organometallic acetylacetonate systems, Glass and Tobias (43) observed that the order of increasing exchange rate with acetylacetone is $Cl_2Sn(acac)_2 << (CH_3)_2Au(acac) \approx CH_3ClSn(acac)_2 \approx (CH_3)_2Ga(acac) < (C_6H_5)_2Sn(acac)_2 < (CH_3)_2Sn(acac)_2 < (CH_3)_2Tl(acac)$. Further, exchange of acetylacetone between $(CH_3)_2Sn(acac)_2$ and $(C_6H_5)_2Sn(acac)_2$ was found to be slower than in $(CH_3)_2Sn(acac)_2$-Hacac and $(C_6H_5)_2Sn(acac)_2$-Hacac systems. The proposed mechanism for the exchange process is similar to that of Adams and Larsen (30) for $M(dik)_4$-Hdik exchange (vide supra). Eyring activation parameters were also reported; unfortunately, these were calculated from exchange rates computed from

approximate equations discussed earlier in this work. Nevertheless, the suggestion was made that the rate-determining step involves a M-O bond rupture but no data was reported to substantiate the possible step(s) in the mechanism which might be rate-determining.

Radioactive tracer studies using labelled ^{14}C-acetylacetone to investigate the kinetics and mechanisms of isotopic ligand exchange have likewise been reported. Thus, Saito and Masuda (102) have studied the exchange of ^{14}C-Hacac with $Al(acac)_3$ in tetrahydrofuran (THF). The exchange rate was observed to be independent of the concentration of acetylacetone but dependent on that of water. The rate equation is (102):

$$R = k_1[Al(acac)_3] + k_2[Al(acac)_3][H_2O] \qquad 39$$

where at 25°, $k_1 = 6 \times 10^{-5}$ min^{-1} and $k_2 = 2.0 \times 10^{-2} M^{-1} min^{-1}$. The activation energy for the k_2 path was 22 kcal/mol. The isotopic ligand exchange is also acid-catalyzed, the stronger the acid the greater the catalytic effect. Acids used were (102): Cl_3COOH (pK = 0.635), $m\text{-}CH_3C_6H_4COOH$ (pK = 4.272), and C_6H_5OH (pK = 9.99_8). The rate equation in this case was found to be

$$R = k_1[Al(acac)_3] + k_1'[Al(acac)_3][acid] + k_2'[Al(acac)_3][H_2O] + k_2''[Al(acac)_3][H_2O][acid] \qquad 40$$

Experimental results indicated that the mechanism of

isotopic ligand exchange is a dissociative one, the rate-determining step being the liberation of a coordinated acetylacetonate ligand from the $Al(acac)_3$ complex. Since simultaneous rupture of two M-O bonds is not very probable, it was suggested (102) that one of the three ligands in the complex is present as a unidentate ligand, and break of its remaining M-O bond will bring about ligand exchange. The mechanism is shown below

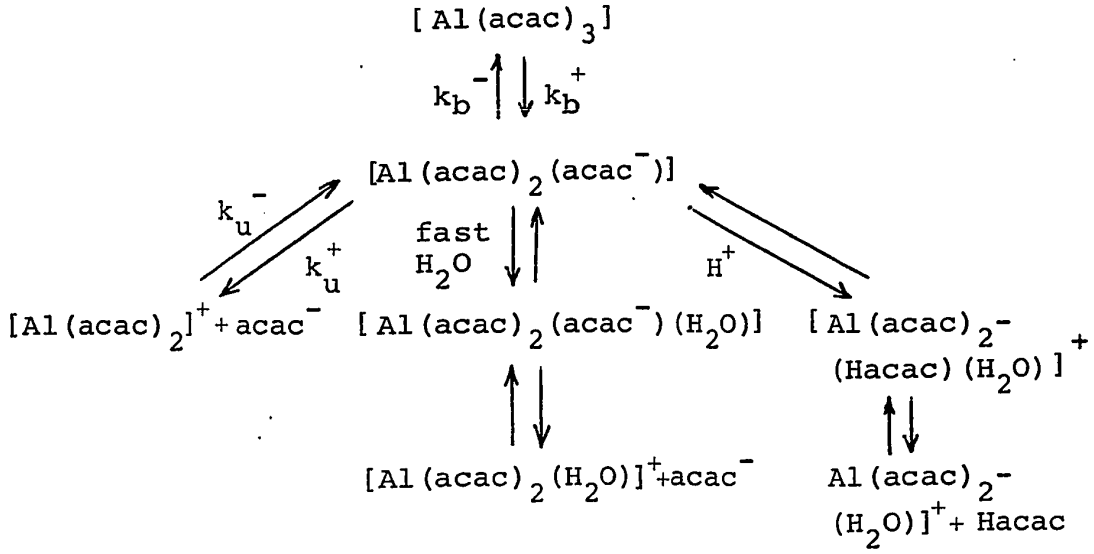

where $k_1 = k_b^+ k_u^+ / k_b^-$ and k_b^+ is the rate constant for M-O bond rupture in the bidentate ligand, k_u^+ is for the M-O bond rupture in the unidentate ligand, and k_b^- is the rate constant for the M-O bond formation to yield the coordinated bidentate ligand. The small value of k_1 ($6 \times 10^{-5} min^{-1}$) reflects the ease of recombination of the unidentate ligand to aluminum (102). The k_2 term in the rate law 39 is very

significant - apparently the H_2O is present as being coordinated to aluminum in the reaction intermediate since on addition of petroleum ether to a solution of $Al(acac)_3$ in THF (containing a large amount of water, > 0.1 M) yielded (102) a gelatinous precipitate of aluminum (probably as the hydroxide). The second term in rate equation 40 (k_1') was found to be insignificant vis-á-vis the k_2'' term. This latter term apparently reflects the establishment of the $HX + H_2O \rightleftarrows X^- + H_3O^+$ equilibrium. It seems that direct transfer of H^+ from the acid to the complex is difficult; rather, specific proton transport to the complex occurs via H_3O^+ formation. This is not unreasonable if one considers the free end of the unidentate acetylacetonate ligand to remain in the neighbourhood of the metal ion; then, only a small particle like H_3O^+ can approach the unidentate species to hand over the proton to the unidentate acetylacetonate ligand, while the H_2O molecule coordinates to the metal ion in the sixth octahedral position. The role of acetylacetone (pK = 5.824) as a possible catalyst was discounted on the basis that the effective acid strength of acetylacetone in THF - H_2O to yield H_3O^+ is (thermodynamically) probably much weaker than expected (102). However, it should be noted that a mechanism in which $Al(acac)_3$ is directly attacked by water molecules to yield a seven-coordinate species as well as a mechanism in which a H^+ attacks an oxygen atom in the $Al(acac)_3$ complex could not be precluded on the basis of the experimental data alone.

But because liberation of a coordinated acetylacetonate ligand is possible - although small - without catalytic action (102), the mechanism is more readily understood and more consistent with a reaction intermediate such as $[Al(acac)_2(acac^-)]$.

A similar mechanism was postulated (103) for the ligand exchange between $Ga(quinol)_3$ and 8-hydroxyquinoline (Hquinol) in which the reaction species is $Ga(quinol)_2(quinol^-)$. The rate-determining step in the spontaneous uncatalyzed path (k_o) is rupture of the remaining metal-ligand bond to yield $[Ga(quinol)_2]^+$ and $quinol^-$, while the slow step in the acid-catalyzed path (k_a) is rupture of a metal-ligand bond in $[Ga(quinol)_2(Hquinol)]^+$ to yield $[Ga(quinol)_2]^+$ and 8-hydroxyquinoline (103). The rate expression is given by

$$R = k_o[Ga(quinol)_3] + k_a[Ga(quinol)_3][acid] \qquad \underline{41}$$

where the activation energy for the k_o path is 18.6 kcal/mol. No concrete evidence was found to suggest that the force constants of metal-ligand bonds are in any way simply related to the stability of and lability of the complexes.

Saito and Masuda (104) have extended their isotopic ligand exchange studies between $Al(acac)_3$ and C-14 labelled acetylacetone to solvents other than tetrahydrofuran, viz., ethylacetate, toluene, and the xylenes. In the absence of acids the rate expression was the same as

rate law 39 but in the presence of acids (m-toluic acid), the rate equation was

$$R = k_1[Al(acac)_3] + k_2[Al(acac)_3][H_2O] + k_1'[Al(acac)_3][acid] + k_2'[acid][H_2O][Al(acac)_3] \quad 42$$

Again, exchange of ligands was independent of the acetylacetone concentration. The exchange can occur either by (1) rupture of one M-O bond as the rate-determining step and the remaining bond breaks rapidly or (2) one of the acetylacetonate ligands is present as a unidentate ligand with a "long" lifetime and the break of the remaining metal-oxygen bond is rate-determining. The catalytic action by acids was rationalized by considering water to occupy the sixth position on the aluminum complex $[Al(acac)_2(acac^-)]$ and the acid to protonate the free end of the dangling unidentate ligand so that recombination of the free ligand end to get the original six-coordinate $Al(acac)_3$ complex is retarded. Experimental results favor mechanism (2) above (104). If mechanism (1) were operating, the ease of one M-O bond rupture should be affected by catalysts and $\Delta H^{\neq}$ values would be expected to be different for the k_1, k_2, k_1', and k_2' paths. In fact, $\Delta H^{\neq}$ = 21.4 kcal/mol in ethylacetate for all the k paths and $\Delta H^{\neq}$ = 19.2 kcal/mol in toluene for the uncatalyzed path k_o ($= k_1 + k_2[H_2O]$). However, when mechanism (2) operates, the rate constants are dependent on the ease with which the free end of the unidentate ligand recombines with aluminum. The transition

state is then viewed (104) as elongation of the remaining M-O bond which would not be affected by protonation of the free ligand end nor by occupation of the sixth coordination site on the aluminum ion by water. In toluene and in the xylenes $k_1 = 0$ but in tetrahydrofuran and ethylacetate $k_1 = 6 \times 10^{-6} min^{-1}$. Entropies of activation (104) for the uncatalyzed k_o path are -7.8 (THF), -8.0 ($CH_3COOC_2H_5$), and -12.2 (Toluene) eu, while for the k_1 path $\Delta S^{\neq} = -12.2$ eu ($CH_3COOC_2H_5$), for the k_2 path $\Delta S^{\neq} = +0.04$ ($CH_3COOC_2H_5$) and -3.8 (Toluene) eu; for the acid-catalyzed path in ethylacetate $\Delta S^{\neq}$ values are +1.4 eu (k_1' path) and +9.5 eu (k_2' path). These values for the uncatalyzed paths as well as the k_1 values in the various solvents have been rationalized (104) in terms of polar solvents solvating the free end of the unidentate ligand and/or the sixth coordination site on the complex thus retarding the recombination of the free end of the ligand to the aluminum ion. However, differences in k_1 values can also be accounted for (104) by suggesting that the polar solvent coordinates to the aluminum thereby decreasing the effective charge on the aluminum ion and thus making the remaining Al-O bond easier to rupture. The mechanism is described below. It was also suggested that in toluene and xylenes, the acid acts as the proton carrier in the k_1' path but in the k_2' path both acid and water cooperate to form H_3O^+ which is the proton carrier. Further, in toluene and xylenes, the acid molecules or their anions

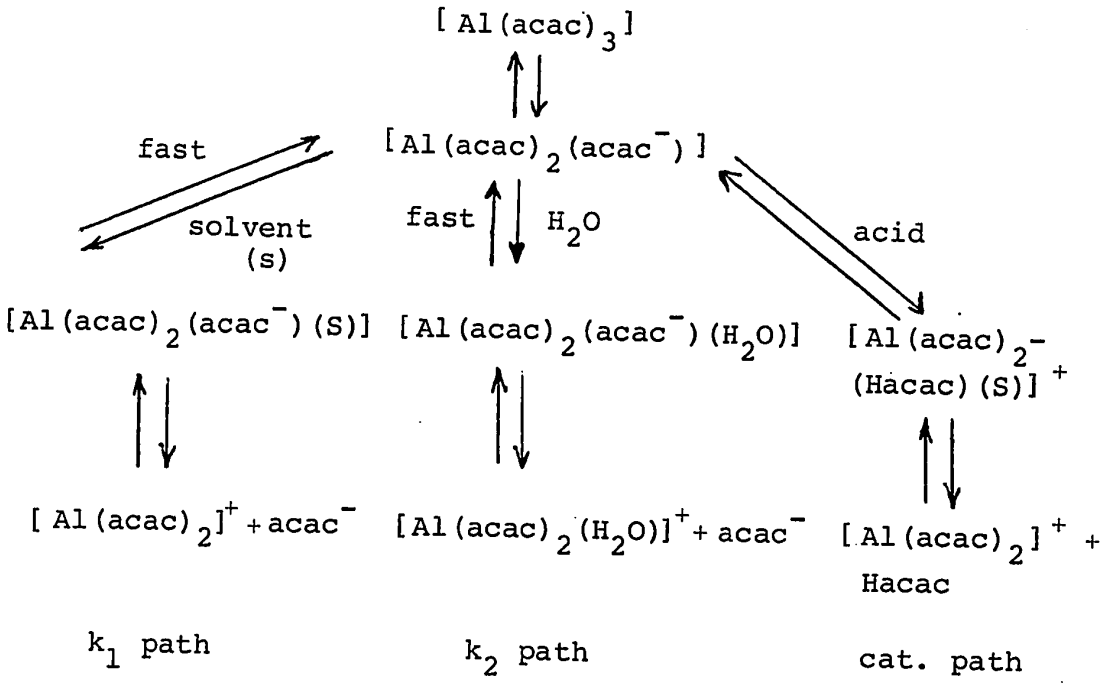

could be used to occupy the vacant coordination site in $[Al(acac)_2(acac^-)]$.

No dependence on the concentration of water (0.017 to 0.12 M) was found in the isotopic ligand exchange studies (105) between $Pd(acac)_2$ and C-14 labelled acetylacetone for which the rate equation was reported to be

$$R = k_1[Pd(acac)_2] + k_2[Pd(acac)_2][Hacac] + k_3[Pd(acac)_2][acid] \qquad 43$$

The k_2 path (S_N2) represents a direct attack by the free ligand acetylacetone and not by the acetylacetonate anion since k_2 values are not affected by presence of acids stronger than acetylacetone. The k_1 path is a dissociative

path in which the rate-determining step is rupture of the remaining M-O bond in the unidentate ligand. Three kinds of mechanisms were suggested for the k_3 path: (a) displacement of a coordinated ligand through a nucleophilic attack by an acid molecule or its anion; (b) dissociation of one end of the ligand as the rate-determining step and the other end dissociates fast - presumably, protons attack a coordinated oxygen and accelerate the first step of the bond rupture process between Pd(II) and oxygen - and (c) one of the ligands is present as a "rather stable" unidentate species and rupture of the remaining Pd-O bond is rate-determining - here the protons would trap the free end of the ligand and would retard its recombination so as to increase the exchange rate. Experimental data and arguments were used to deduce that the k_3 path occurs either via (b) and/or (c) above, but the data could not differentiate these two. However, kinetic studies (106) of substitution reaction of $Pd(acac)_2$ in H_2O-CH_3OH showed that acid catalysis occurs via path (c); in addition, path (c) was used to rationalize the kinetics of exchange between $Al(acac)_3$ and C-14 labelled acetylacetone (103,104).

Radioactive tracer techniques have also been employed to follow the kinetics of isotopic ligand exchange between $Be(acac)_2$ and C-14 labelled acetylacetone in which an associative mechanism to yield a five-coordinate beryllium(II) intermediate is precluded (107). The rate law for the exchange is

$$R = k_1[Be(^{14}C\text{-acac})_2] + k_2[Be(^{14}C\text{-acac})_2][Hacac] \qquad 44$$

Although the k_2 path appears to be an associative mechanism, it has been rationalized by admitting a one-ended dissociation as a first fast step. This has been found experimentally to be operative (vide supra) in ligand redistribution reactions for several classes of complexes with bidentate ligands (108,109). The experimental rates (107) are consistent with two processes: a monomolecular S_N1 path (k_1) and a bimolecular S_N2 path (k_2). In chloroform and dichloromethane the k_1 path is negligible while in cyclohexane, benzene, and acetonitrile the k_1 process is small; but in nitromethane and tetrahydrofuran, the k_1 path becomes more significant and predominant whilst in methanol the mechanism of ligand exchange appears to be exclusively S_N1, though more probably pseudo-S_N1 because of possible solvation of the beryllium ion. In addition, it was demonstrated that it is the enol form of acetylacetone which reacts in the rate-determining step. The proposed mechanism for both the k_1 and k_2 paths is summarized below (R = CH_3).

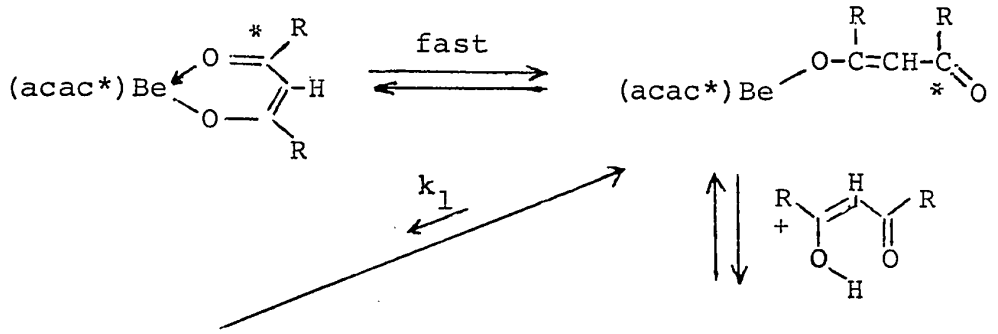

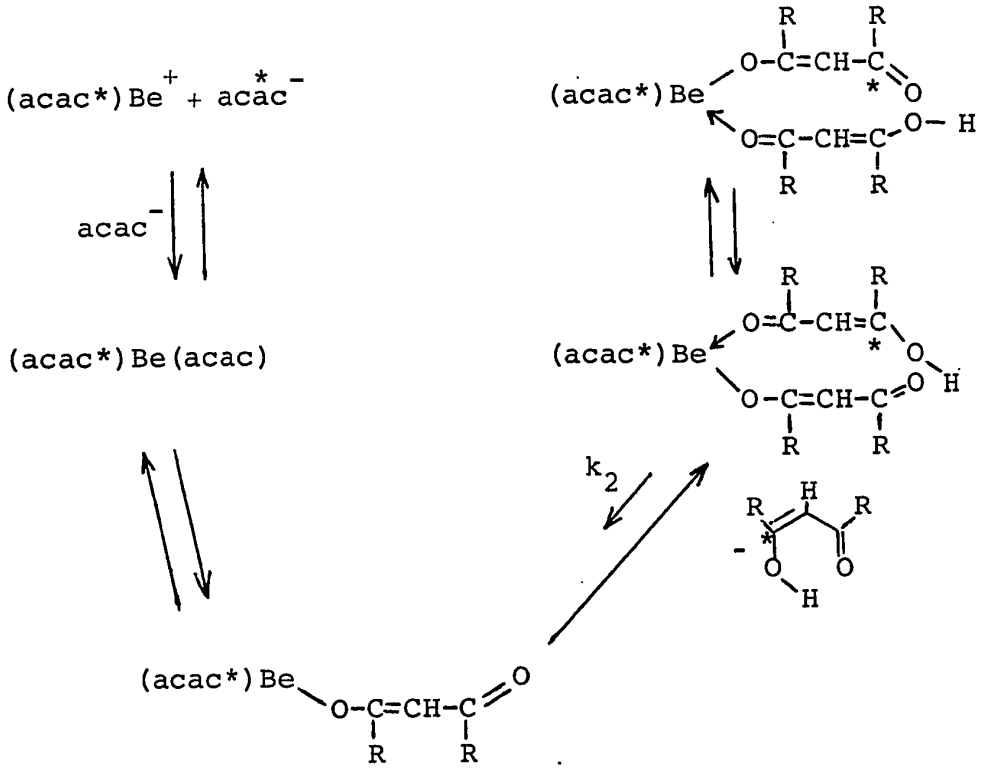

The main feature to note from all the previous work done on the kinetics and mechanisms of ligand exchange is that the first step involves a fast equilibrium step, thus

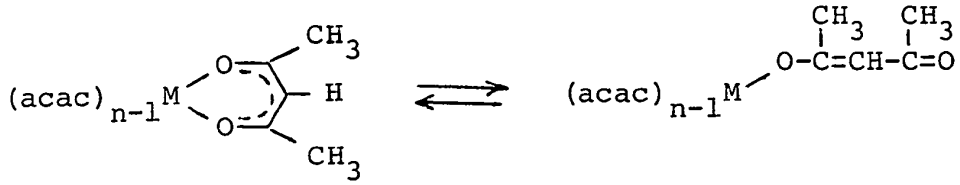

and as a second step in the first order paths, rupture of the remaining M-O bond to yield

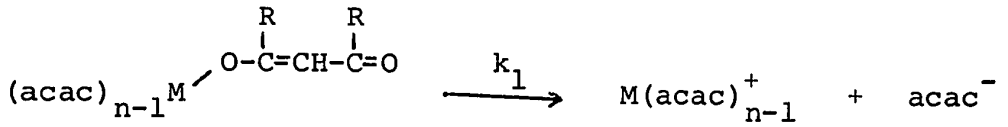

A more recent study reports on the ligand exchange mechanism between $In(CF_3COCHCOR)_3$ where R is methyl, i-butyl, phenyl, 2-naphthyl, and 2-thienyl by ^{19}F nmr spectroscopy (110). The ^{19}F nmr linewidths indicated that exchange was first order in $[In(dik)_3]$ but zero order in free ligand concentration. From dependences of the linewidths on the concentration of free ligand, [HL], and complex, $[InL_3]$, the relaxation times were reported as being

$$\frac{1}{\tau_{HL}} = \frac{k[In(tfac)_3]}{[Htfac]} \quad \text{and} \quad \frac{1}{\tau_{InL_3}} = k$$

The mechanism proposed is very similar to that proposed by Adams and Larsen (30) (vide supra), but the rate-controlling step (step 3) was identified as the rotation of one monodentate ligand about a partial double bond prior to intramolecular proton transfer to a second monodentate ligand. This was inferred by comparison of $\Delta G^{\neq}$ data for the ligand exchange process with those from restricted rotation of $N(Me)_2$ group about a C-N bond in N,N-dimethyl amide compounds. It should be noted, however, that any correlation in $\Delta G^{\neq}$ is simply coincidental since the $\Delta G^{\neq}$ parameter is somewhat "insensitive" to configurational changes -

activation energies should be compared!

(b) Exchange Studies in $(C_6H_5)_2Sn(acac)_2$-$(CH_3)_2Sn(acac)_2$

In order to investigate the possible mechanism(s) for the ligand exchange between $(C_6H_5)_2Sn(acac)_2$ and $(CH_3)_2Sn(acac)_2$, values of the mean residence times in site A, $(C_6H_5)_2Sn(acac)_2$, and in site B, $(CH_3)_2Sn(acac)_2$, were determined as a function of the concentration of $(CH_3)_2Sn(acac)_2$ and of the concentration of $(C_6H_5)_2Sn(acac)_2$, respectively. Two series of solutions were prepared in bromoform: series "A" consisted of five solutions all with a fixed concentration of $(C_6H_5)_2Sn(acac)_2$ and varying concentrations of $(CH_3)_2Sn(acac)_2$ (Table XXIII); series "B" consisted of five solutions all fixed in the concentration of $(CH_3)_2Sn(acac)_2$ and differing in the concentrations of $(C_6H_5)_2Sn(acac)_2$ (Table XXIV). Spectra of these solutions were recorded at 70° and are shown in Figures 16 and 17. Mean residence times τ_A and τ_B were determined from Total Line-Shape Analysis of the nmr spectra as described earlier (see eg., Sections II C 4b and III B 5a). The results of the analysis are listed in Tables XXIII and XXIV along with the rates $1/\tau_i$, and $\delta\nu$ values from the computer-calculated nmr spectra which are also displayed in Figures 16 and 17. Solid circles represent experimental points, solid triangles calculated points, while open circles denote perfect fit between the experimental and calculated points. Two features are noteworthy in Tables XXIII and

Figure 16.- Nmr spectra for the acetylacetonate methyl proton region as a function of the concentration of $(CH_3)_2Sn(acac)_2$ in bromoform at 70°; (a) experimental spectra; (b) comparison of experimental and calculated spectra, solid circles represent experimental points, solid triangles calculated points, open circles denote perfect fit between experimental and calculated points.

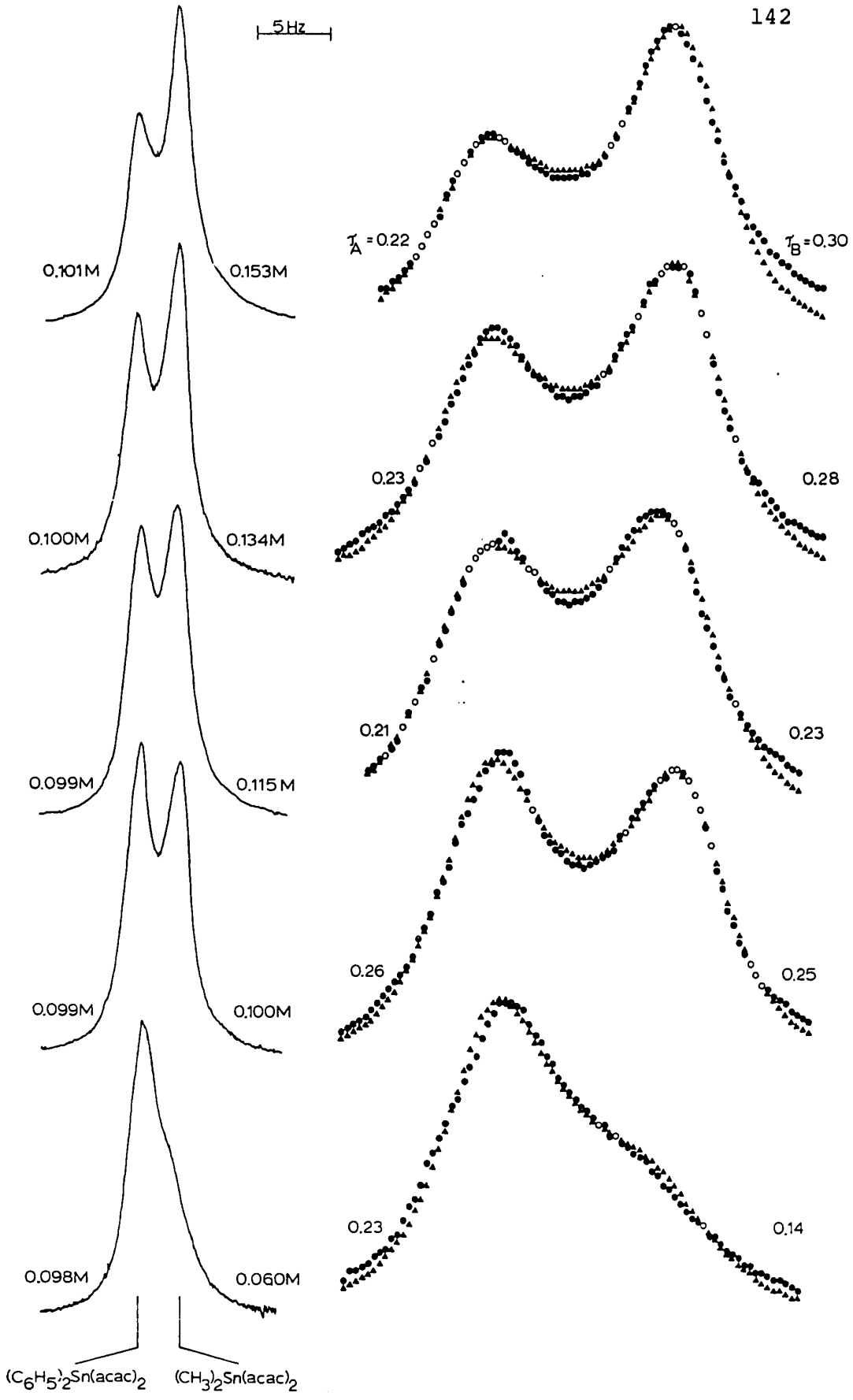
5 Hz
0.101M
0.153M
0.100M
0.134M
0.099M
0.115 M
0.099M
0.100M
0.098M
0.060M
$(C_6H_5)_2Sn(acac)_2$
$(CH_3)_2Sn(acac)_2$
τ_A = 0.22
τ_B = 0.30
0.23
0.28
0.21
0.23
0.26
0.25
0.23
0.14
(a)
(b)

Figure 17.- Nmr spectra for the acetylacetonate methyl proton region as a function of the concentration of $(C_6H_5)_2Sn(acac)_2$ in bromoform at 70°; (a) experimental spectra; (b) comparison of experimental and calculated spectra, solid circles represent experimental points, solid triangles calculated points, open circles denote perfect fit between experimental and calculated points.

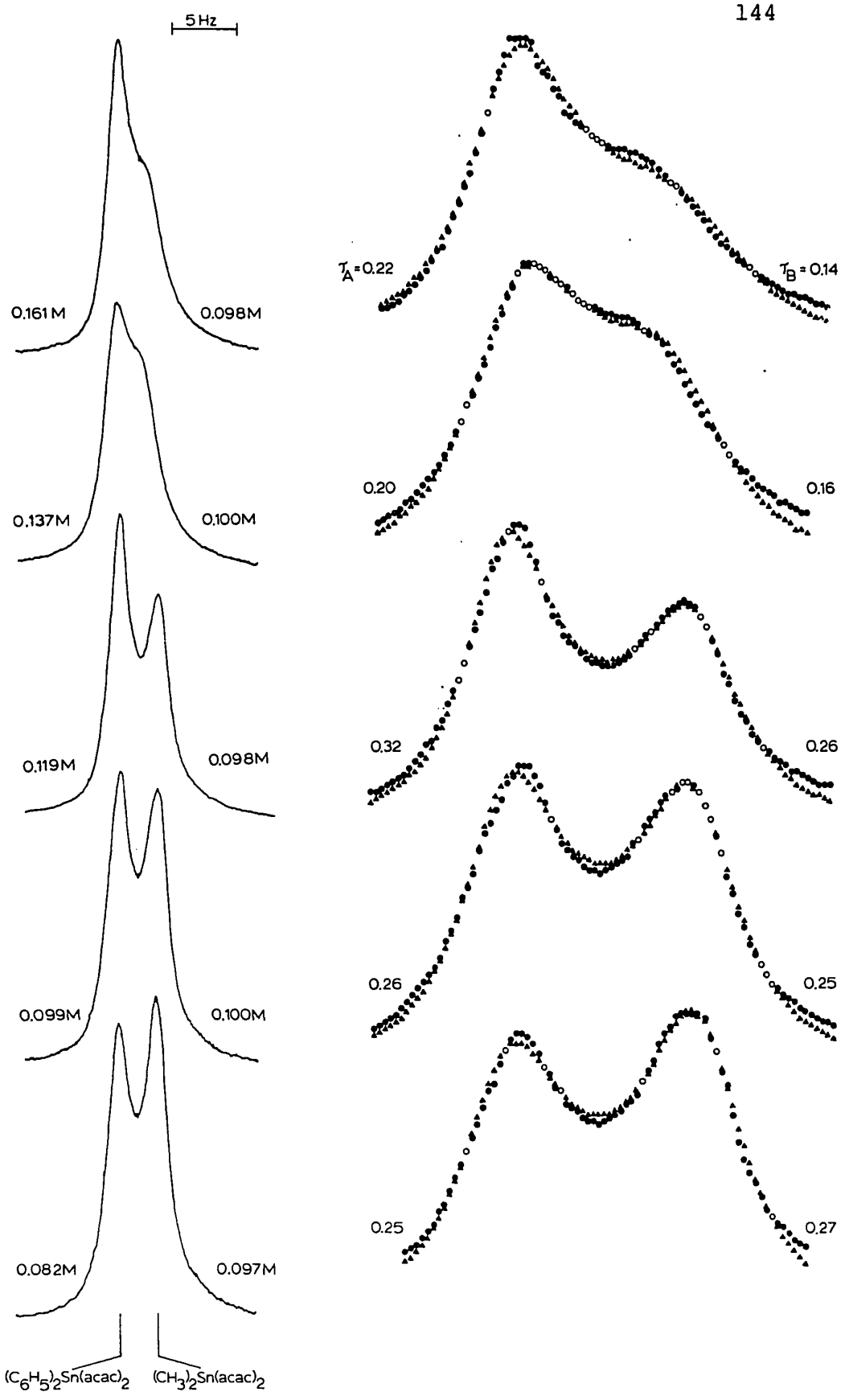
5 Hz
0.161 M
0.098M
0.137M
0.100M
0.119M
0.098M
0.099M
0.100M
0.082M
0.097M
$(C_6H_5)_2Sn(acac)_2$
$(CH_3)_2Sn(acac)_2$
(a)
τ_A = 0.22
τ_B = 0.14
0.20
0.16
0.32
0.26
0.26
0.25
0.25
0.27
(b)

Table XXIII.- Dependence of the Inverse Mean Lifetime $1/\tau_A$ on the Concentration of $(CH_3)_2Sn(acac)_2$ in Bromoform at 70°

Solution	$[(C_6H_5)_2Sn(acac)_2]$ [A]	$[(CH_3)_2Sn(acac)_2]$ [B]	τ_A (sec)	τ_B (sec)	$1/\tau_A$ (sec^{-1})	$\delta\nu_o$ (Hz)
A_1	0.1005	0.1530	0.22	0.30	4.5	3.68
A_2	0.1003	0.1341	0.23	0.28	4.4	3.73
A_3	0.0999	0.1154	0.21	0.23	4.8	3.70
A_4	0.0987	0.1000	0.26	0.25	3.9	3.68
A_6	0.0981	0.0605	0.23	0.14	4.3	3.49

Table XXIV.- Dependence of the Inverse Mean Lifetime $1/\tau_B$ on the Concentration of $(C_6H_5)_2Sn(acac)_2$ in Bromoform at 70°

Solution	$[(C_6H_5)_2Sn(acac)_2]$ [A]	$[(CH_3)_2Sn(acac)_2]$ [B]	τ_A (sec)	τ_B (sec)	$1/\tau_B$ (sec^{-1})	[A]/[B]	$\delta\nu_o$ (Hz)
B_1	0.1613	0.0977	0.22	0.14	7.1	1.6506	3.72
B_2	0.1373	0.1004	0.20	0.16	6.3	1.3678	3.46
B_3	0.1194	0.0982	0.32	0.26	3.9	1.2161	3.61
B_4	0.0987	0.1000	0.26	0.25	4.0	0.9864	3.68
B_5	0.0822	0.0966	0.25	0.27	3.7	0.8505	3.71

XXIV: first, the rate of exchange of an acetylacetonate ligand from site A to site B, expressed as $1/\tau_A$, is independent of the concentration of $(CH_3)_2Sn(acac)_2$; second, the rate of transfer of an $acac^-$ ligand from site B to site A, expressed as $1/\tau_B$, is dependent on the concentration of $(C_6H_5)_2Sn(acac)_2$. In addition, comparison of rates of exchange between solution B1 and B5 (Table XXIV) indicates that halving the concentration of $(C_6H_5)_2Sn(acac)_2$ from 0.1613 M to 0.0822 M halves the rate (as $1/\tau_B$) from 7.1 to 3.7 sec^{-1}. This indicates that the dependence of the rate of ligand exchange is first order in the concentration of the diphenyltin acetylacetonate complex. The dependence of the inverse mean lifetimes on the concentrations of reactants is pictured in Figure 18 in which are plotted $1/\tau_B$ against $[(C_6H_5)_2Sn(acac)_2]/[(CH_3)_2Sn(acac)_2]$ and $1/\tau_A$ versus $[(CH_3)_2Sn(acac)_2]$. Thus, the rates of exchange can be expressed as

$$\frac{1}{\tau_B} = \frac{k[(C_6H_5)_2Sn(acac)_2]}{[(CH_3)_2Sn(acac)_2]} \qquad 45$$

and

$$\frac{1}{\tau_A} = k \qquad 46$$

where k is the observed rate constant for the ligand exchange process. From the slope of a linear least-squares analysis on the five points of the plot $1/\tau_B$ vs [A] /[B] of Figure 18, k = 4.6 ± 1.2 sec^{-1} (one standard deviation), and the intercept = -0.5 ± 1.8 (one standard

Figure 18.- Plots of the inverse mean lifetimes $1/\tau_A$ and $1/\tau_B$ (see text) as a function of concentration.

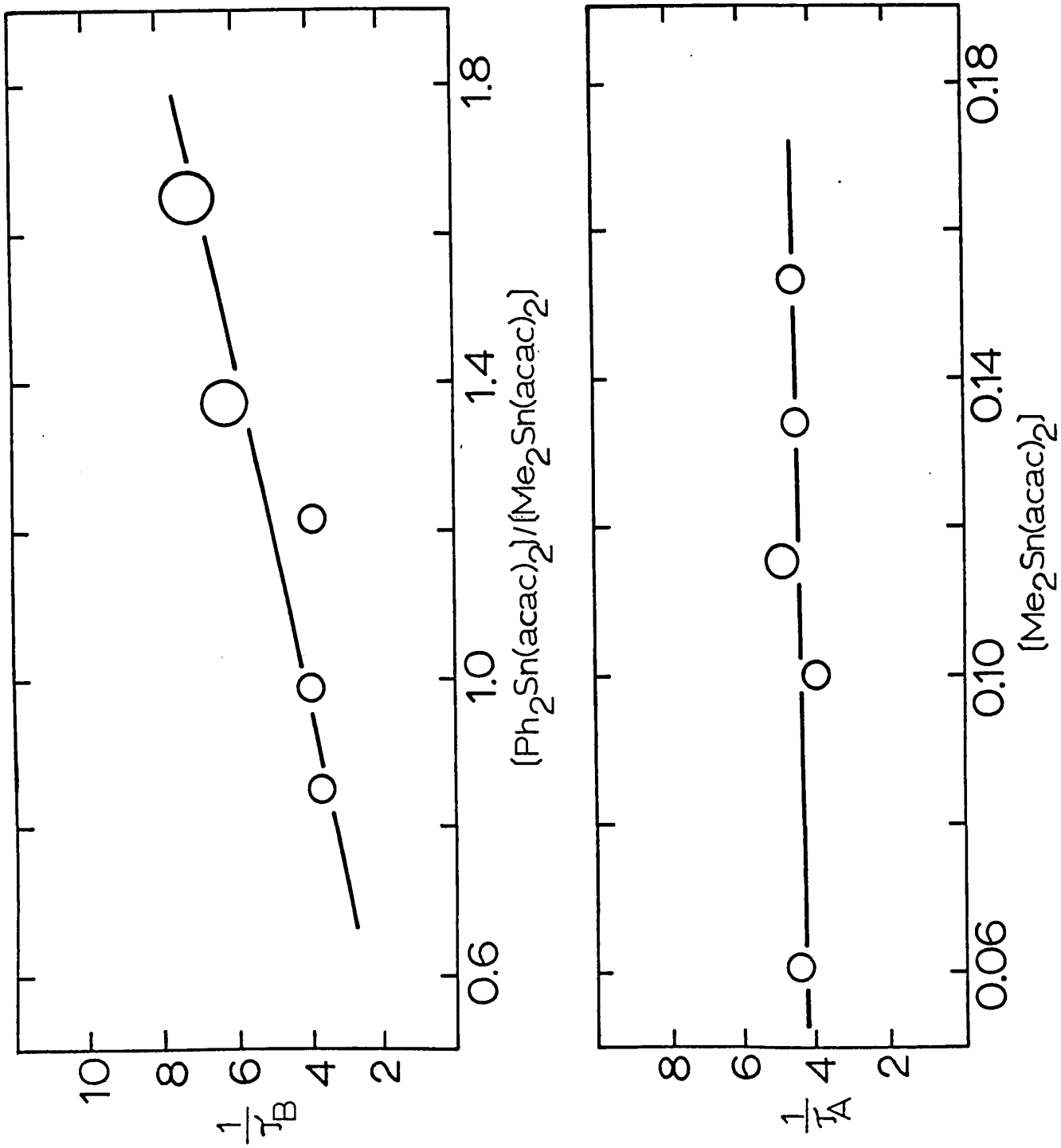
10
8
6
4
2
$\frac{1}{\tau_B}$
0.6
1.0
1.4
1.8
$[Ph_2Sn(acac)_2]/[Me_2Sn(acac)_2]$
8
6
4
2
$\frac{1}{\tau_A}$
0.06
0.10
0.14
0.18
$[Me_2Sn(acac)_2]$

deviation) as expected for the rate equation 45. This value of k is to be compared with k = 4.4 ± 0.3 (one σ) from the average of $1/\tau_A$ values of Table XXIII.

It is now instructive to consider some plausible mechanisms similar and dissimilar to those already discussed earlier in Section III B 6a, and keeping in mind that $1/\tau_A$ is constant and $1/\tau_B$ is a function of the concentration of $(C_6H_5)_2Sn(acac)_2$ only.

Mechanism I:

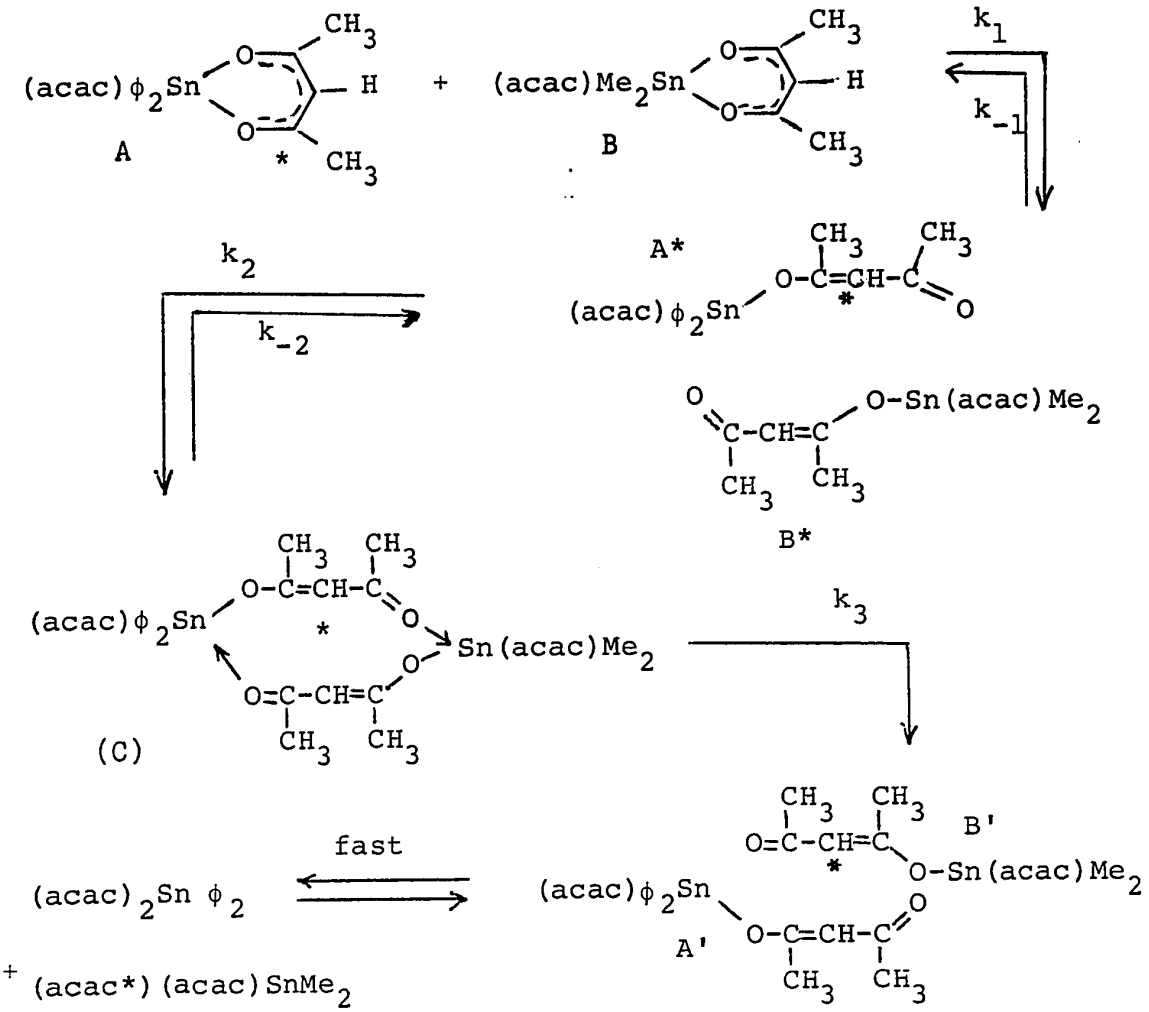

Two cases can be considered here. Case (1): the first step defined by k_1 and k_{-1} is a fast equilibrium step.

$$\frac{d[C]}{dt} = k_2[A^*][B^*] - k_{-2}[C] - k_3[C]$$

and applying the steady state approximation

$$k_2[A^*][B^*] - k_{-2}[C] - k_3[C] = 0 = \frac{d[C]}{dt}$$

from which $[C](k_{-2} + k_3) = k_2[A^*][B^*]$

but $[A^*][B^*] = K_1[A][B]$

$$\rightsquigarrow \quad [C] = \frac{k_2 K_1 [A][B]}{k_{-2} + k_3}$$

Thus $$\frac{d[A']}{dt} = k_3[C] = \frac{K_1 k_2 k_3 [A][B]}{k_{-2} + k_3}$$

from which

$$\frac{1}{\tau_A} = \frac{1}{[A]} \cdot \frac{d[A']}{dt} = \frac{K_1 k_2 k_3 [B]}{k_{-2} + k_3}$$

and $$\frac{1}{\tau_B} = \frac{1}{[B]} \cdot \frac{d[A']}{dt} = \frac{K_1 k_2 k_3 [A]}{k_{-2} + k_3} \qquad 47$$

a) if $k_3 >> k_{-2}$

$$\frac{1}{\tau_A} = K_1 k_2 [B] \quad ; \quad \frac{1}{\tau_B} = K_1 k_2 [A] \qquad 48$$

b) if $k_{-2} >> k_3$

$$\frac{1}{\tau_A} = K_1K_2k_3[B] \quad ; \quad \frac{1}{\tau_B} = K_1K_2k_3[A] \qquad 49$$

Case (2): first step is not a fast equilibrium step.

$$\frac{d[A^*]}{dt} = k_1[A][B] - k_{-1}[A^*][B^*] - k_2[A^*][B^*]$$

from which after applying the steady state approximation we get

$$[A^*]\{k_{-1}[B^*] + k_2[B^*]\} = k_1[A][B]$$

$$[A^*] = \frac{k_1[A][B]}{k_{-1}[B^*] + k_2[B^*]}$$

and $\frac{1}{2}\frac{d[C]}{dt} = k_2[A^*][B^*] = \frac{k_1k_2[A][B][B^*]}{k_{-1}[B^*] + k_2[B^*]}$

Thus, $\frac{1}{2}\frac{d[C]}{dt} = \frac{k_1k_2[A][B]}{k_{-1} + k_2}$

from which

$$\frac{1}{\tau_A} = \frac{1}{2[A]} \cdot \frac{d[C]}{dt} = \frac{k_1k_2[B]}{k_{-1} + k_2} \qquad \text{and}$$

$$\frac{1}{\tau_B} = \frac{1}{2[B]} \cdot \frac{d[C]}{dt} = \frac{k_1k_2[A]}{k_{-1} + k_2} \qquad 50$$

a) for $k_2 >> k_{-1}$

$$\frac{1}{\tau_A} = k_1[B] \quad ; \quad \frac{1}{\tau_B} = k_1[A] \qquad 51$$

b) for $k_{-1} >> k_2$

$$\frac{1}{\tau_A} = K_1[B] \quad ; \quad \frac{1}{\tau_B} = K_1[A] \qquad \underline{52}$$

Since expressions 48, 49, 51, and 52 are not consistent with equation 45 and 46, mechanism I is discarded.

Mechanism II:

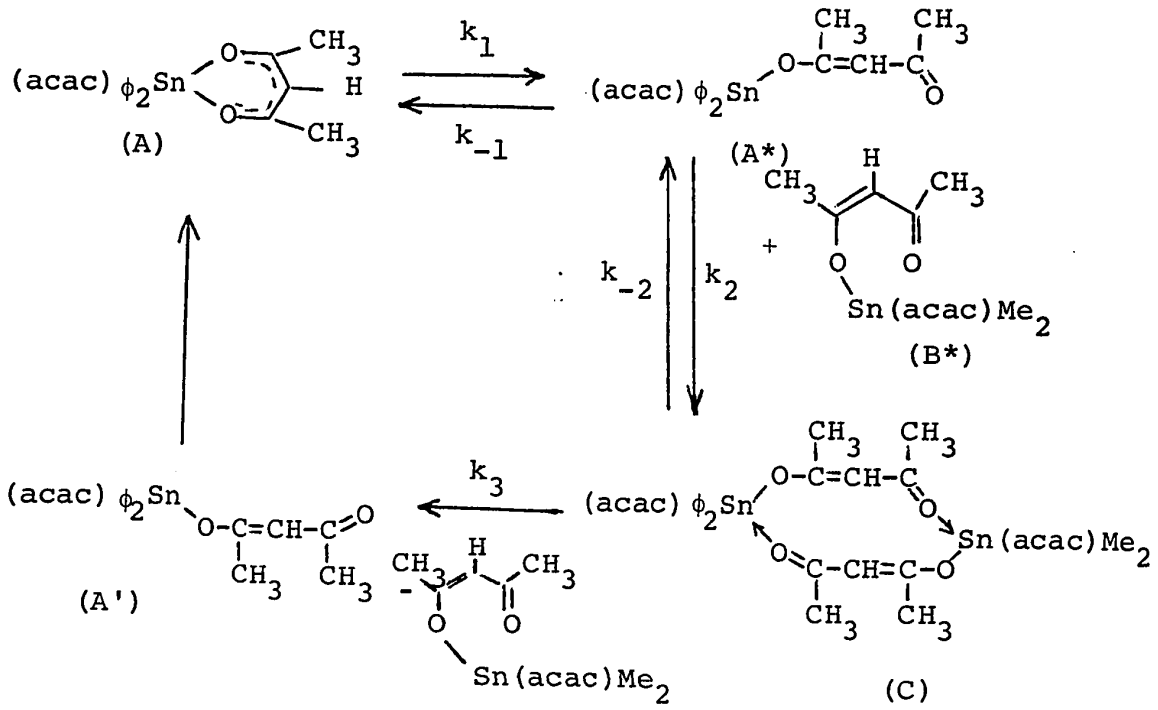

Two cases can be considered here also:

Case (1): Step 1 is a fast equilibrium step similar to mechanistic reports discussed earlier (See Section III B 6a). Also B* is considered formed from B through a fast equilibrium step.

Hence

$$\frac{d[C]}{dt} = k_2[A^*][B^*] - k_{-2}[C] - k_3[C]$$

and applying the steady state approximation we obtain

$$[C] = \frac{k_2[A^*][B^*]}{k_{-2} + k_3}$$

but $[A^*] = K_1[A]$ and $[B^*] = K[B]$

thus $$[C] = \frac{k_1 KK_1[A][B]}{k_{-2} + k_3}$$

$$\frac{d[A']}{dt} = k_3[C] = \frac{k_2 k_3 KK_1[A][B]}{k_{-2} + k_3}$$

from which

$$\frac{1}{\tau_A} = \frac{1}{[A]} \cdot \frac{d[A']}{dt} = \frac{k_2 k_3 KK_1[B]}{k_{-2} + k_3} \quad \text{and} \qquad 53$$

$$\frac{1}{\tau_B} = \frac{1}{[B]} \cdot \frac{d[A']}{dt} = \frac{k_2 k_3 KK_1[A]}{k_{-2} + k_3}$$

whence

a) if $k_3 >> k_{-2}$

$$\frac{1}{\tau_A} = k_2 KK_1[B] \quad ; \quad \frac{1}{\tau_B} = k_2 KK_1[A] \qquad 54$$

b) if $k_{-2} >> k_3$

$$\frac{1}{\tau_A} = k_3 KK_1 K_2[B] \quad ; \quad \frac{1}{\tau_B} = k_3 KK_1 K_2[A] \qquad 55$$

Equations 54 and 55 are not consistent with equations 45 and 46, and thus case (1) for mechanism (II) must be

discarded. It is concluded therefore that rupture of Sn-O bonds in species C is not the rate-determining step as was postulated for $Zr(acac)_4$-Hacac and $Hf(acac)_4$-Hacac systems in chlorobenzene by Adams and Larsen (30).

Case (2): step 3 is a fast step, and B* is formed from B through a fast equilibrium step.

Thus, $$\frac{d[A^*]}{dt} = k_1[A] - k_{-1}[A^*] - k_2[A^*][B^*]$$

and applying the steady state approximation we obtain

$$[A^*] = \frac{k_1[A]}{k_{-1} + k_2[B^*]} \qquad \text{but } [B^*] = K[B]$$

hence

$$[A^*] = \frac{k_1[A]}{k_{-1} + k_2K[B]}$$

and $$\frac{1}{2} \cdot \frac{d[C]}{dt} = k_2[A^*][B^*] = \frac{k_1k_2[A]K[B]}{k_{-1} + k_2K[B]}$$

whence

$$\frac{1}{\tau_A} = \frac{1}{2[A]} \cdot \frac{d[C]}{dt} = \frac{k_1k_2K[B]}{k_{-1} + k_2K[B]} \qquad \text{and}$$

56

$$\frac{1}{\tau_B} = \frac{1}{2[B]} \cdot \frac{d[C]}{dt} = \frac{k_1k_2K[A]}{k_{-1} + k_2K[B]}$$

a) if $k_2K[B] >> k_{-1}$

$$\frac{1}{\tau_A} = k_1 \quad ; \qquad \frac{1}{\tau_B} = k_1\frac{[A]}{[B]} \qquad 57$$

b) if $k_{-1} >> k_2K[B]$

$$\frac{1}{\tau_A} = k_2KK_1[B] \quad ; \quad \frac{1}{\tau_B} = k_2KK_1[A] \qquad \underline{58}$$

Since equations 58 are not consistent with equations 45 and 46, k_2 is not the rate-determining step. But equations 57 are fully consistent with expressions 45 and 46 from which it is concluded that $k_2 >> k_{-1} > k_1$ and so k_1 is rate-determining. The rate law can then be expressed as Rate = $k_1[A]$. Therefore the rate-determining step in the ligand exchange between $(C_6H_5)_2Sn(acac)_2$ and $(CH_3)_2Sn(acac)_2$ appears to be rupture of one Sn-O bond in the former complex. Such a case has not been reported earlier, but has been suggested by several workers as a first step in the intramolecular environmental averaging processes in $(C_6H_5)_2Sn(acac)_2$ (42) and in other transition and post-transition metal acetylacetonate complexes (52, and see for example ref 1).

The kinetic data presented here do not, unfortunately, preclude a mechanism in which the rate-determining step is identified as rotation of one monodentate ligand (in species A*) about a partial double bond in the O-C-C-C-O moiety of the acetylacetonate unidentate ligand. Such a mechanism would have as its first step rupture of a Sn-O bond to yield a five-coordinate species similar to the first step of mechanism II above. However, once this five-coordinate species is formed and before it

reacts with species B*, the unidentate acetylacetonate ligand may undergo rotation about the partial double bond in O-C-C-C-O. The remaining steps in this mechanism (see below) may be the same as those of mechanism II.

$$A \underset{k_{-1}}{\overset{k_1}{\rightleftharpoons}} A^* \xrightarrow{k_{rot}} A^*_{rot} \xrightarrow[B^*_{rot}]{} C \longrightarrow \ldots.$$

If the rate of ligand exchange is defined by

$$\frac{d[A^*_{rot}]}{dt} = k_{rot}[A^*] \qquad 59$$

where A^*_{rot} is the "rotated form" of A*, then one obtains expression for τ_A^{-1}, τ_B^{-1} and the rate as in equations 60 and 61 which are also consistent with our data. From these

$$\frac{1}{\tau_A} = \frac{k_{rot}k_1}{k_{-1} + k_{rot}} \; ; \; \frac{1}{\tau_B} = \frac{k_{rot}k_1}{k_{-1} + k_{rot}} \cdot \frac{[A]}{[B]} \qquad 60$$

$$\text{Rate} = \frac{k_1 k_{rot}}{k_{-1} + k_{rot}} \cdot [A] \qquad 61$$

it can also be concluded that if $k_{rot} >> k_{-1}$, then $\tau_A^{-1} = k_1$ and $\tau_B^{-1} = k_1[A]/[B]$ and k_1 is again the rate-controlling step; but if $k_{-1} >> k_{rot}$, then $\tau_A^{-1} = k_{rot}K_1$ and $\tau_B^{-1} = k_{rot}K_1[A]/[B]$ and k_{rot} would be the rate-determining step.

It is tempting at this point to compare activation parameters for the intermolecular ligand exchange

reported here to those from the intramolecular configurational rearrangements in the $(C_6H_5)_2Sn(acac)_2$ complex (44). For the intermolecular process ($CDCl_3$): E_A = 7.5 ± 1.5 kcal/mole, $\Delta S^{\neq}_{298}$ = -33 ± 5 eu, k_{298} = 3.8 ± 0.6 sec^{-1}; for the intramolecular process ($CDCl_3$): E_A = 8.1 ± 0.3 kcal/mole, $\Delta S^{\neq}_{298}$ = -21.7 ± 1.4 eu, k_{298} = 369 sec^{-1}. It is thus noteworthy that the entropies of activation in the latter process are ca. 11 eu more positive and k_{298} is larger by a factor of 10^2 indicating a faster intramolecular methyl group exchange process. If this process proceeded through a bond rupture mechanism - which cannot be unequivocally established (cf. ref 1) - then one would expect that the activation parameters be the same, within experimental error, for both processes; only the activation energies appear to be the same. The differences in the values of the other parameters could probably be rationalized in terms of k_{rot} as the rate-controlling step and that the similarity in the energies of activation may be coincidental. What argues against k_{rot} as the rate-determining step, however, is that if rotation of the unidentate acac ligand in the A* species must occur, so as to be in the proper configuration prior to exchange, then surely rotation of the unidentate acac ligand in B* will occur also - and if rotation is slow in A*, it is not inconceivable that it also be slow in B*, that it be experimentally detectable (provided one admits the existence of B*), and therefore that the rate be first order in the concentration of $(CH_3)_2Sn(acac)_2$

(this was not observed). In addition, the errors in $\Delta S^{\neq}$ and E_A (Table XVI) are large. An error of +5 eu in $\Delta S^{\neq}$ or an error of 1.5 kcal/mole in E_A will increase k_{298} by a factor of ∿10; when both of these errors are considered together, k_{298} increases by a factor of ∿200 (k_{298} = 540 sec^{-1} if E_A = 6.0 kcal/mole and $\Delta S^{\neq}$ = -28 eu). Thus, comparison of values of activation parameters between the ligand exchange process in $(C_6H_5)_2Sn(acac)_2$-$(CH_3)_2Sn(acac)_2$ and the intramolecular configurational rearrangement in $(C_6H_5)_2Sn(acac)_2$ is at best tenuous. It would be even more tenuous if the latter process occured *via* twisting mechanisms (*cf.* ref 1).

The strongest evidence against rotation of the dangling acetylacetonate ligand in the A* species arises from studies on the stereochemical lability of some triorganosilicon acetylacetonates (111). These complexes possess an open-chain enol ether structure and give rise to configurations in which the uncoordinated carbonyl oxygen atom is positioned either *cis* or *trans* to the siloxy group.

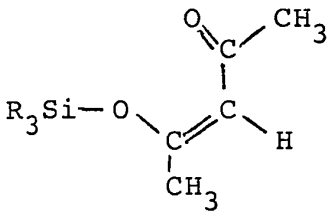

cis

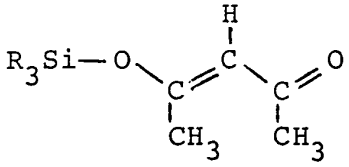

trans

Apparently, cis isomers undergo a rapid, intramolecular rearrangement process which interchanges the allylic and acetyl methyl groups on the acetylacetonate moiety. This rearrangement is believed (111) to occur via a five-coordinate silicon intermediate; however, a similar process for the trans isomers is restricted by rotation about the C=C bond (111) as the nmr spectra of these reveal a =CH- multiplet, two acetylacetonate methyl doublets, and a Si-CH_3 singlet (when R is CH_3). No broadening of the acetylacetonate methyl lines for the trans isomer of $(CH_3)_3Si(acac)$ was observed in the temperature range -70 to 120°.

Further, the data presented here do not preclude a solvent-assisted path in the rupture of a Sn-O bond in mechanism II, case (2). That the solvent does not play an insignificant role is suggested by comparing activation parameters in deuteriochloroform and bromoform (see Table XVI). Values of $\Delta S^{\neq}$ for the ligand exchange process are rather low, -42 eu ($CHBr_3$) and -33 eu ($CDCl_3$), for a reaction involving a bond rupture rate-determining step. Brown (82) has pointed out that activation entropies should be positive for a dissociative mechanism and negative for an associative one, in the absence of strong solvent effects. These low negative values of the entropies probably reflect the fact that the free end of the unidentate acetylacetonate ligand in the reaction intermediate (A*) does not get very far away from its original coordination

site but remains in the neighbourhood; and $CHBr_3$, through solvation of the intermediate, might well force the free end to stay close to its original position. This would also explain the lower value of $\Delta S^{\neq}$ in $CHBr_3$ than in $CDCl_3$ since the latter solvent, in its attempt to coordinate to the "vacant" sixth position, would force the free ligand end away from the coordination neighbourhood and thus leading to an increase in $\Delta S^{\neq}$ for $CDCl_3$ solutions.

In view of the above arguments, it appears that solvents may play an important role in the various steps of mechanism II. Further work would have to be carried out with other solvents of increasing coordinating behaviour, and increasing dielectric constant in an attempt to establish the extent to which solvent molecules contribute to the kinetics and mechanisms of ligand exchange reactions. Also, a change in the nature of the bidentate ligands may perhaps lead to differentiation of the k_1 *versus* k_{rot} as the rate-controlling step in ligand exchange.

IV. A P P E N D I X

Table XXV.- Summary of Data of Ligand Exchange Studies on MO_6 Core Complexes at 25°[a]

Type of Exchange[b]	System	Solvent	K_{fi}	ΔH kcal/mole	ΔS eu	Ref.
I	$Al(acac)_3$-$Al(bzbz)_3$	C_6H_6	K_{f1}, 2.27	0.03±0.20	2.63±0.51	39
			K_{f2}, 2.43	0.16±0.14	2.30±0.39	
		$1,2\text{-}C_2H_4Cl_2$	K_{f1}, 2.86	-0.06±0.05	1.89±0.13	39
			K_{f2}, 2.97	-0.03±0.05	2.04±0.10	
	$Ga(acac)_3$-$Ga(bzbz)_3$	C_6H_6	K_{f1}, 2.59±0.11	0.32±0.25	2.98±0.74	37
			K_{f2}, 2.47±0.10	0.04±0.24	1.91±0.71	
II	$Al(acac)_3$-$Al(hfac)_3$	Dioxane	K_{f1}, 2.11×10^2	-1.39±0.22	6.03±0.56	39
			K_{f2}, 2.88×10^2	-1.80±0.20	5.20±0.50	
		C_6H_5Cl	K_{f1}, 3.25×10^2	-1.81±0.22	5.42±0.64	39
			K_{f2}, 3.09×10^2	-1.44±0.22	6.52±0.63	
		$1,2\text{-}C_2H_4Cl_2$	K_{f1}, 2.05×10^2	-1.70±0.21	4.88±0.58	39
			K_{f2}, 1.92×10^2	-1.62±0.17	5.01±0.46	
		$C_6H_5NO_2$	K_{f1}, 3.46×10^2	-1.95±0.30	5.08±0.81	39
			K_{f2}, 3.26×10^2	-1.98±0.50	4.89±1.20	
	$Ga(acac)_3$-$Ga(hfac)_3$	C_6H_6	K_{f1}, $1.12\pm0.21\times10^3$	-4.1±0.8	0.1±2.4	37
			K_{f2}, $1.22\pm0.27\times10^3$	-4.5±1.0	-0.9±2.9	

Table XXV - Cont'd

Values for a random distribution of ligands:				
$M(dik)_3$-$M(dik')_3$	-	K_{f1}, 3.00	0.00	2.18
		K_{f2}, 3.00	0.00	2.18

[a] These data refer to the formation of one mole of mixed ligand complex from the corresponding parent complexes as defined by the equation

$$\frac{i}{3} M(dik)_3 + \frac{3-i}{3} M(dik')_3 \xrightleftharpoons{K_{fi}} M(dik)_i(dik')_{3-i}$$

[b] For meaning of Type of exchange, see text.

Table XXVI.- Summary of Data of Ligand Exchange Studies on MO_8 Core Complexes[a]

Type of Exchange[b]	System	Solvent	K_{fi}	ΔH, kcal/mole	ΔS, eu	Ref.
I	$Zr(acac)_4$-$Zr(bzbz)_4$ at 35°	CH_2Cl_2	K_{f1}, 1.3±1.0	-	-	39
			K_{f2}, 2.9±1.5	-	-	
			K_{f3}, 3.1±1.0	-	-	
	$Zr(acac)_4$-$Zr(\beta\text{-T})_4$ at 35°	C_6H_6-$C_6H_6NO_2$	K_{f1}, 1.83±0.6	-	-	39
			K_{f2}, 4.90±1.5	-	-	
			K_{f3}, 3.27±1.1	-	-	
II	$Zr(acac)_4$-$Zr(hfac)_4$ (data at 25°)	C_6H_6	K_{f1}, 3.89×10^3	-3.48±0.16	4.75±0.50	39
			K_{f2}, 7.63×10^4	-5.24±0.23	4.79±0.74	
			K_{f3}, 4.80×10^3	-4.15±0.16	2.93±0.51	
	$Zr(dpm)_4$-$Zr(hfac)_4$ (data at 35°)	C_6H_6	K_{f1}, $2.33\pm0.31\times10^4$	-	-	39
			K_{f2}, $2.79\pm0.65\times10^5$	-	-	
			K_{f3}, $2.85\pm0.20\times10^4$	-	-	
III	$Zr(acac)_4$-$Zr(tfac)_4$[c] (data at 25°)	C_6H_6	K_{f1}, 17.2	0.00±0.25	5.5±0.9	34,39
			K_{f2}, 42.7	-0.02±0.35	7.2±1.2	
			K_{f3}, 16.5	0.02±0.42	5.3±1.5	

Table XXVI - Cont'd

CCl_4	K_1[d], 5.9±0.6(2.67)[e]	-0.10±0.19	3.1±0.8(1.95)[e]	
	K_2, 6.0±0.8(2.25)	0.25±0.18	4.5±0.7(1.61)	34
	K_3, 8.0±1.1(2.67)	-0.20±0.25	3.4±0.9(1.95)	
Values for a random distribution of ligands:				
$M(dik)_4$-$M(dik')_4$	K_{f1}, 4.00	0.00	2.75	
	K_{f2}, 6.00	0.00	3.56	
	K_{f3}, 4.00	0.00	2.75	

[a] All data refer to the formation of one mole of mixed ligand complex from the corresponding parent complexes as defined by the equation

$$\frac{i}{4} M(dik)_4 + \frac{4-i}{4} M(dik')_4 \overset{K_{fi}}{\rightleftharpoons} M(dik)_i(dik')_{4-i}$$

[b] For meaning of Type of exchange, see text. [c] These data were calculated (39) from data reported in reference 34. [d] These data refer to reactions 11, 12, and 13, respectively - see text. [e] Values for a random distribution of ligands as exemplified by reactions 11, 12, and 13 - see text.

Table XXVII.- Dependence of Equilibrium Quotients for the [pip][Y(hfac)$_4$]-[pip][Y(tfac)$_4$] System on Solute Composition[a] at -58.0°

Solution No.	f_{hfac}	K_1	K_2	log K_2	K_3	log K_3
4	0.164	-	-	-	12.06	1.0814
					11.30	1.0531
					12.10	1.0828
					13.10	1.1173
					11.20	1.0492
					11.95±0.89[b]	
5	0.225	-	-	-	11.59	1.0641
					10.10	1.0043
					12.15	1.0846
					12.26	1.0885
					11.81	1.0737
					11.58±1.08	
6	0.286	-	-	-	9.85	0.9934
					11.61	1.0648
					10.86	1.0358
					11.26	1.0516
					11.43	1.0581
					11.00±0.87	
7	0.342	-	-	-	10.08	1.0035
					8.44	0.9264
					9.62	0.9832
					8.98	0.9533
					9.20	0.9638
					9.26±0.76	
8	0.418	-	12.10	1.0828	9.01	0.9547
			12.98	1.1133	7.95	0.9004
			12.06	1.0814	8.29	0.9186
			11.39	1.0565	8.31	0.9196
			11.20	1.0492	8.32	0.9201
			11.95±0.87		8.38±0.48	
9	0.482	-	10.63	1.0265	-	-
			10.51	1.0216		
			11.21	1.0492		
			11.05	1.0434		
			10.73	1.0306		
			10.83±0.36			
Mean of all Spectral Measurements			11.39±0.56		10.43±0.64	

Table XXVII - Cont'd

Statistical equilibrium quotients	2.67	2.25	2.67

[a] Deuteriochloroform solution; total solute molarity is 0.35 M. [b] Standard deviation of the mean ($\sigma_m = \sigma t/\sqrt{n}$) at the 95% confidence level.

Table XXVIII.- Dependence of Equilibrium Quotients for the $[pip][Y(hfac)_4]$-$[pip][Y(tfac)_4]$ System on Solute Composition[a] at -50.5°

Solution No.	f_{hfac}	K_1	K_2	log K_2	K_3	log K_3
4	0.164	-	-	-	8.42	0.9253
					7.72	0.8876
					8.67	0.9380
					7.92	0.8987
					8.11	0.9090
					8.17±0.47[b]	
5	0.225	-	-	-	8.39	0.9238
					8.88	0.9484
					8.77	0.9430
					8.00	0.9031
					7.63	0.8825
					8.33±0.64	
6	0.286	-	-	-	7.83	0.8938
					7.53	0.8768
					7.52	0.8762
					7.50	0.8751
					8.46	0.9274
					7.77±0.47	
7	0.342	-	9.33	0.9699	6.07	0.7832
			10.19	1.0082	6.93	0.8407
			8.76	0.9425	5.43	0.7348
			8.51	0.9299	6.59	0.8189
			9.08	0.9581	6.81	0.8332
			9.17±0.80		6.37±0.77	
8	0.418	-	9.98	0.9991	6.84	0.8351
			9.38	0.9722	6.27	0.7973
			9.56	0.9805	7.09	0.8507
			8.90	0.9494	7.32	0.8645
			9.64	0.9841	6.84	0.8351
			9.49±0.49		6.87±0.33	
9	0.482	-	10.31	1.0133	-	-
			9.79	0.9908		
			10.16	1.0069		
			9.97	0.9983		
			9.12	0.9600		
			9.87±0.57			
Mean of all Spectral Measurements		-	9.51±0.32		7.50± 0.37	

Table XXVIII - Cont'd

Statistical equilibrium quotients	2.67	2.25	2.67

[a] Deuteriochloroform solution; total solute molarity is 0.35 M. [b] Standard deviation of the mean ($\sigma_m = \sigma t/\sqrt{n}$) at the 95% confidence level.

Table XXIX.- Dependence of Equilibrium Quotients for the [pip][Y(hfac)$_4$] - [pip][Y(tfac)$_4$] System on Solute Composition[a] at -41.5°

Solution No.	f_{hfac}	K_1	K_2	log K_2	K_3	log K_3
4	0.164	-	-	-	5.54	0.7435
					5.38	0.7308
					5.57	0.7459
					5.08	0.7059
					5.85	0.7672
					5.48±0.35[b]	
5	0.225	-	-	-	8.27	0.9175
					7.58	0.8797
					7.75	0.8893
					7.98	0.9020
					8.15	0.9112
					7.95±0.35	
6	0.286	-	-	-	7.55	0.8779
					7.69	0.8859
					7.22	0.8585
					7.13	0.8531
					5.89	0.7701
					7.10±0.88	
7	0.342	-	6.07	0.7832	7.23	0.8591
			6.42	0.8075	7.38	0.8681
			6.58	0.8182	7.98	0.9020
			7.17	0.8555	7.41	0.8698
			6.64	0.8222	7.47	0.8733
			6.57±0.45		7.51±0.35	
8	0.418	-	8.59	0.9340	5.66	0.7528
			8.60	0.9345	6.14	0.7882
			8.82	0.9455	5.38	0.7308
			9.61	0.9827	5.51	0.7412
			9.14	0.9609	5.79	0.7627
			8.95±0.53		5.70±0.34	
9	0.482	-	9.62	0.9832	-	-
			9.26	0.9666		
			9.48	0.9768		
			10.05	1.0022		
			9.42	0.9741		
			9.56±0.37			
10	0.544	-	7.85	0.8949	-	-
			7.83	0.8938		
			7.84±0.05			
Mean of all spectral measurements		-	8.30±0.67		6.74±0.44	

Table XXIX - Cont'd

Statistical equilibrium quotients	2.67	2.25	2.67

[a] Deuteriochloroform solution; total solute molarity is 0.35 M. [b] ± Standard deviation of the mean ($\sigma_m = \sigma t/\sqrt{n}$) at the 95% confidence level.

Table XXX.- Dependence of Equilibrium Quotients for the $[pip][Y(hfac)_4] - [pip][Y(tfac)_4]$ System on Solute Composition[a] at -37.5°

Solution No.	f_{hfac}	K_1	K_2	log K_2	K_3	log K_3
4	0.164	-	-	-	6.86	0.8363
					6.21	0.7931
					5.99	0.7774
					6.49	0.8123
					8.11	0.9090
					6.68	0.8248
					6.72±0.79[b]	
5	0.225	-	-	-	6.46	0.8102
					6.66	0.8235
					6.52	0.8143
					6.47	0.8109
					7.47	0.8733
					6.72±0.53	
6	0.286	-	-	-	6.93	0.8407
					8.89	0.9489
					8.60	0.9345
					9.02	0.9552
					8.81	0.9449
					8.45±1.16	
7	0.342	-	7.29	0.8627	8.79	0.9440
			8.06	0.9063	9.23	0.9652
			8.13	0.9101	7.81	0.8927
			8.77	0.9430	9.00	0.9543
			7.55	0.8779	8.50	0.9294
			7.96±0.71		8.67±0.68	
8	0.418	-	8.19	0.9133	8.33	0.9206
			8.93	0.9509	6.99	0.8445
			8.19	0.9133	8.03	0.9047
			9.01	0.9547	6.89	0.8382
			9.19	0.9633	8.11	0.9090
			8.70±0.59		7.67±0.59	
9	0.482	-	7.53	0.8768	-	-
			8.36	0.9222		
			9.13	0.9605		
			8.62	0.9355		
			7.80	0.8921		
			8.29±0.79			

Table XXX - Cont'd

10	0.544	-	8.05 8.06 7.83 8.23 7.96 8.03±0.18	0.9058 0.9063 0.8938 0.9154 0.9009	-	-
Mean of all spectral Measurements		-	8.24±0.25		7.61±0.42	
Statistical equilibrium quotients		2.67	2.25		2.67	

[a] Deuteriochloroform solution; total solute molarity is 0.35 M. [b] Standard deviation of the mean ($\sigma_m = \sigma t/\sqrt{n}$) at the 95% confidence level.

Table XXXI.- Dependence of Equilibrium Quotients for the [pip][Y(hfac)$_4$]-[pip][Y(tfac)$_4$] System on Solute Composition[a] at -28.5°[4]

Solution No.	f_{hfac}	K_1	K_2	log K_2	K_3	log K_3
4	0.164	-	-	-	5.86	0.7679
					5.52	0.7419
					6.54	0.8156
					5.37	0.7299
					6.12	0.7868
					5.88±0.58[b]	
5	0.225	-	-	-	6.45	0.8096
					5.37	0.7299
					6.84	0.8351
					6.95	0.8420
					7.72	0.8876
					6.66±1.07	
6	0.286	-	-	-	6.96	0.8426
					7.62	0.8819
					7.28	0.8621
					6.78	0.8312
					4.88	0.6884
					6.70±1.32	
7	0.342	-	-	-	7.64	0.8831
					7.35	0.8663
					6.85	0.8357
					6.62	0.8209
					8.32	0.9201
					7.35±0.84	
8	0.418	-	9.38	0.9722	6.41	0.8069
			10.31	1.0133	6.28	0.7979
			10.29	1.0124	5.62	0.7497
			-		6.01	0.7789
			-		6.44	0.8089
			9.99±1.32		6.15±0.42	
9	0.482	-	9.08	0.9581	5.96	0.7753
			8.49	0.9289	5.38	0.7308
			8.21	0.9144	7.30	0.8633
			9.08	0.9581	5.85	0.7672
			9.12	0.9600	7.65	0.8837
			8.80±0.52		6.42±1.23	
10	0.544	-	6.83	0.8344	-	-
			7.02	0.8463		
			7.03	0.8469		
			6.77	0.8306		
			6.64	0.8222		
			6.86±0.21			

Table XXXI - Cont'd

11	0.614	-	5.80 5.20 5.76 6.15 6.75 5.93±0.70	0.7634 0.7160 0.7604 0.7889 0.8293	-	-
Mean of all spectral Measurements		-	7.66±0.80		6.53±0.31	
Statistical equilibrium quotients		2.67	2.25		2.67	

[a] Deuteriochloroform solution; total solute molarity is 0.35 M. [b] Standard deviation of the mean ($\sigma_m = \sigma t/\sqrt{n}$) at the 95% confidence level.

Table XXXII.- Dependence of Equilibrium Quotients for the [pip][Y(hfac)$_4$]-[pip][Y(tfac)$_4$] System on Solute Composition[a] at -16.0°

Solution No.	f_{hfac}	K_1	K_2	log K_2	K_3	log K_3
4	0.164	-	-	-	6.63	0.8215
					6.50	0.8129
					7.04	0.8476
					6.66	0.8235
					6.98	0.8439
					6.76±0.29[b]	
5	0.225	-	-	-	6.74	0.8287
					8.96	0.9523
					8.17	0.9122
					10.23	1.0099
					8.01	0.9036
					8.42±1.60	
6	0.286	-	-	-	6.78	0.8312
					7.81	0.8927
					7.44	0.8716
					6.51	0.8136
					7.51	0.8757
					7.21±0.67	
7	0.342	-	-	-	7.66	0.8842
					7.29	0.8627
					6.97	0.8432
					7.85	0.8949
					7.65	0.8837
					7.48±0.44	
8	0.418	-	-	-	6.99	0.8445
					7.54	0.8774
					5.67	0.7536
					8.01	0.9036
					7.05±1.61	
9	0.482	-	-	-	6.71	0.8267
					7.08	0.8500
					7.41	0.8698
					7.88	0.8965
					5.98	0.7767
					7.01±1.38	
10	0.544	-	8.84	0.9465	-	-
			8.54	0.9315		
			8.59	0.9340		
			7.71	0.8871		
			8.21	0.9144		
			8.37±0.54			

Table XXXII - Cont'd

11	0.614	-	6.28	0.7980	-	-
			6.18	0.7910		
			6.09	0.7846		
			6.65	0.8228		
			6.74	0.8287		
			6.38±0.40			
Mean of all spectral Measurements		-	7.38±0.79		7.33±0.32	
Statistical equilibrium quotients		2.67	2.25		2.67	

---

[a] Deuteriochloroform solution; total solute molarity is 0.35 M. [b] Standard deviation of the mean ($\sigma_m = \sigma t/\sqrt{n}$) at the 95% confidence level.

V. REFERENCES

1. N. Serpone and D.G. Bickley, Progr. Inorg. Chem., 17, 391 (1972).

2. J.J. Fortman and R.E. Sievers, Coord. Chem. Rev., 6, 331 (1971).

3. D.W. Thompson, Struct. Bond. (Berlin), 9, 27 (1971).

4. S.E. Livingstone, Coord. Chem. Rev., 7, 59 (1971).

5. M. Cox and J. Darben, Coord. Chem. Rev., 7, 29 (1971).

6. R.C. Fay, Ann. N.Y. Acad. Sci., 159, 152 (1969).

7. R.M. Pike, Coord. Chem. Rev., 2, 163 (1967).

8. S.J. Lippard, Progr. Inorg. Chem., 8, 109 (1967); and references therein.

9. J.P. Fackler, Jr., Progr. Inorg. Chem., 7, 361 (1966).

10. G. Calingaert and J.A. Beatty, J. Amer. Chem. Soc., 61, 2748 (1939).

11. G. Calingaert and J.A. Beatty in "Organic Chemistry, An Advanced Treatise", Vol. 2, H. Gilman, Ed., John Wiley and Sons, Inc., New York, N.Y., 1950, p. 1806.

12. T.S. Moore and M.W. Young, J. Chem. Soc., 2694 (1932).

13. K. Moedritzer, Adv. Organomet. Chem., 6, 171 (1968).

14. M. Krauss, Ed., "Redistribution Reactions in Chemistry", Annals of the New York Academy of Sciences, Vol. 159, Art. 1, New York, N.Y., 1969.

15. J.C. Lockhart, "Redistribution Reactions", Academic Press, New York, N.Y., 1970.

16. H. Sigel and D.B. McCormick, Accts. Chem. Res., 3, 201 (1970).

17. E.L. Muetterties and C.M. Wright, Quart. Revs., 21, 109 (1967); and references therein.

18. M.J. Bennett, F.A. Cotton, P. Legzdins, and S.J. Lippard, Inorg. Chem., 7, 1770 (1968).

19. H. Bauer, J. Blanc, and D.L. Ross, J. Amer. Chem. Soc., 86, 5125 (1964).

20. L.R. Melby, N.J. Rose, E. Abramson, and J.C. Caris, J. Amer. Chem. Soc., 86, 5117 (1964).

21. S.J. Lippard, Proc. Int. Conf. Coord. Chem., 1966, 9, 476 (1966).

22. C.A. Hutchison, Jr., and N.J. Elliott, J. Chem. Phys., 16, 920 (1948).

23. L. Sacconi, Atti Accad. Nat. Lincei, Cl. Sci. Fis. Mat. Natur., Rend., (8), 6, 639 (1949).

24. S.J. Lippard, J. Amer. Chem. Soc., 88, 4300 (1966).

25. R.G. Charles and E.P. Riedel, J. Inorg. Nucl. Chem., 28, 3005 (1966).

26. H.A. Swain, Jr., and D.G. Karraker, Inorg. Chem., 9, 1766 (1970).

27. K.J. Eisentraut and R.E. Sievers, J. Inorg. Nucl. Chem., 29, 1931 (1967).

28. R.E. Sievers, K.J. Eisentraut, C.S. Springer, Jr., and D.W. Meek, Advan. Chem. Series, No 71, 141 (1967).

29. R.W. Moshier and R.E. Sievers, "Gas Chromatography of Metal Chelates", Pergamon Press Inc., New York, N.Y., 1965, and references therein.

30. A.C. Adams and E.M. Larsen, Inorg. Chem., 5, 814 (1966).

31. R.C. Fay and T.J. Pinnavaia, Inorg. Chem., 7, 508 (1968).

32. R.C. Fay and N. Serpone, J. Amer. Chem. Soc., 90, 5701 (1968).

33. A.C. Adams and E.M. Larsen, Inorg. Chem., 5, 228 (1966).

34. T.J. Pinnavaia and R.C. Fay, Inorg. Chem., 5, 233, (1966).

35. F.A. Cotton, P. Legzdins, and S.J. Lippard, J. Chem. Phys., 45, 3461 (1966).

36. A.C. Adams and E.M. Larsen, J. Amer. Chem. Soc., 85, 3508 (1963).

37. T.J. Pinnavaia and S.O. Nweke, Inorg. Chem., 8, 639 (1969).

38. J.J. Fortman and R.E. Sievers, Inorg. Chem., 6, 2022, (1967).

39. T.J. Pinnavaia, M.T. Mocella, B.A. Averill, and J.T. Woodward, Inorg. Chem., 12, 763 (1973).

40. T.H. Siddall and W.E. Stewart, Chem. Commun., 922 (1969).

41. N. Serpone and R. Ishayek, Inorg. Chem., 10, 2650 (1971).

42. N. Serpone and K.A. Hersh, Inorg. Nucl. Chem. Letters, 7, 115 (1971).

43. G.E. Glass and R.S. Tobias, J. Organomet. Chem., 15, 481 (1968).

44. K.A. Hersh, M.Sc. Thesis, Sir George Williams University, Montreal 107, (1973).

45. T.J. Pinnavaia and R.C. Fay, Inorg. Syntheses, 12, 88 (1970).

46. N. Serpone, Ph.D. Dissertation, Cornell University, Ithaca, N.Y. 14850 (1968).

47. M.M. McGrady and R.S. Tobias, J. Amer. Chem. Soc., 87, 1909 (1965).

48. R. Uceda, Y. Kawasaki, T. Tanaka, and R. Okawara, J. Organomet. Chem., 5, 194 (1966).

49. Y. Kawasaki, T. Tanaka, and R. Okawara, Bull. Chem. Soc. Japan, 37, 903 (1964).

50. P.J. Paulsen and W.D. Cooke, Anal. Chem., 35, 1560 (1963).

51. G.V.D. Tiers, "NMR Summary", Minnesota Mining and Manufacturing Company, St. Paul, Minn., January 15, 1962.

52. R.W. Jones, Jr., Ph.D. Dissertation, Cornell University, Ithaca, N.Y., 14850 (1971).

53. A. Allerhand, H.S. Gutowsky, R.A. Meinzer, and J. Jonas, J. Amer. Chem. Soc., 88, 3185 (1966).

54. J.A. Pople, W.G. Schneider, and H.J. Bernstein, "High Resolution Nuclear Magnetic Resonance", McGraw-Hill Book Co., Inc., New York, N.Y., 1959, p 458.

55. H.S. Gutowsky and C.H. Holm, J. Chem. Phys., 25, 1228 (1956).

56. J. Jonas, A. Allerhand, and H.S. Gutowsky, J. Chem. Phys., 42, 3396 (1965).

57. L.W. Reeves and R.N. Shaw, Can. J. Chem., 48, 3641 (1970).

58. For more details see the Operating and Service Manual (1965) for Type F-3B Line Follower, Hewlett-Packard, San Diego, California.

59. We thank Professor L.D. Colebrook for a copy of this program.

60. For a description of this program see A. Granata, M.Sc. Thesis, Sir George Williams University, Montreal 107, (1972).

61. N. Filipescu, C.R. Hurt, and N. McAvoy, J. Inorg. Nucl. Chem., 28, 1753 (1966).

62. C. Becher, H. Samelson, and A. Lempicki, J. Chem. Phys., 42, 1081 (1965).

63. E.P. Riedel and R.G. Charles, J. Appl. Phys., 36, 3954 (1965).

64. L.J. Nugent, M.L. Bhaumik, S. George, and S.M. Lee, J. Chem. Phys., 41, 1305 (1964).

65. N. Filipescu, G. Mushrush, C.R. Hurt, and N. McAvoy, Nature (London), 211, 960 (1966).

66. T.M. Shepherd, Nature (London), 212, 745 (1966).

67. H. Samelson, C. Brecher, and A. Lempicki, J. Mol. Spectry., 19, 349 (1966).

68. T. Shigematsu, M. Matsui, and K. Utsunomiya, Bull. Chem. Soc. Japan, 42, 1278 (1969).

69. In these calculations we have used the hard sphere model after D.L. Kepert, J. Chem. Soc., 4736 (1965).

70. A.D. Buckingham, Can. J. Chem., 38, 300 (1960).

71. J.I. Musher, J. Chem. Phys., 37, 34 (1962).

72. J.A.S. Smith and E.J. Wilkins, J. Chem. Soc., A, 1749 (1966).

73. R.C. Fay and T.S. Piper, J. Amer. Chem. Soc., 84, 2303 (1962).

74. R.C. Fay and T.S. Piper, J. Amer. Chem. Soc., 85, 500 (1963).

75. R.C. Fay and R.N. Lowry, Inorg. Chem., 9, 2048 (1970).

76. R.J. Abraham, Mol. Phys., 4, 369 (1961).

77. R. Kaiser, Can. J. Chem., 41, 430 (1963).

78. Previous studies have not been conclusive as to the site of hydrogen bonding [cf. T.S. Davis and J.P. Fackler, Jr., Inorg. Chem., 5, 242 (1966)].

79. P. Laszlo, Progr. Nucl. Magn. Res. Spectry., 3, 231 (1967).

80. T.J. Pinnavaia, Ph.D. Dissertation, Cornell University, Ithaca, N.Y., 14850 (1967).

81. R.C. Fort, Abstracts of Papers, 152nd National Meeting of the American Chemical Society, New York, N.Y., September, 1966.

82. See for example T.L. Brown, Accts. Chem. Res., 1, 23 (1968); C.H. Langford and H.B. Gray, "Ligand Substitution Processes", Benjamin, New York, 1966.

83. Reference 54, Chapter 10.

84. L.W. Reeves, Advan. Phys. Org. Chem., 3, 187 (1965).

85. C.S. Johnson, Jr., Advan. Magn. Res., 1, 33 (1965).

86. K.C. Williams and T.L. Brown, J. Amer. Chem. Soc., 88, 4134 (1966).

87. T.L. Brown and J.A. Ladd, Department of Chemistry, University of Illinois, Urbana, Illinois 61801.

88. We thank Professor R.C. Fay of Cornell University, Ithaca, New York 14850, for providing us with the modified version of this program.

89. T.J. Pinnavaia, J.M. Seleson, II, and D.A. Case, Inorg. Chem., 8, 644 (1969).

90. R.R. Shoup, E.D. Becker, and M.L. McNeil, J. Phys. Chem., 76, 71 (1972).

91. E. Greenwald, A. Loewenstein, and S. Meiboom, J. Chem. Phys., 27, 630 (1957).

92. A. Loewenstein and S. Meiboom, J. Chem. Phys., 27, 1067 (1957).

93. M.T. Rogers and J.C. Woodbrey, J. Phys. Chem., 66, 540 (1962).

94. L.H. Piette and W.A. Anderson, J. Chem. Phys., 30, 899 (1959).

95. M. Takeda and E.O. Stejskal, J. Amer. Chem. Soc., 82, 25 (1960).

96. R.W. Jones, Jr., and R.C. Fay, submitted for publication; R.W. Jones, Jr., Ph.D. Thesis, Cornell University, Ithaca, N.Y., 14850, (1971).

97. T.S. Davis, and J.P. Fackler, Jr., Inorg. Chem., 5, 242 (1966).

98. The Chemical Rubber Company, "Handbook of Chemistry and Physics", 51st Edition, 1970-1971.

99. J.P. Collman and J.Y. Sun, Inorg. Chem., 4, 1273 (1965).

100. J.M. Bull, M.J. Frazer and J. Measures, Chem. Commun., 1310 (1968).

101. W.G. Movius and N.A. Matwiyoff, J. Amer. Chem. Soc., 90, 5452 (1968).

102. K. Saito and K. Masuda, Bull. Chem. Soc. Japan, 41, 384 (1968).

103. K. Saito and K. Masuda, Bull. Chem. Soc. Japan, 42, 3184 (1969).

104. K. Saito and K. Masuda, Bull. Chem. Soc. Japan, 43, 119 (1970).

105. K. Saito and M. Takahashi, Bull. Chem. Soc. Japan, 42, 3462 (1969).

106. R.G. Pearson and D.A. Johnson, J. Amer. Chem. Soc., 86, 3983 (1964).

107. A. Barabas, Inorg. Nucl. Chem. Letters, 6, 775 (1970).

108. C.A. Bunton, J.H. Carter, D.R. Llewellyn, C. O'Connor, A.L. Odell and S.Y. Yih, J. Chem. Soc., 4615 (1964); ibid., 4627 (1964).

109. R.A. Pratt, E. Sherwin, and G.J. Weston, J. Chem. Soc., 476 (1962).

110. G.M. Tanner, D.G. Tuck, and E.J. Wells, Can. J. Chem., 50, 3950 (1972).

111. T.J. Pinnavaia, W.T. Collins, and J.J. Howe, J. Amer. Chem. Soc., 92, 4544 (1970); J.J. Howe and T.J. Pinnavaia, ibid., 91, 5378 (1969).